Accepted Manuscript

Micro-scale to nano-scale generators for energy harvesting: Self powered piezoelectric, triboelectric and hybrid devices

Sundaram Chandrasekaran, Chris Bowen, James Roscow, Yan Zhang, Dinh Khoi Dang, Eui Jung Kim, R.D.K. Misra, Libo Deng, Jin Suk Chung, Seung Hyun Hur

PII: S0370-1573(18)30299-0
DOI: https://doi.org/10.1016/j.physrep.2018.11.001
Reference: PLREP 2035

To appear in: *Physics Reports*

Accepted date : 1 November 2018

Please cite this article as: S. Chandrasekaran, C. Bowen, J. Roscow et al., Micro-scale to nano-scale generators for energy harvesting: Self powered piezoelectric, triboelectric and hybrid devices, *Physics Reports* (2018), https://doi.org/10.1016/j.physrep.2018.11.001

This is a PDF file of an unedited manuscript that has been accepted for publication. As a service to our customers we are providing this early version of the manuscript. The manuscript will undergo copyediting, typesetting, and review of the resulting proof before it is published in its final form. Please note that during the production process errors may be discovered which could affect the content, and all legal disclaimers that apply to the journal pertain.

ACCEPTED MANUSCRIPT

Micro-scale to Nano-scale Generators for Energy Harvesting: Self Powered Piezoelectric, Triboelectric and Hybrid Devices

Sundaram Chandrasekaran[a, b], Chris Bowen[c*], James Roscow[c], Yan Zhang[c*], Dinh Khoi Dang[a], Eui Jung Kim[a], RDK Misra[d], Libo Deng[b], Jin Suk Chung[a], Seung Hyun Hur[a*]

[a]School of Chemical Engineering, University of Ulsan, Daehak-ro, 102, Nam-gu, Ulsan 680-749, South Korea

[b]College of Chemistry and Environmental Engineering, Shenzhen University, Shenzhen 518060, China

[c]Department of Mechanical Engineering, University of Bath, BA2, 7AY, Bath, UK

[d]Department of Metallurgical, Materials and Biomedical Engineering, University of Texas at El Paso, USA.

*Corresponding authors:

Prof. Chris Bowen: c.r.bowen@bath.ac.uk; Dr. Yan Zhang: Y.Zhang2@bath.ac.uk

Prof. Seung Hyun Hur: shhur@mail.ulsan.ac.kr

Abstract

This comprehensive review focuses on recent advances in energy harvesting of micro-scale and nano-scale generators based on piezoelectric and triboelectric effects. The development of flexible and hybrid devices for a variety of energy harvesting applications are systematically reviewed. A fundamental understanding of the important parameters that determine the performance of piezoelectric, triboelectric and hybrid devices are summarized. Current research directions being explored and the emerging factors to improve harvester functionality and advance progress in achieving high performance and durable energy conversion are provided. Investigations with regard to integrating flexible matrices and optimizing the composition of the piezoelectric and triboelectric materials are examined to enhance device performance and improve cost-effectiveness for the commercial arena. Finally, future research trends, emerging device structures and novel materials in view of imminent developments and harvesting applications are presented.

Keywords: micro generator, nanogenerator, piezoelectric, triboelectric, energy harvesting, blue energy.

ACCEPTED MANUSCRIPT

1. Introduction

There are a variety of ambient energy sources in the environment, including mechanical, thermal, chemical, electromagnetic and solar energy, which have a wide range of energy densities. As the size and power consumption of electronic devices continues to shrink, harvesting energy from the surrounding environment to power such systems is a promising approach to provide autonomous devices. In this context, a wide range of energy harvesting materials and mechanisms has been considered thanks to the initial discovery of piezoelectricity. The development of nanostructured piezoelectric materials, however, is a relatively recent development and the understanding of nanoscale effects on ferroelectric and piezoelectric properties continues to be formulated, along with novel fabrication methods and new applications [1-3].

Mechanical energy, in contrast to a number of other energy sources, is almost ubiquitously available. However, the frequency and amplitude of the mechanical vibrations in the environment is often highly variable [4]. Therefore, it is essential to find appropriate energy harvesting methodologies that have a tolerance for variable environments; this is in contrast to traditional cantilever based resonators [5, 6] based on a fixed frequency electrical generator [7]. In 2001, Glynne-Jones et al. [8] proposed a "piezoelectric vibration-powered microgenerator" and in 2006 a new ZnO piezoelectric nanogenerator (PENG) technology was advanced by Z. L. Wang et al. [9]. The PENG converts random mechanical energy into electric energy and has the potential to operate in a wide frequency and motion range. Piezoelectric nanomaterials, such as ZnO, $BaTiO_3$ and lead zirconate titanate (PZT), have the ability to transform mechanical energy to electrical energy, and vice versa. ZnO nanostructures have attracted attention as functional elements for nanogenerators due to their

ACCEPTED MANUSCRIPT

advantages such as high transparency, lead-free chemical composition, ease of nanostructure design, chemical stability and potential for exploiting their combination of semiconducting and piezoelectric properties [10-13]. After the first nanogenerator (NG) was demonstrated in 2006 [9], numerous designs with a variety of nanostructures and architectures have been reported for the efficient conversion of mechanical energy into electric energy, principally by the use of either piezoelectric [14] and triboelectric effects [15-17].

More recently, nanogenerators with an additional function of mechanical flexibility have been developed that are promising in offering energy generation solutions for compliant and stretchable electronics, [12, 18-21] whereby the flexible nanogenerators consist of piezoelectric nanowire or nanorod arrays that are sandwiched between two electrodes formed on flexible substrates. Flexible electronic devices are attracting significant attention because of their promising applications in several research areas, such as bendable LED displays [22-25], self-powered wearable electronics [26-30] and artificial skins [31-34], although progress is somewhat limited due to the need to also simultaneously develop flexible power storage and delivery systems [28]. Such flexible devices must have the ability to bend, fold, twist and stretch, and provide harvested mechanical energy, whilst also maintaining their electronic and structural integrity across a relatively harsh working environment. To date, significant research effort has been devoted to improving the performance of flexible nanogenerator devices in order to broaden their range of potential applications and operating conditions [12, 28, 35].

The functioning mechanism of piezoelectric nanogenerators can be generally described as a transient flow of electrons driven by a piezoelectric potential [36, 37]. Piezoelectric materials have non-centrosymmetric crystal structures and their centers of

ACCEPTED MANUSCRIPT

positive charge and negative charge are under mechanical stress, as shown in **Fig. 1**. As piezoelectricity arises from the arrangement of the crystal structure, these materials can be reduced in size and assimilated into nanoscale devices whilst retaining their functional properties. Recently, both rigid and flexible nanogenerators have been constructed from one-dimensional piezoelectric and/or ferroelectric nanostructures [37]; these include wurtzite ZnO thin films [38], perovskite lead zirconate titanate (PZT) nanofibers [39], $BaTiO_3$ [40], InN nanowires [41-43], $NaNbO_3$ [44], $ZnSnO_3$ microbelts [45, 46], CdTe [47], CdS [48, 49], ZnS [50, 51], GaN nanowires [52, 53] and polymers based on PVDF [54], along with composite systems. When the piezoelectric structures are distorted via a mechanical load, such as a human motion, acoustic waves, wind or machine vibration, the process of charge separation develops a piezoelectric potential that induces an electric current for driving low power electronics. One of the primary applications for nanogenerators is self-powered systems, which harvest energy from the working environment and convert it into electricity to achieve maintenance-free and autonomous operation of a system. In addition, the harvesting materials can also act as a sensor element, whereby an electrical signal is generated [55] when activated by a mechanical or thermal excitation.

This review provides an emphasis on recent developments on manufacturing methods, applications and advancements of self-powered energy harvesting systems, which includes piezoelectric nanogenerators (PENGs), triboelectric nanogenerators (TENG) and flexible hybrid nanogenerators (FHNGs). The wide-ranging applications of these nanogenerators are described. Finally, perspectives of future directions for the technology of energy harvesting nanogenerators are discussed.

2. Pre-2006. Piezoelectric micro-generators

ACCEPTED MANUSCRIPT

The piezoelectric material chosen for an energy harvesting application can have a major impact on the harvesting device functionality and performance. To date, a number of piezoelectric materials have been developed for micro-scale and nano-scale generator applications. The most common type of piezoelectric used in energy harvesting is lead zirconate titanate (PZT), which is a ferroelectric ceramic. Although PZT has been widely used as a harvesting material since the early 21st century, the brittle nature of the material limits the maximum strain that can be achieved without fracture. Images of traditional bimorph and unimorph structures used to create piezoelectric energy harvesters are shown in **Fig. 2(a)**. Kong et al. [56] introduced atomic force microscopy (AFM) as a tool for surface mapping features with a resolution of less than 10 nm, as shown in **Fig. 2 (b)**, and we will see later in this review that this is an important tool for characterizing piezoelectric nanowires and nanorods. This method provides the possibility of incorporating both electronic drive and sensing circuitry into the microprobe for multichannel AFM systems for piezoelectric measurements at the nanoscale. In 1999, Beach et al. [57] deduced the piezoelectric field and charge distribution for numerous III-nitride hetero-structures, as shown in **Fig. 2 (c)**. Their findings included the impact of doping effects and strain energy minimization for piezoelectric effects in strained layers. Later, the structure and micro-fabrication of a novel micro-scanning force microscopy (SFM) device were advanced by Chu et al. [58], which is presented in **Fig. 2(d)**.

Likewise, piezoelectric-fiber based energy harvesting materials were also investigated by Churchill et al. (2003) [59] who examined composites based on unidirectional aligned PZT fibers of 250 µm diameter embedded in a resin matrix. When a 0.38 mm thick sample of 150 mm length and 13 mm width was subjected to a 180 Hz vibration at a strain

ACCEPTED MANUSCRIPT

level of 300 με, the composite could harvest ~7.5 mW of power. The results of this study show that a relatively small fiber-based piezoelectric power harvester could generate sufficient power for wireless transmission. Finally, the single bridge piezoelectric device exhibited sensitivities of 0.32 nA/nm and 70-80 nm/V in a vertical direction and a lateral direction respectively. Moreover, Mohammadi et al. [60] fabricated PZT fibers of different diameters (15, 45, 120, and 250 μm) that were aligned, laminated and molded into an epoxy. This led to flexible composites with 40 vol.% of aligned piezoelectric fibers. A number of samples were made in which several 34 mm × 11 mm rectangular plates of a range of thicknesses (1.2-5.8 mm) were diced to form a composite with fibers oriented in the plate thickness direction. The output voltage of the composites was determined by dropping a 33.5 g weight on them from a height of 10 cm. A maximum voltage of 350 V and output power of 120 mW was produced for the thickest transducer, 5.85 mm thick, with the smallest fiber diameter of 15 μm and it was determined that thicker plates had the ability to achieve larger fiber displacements, and that samples with smaller diameter fibers had the highest piezoelectric coefficient (d_{33}) and lowest dielectric constant, both of which contributed towards the composite achieving greater power outputs and higher efficiency systems.

In 2005, Lee et al. [61] reported on the susceptibility of piezoelectric ceramics to fatigue crack growth when exposed to high frequency cyclic loading, which indicates a potential limitation of the materials for high strain/bending applications. In order to eliminate these disadvantages of piezoelectric ceramic materials and increase their efficiency, researchers have developed more flexible piezoelectric materials that can be used in energy harvesting applications [62]. For example, Mossi et al. (2005) [63] created a unimorph pre-stressed bender. This is an initially curved, arc-shaped, rectangular piezoelectric device that

ACCEPTED MANUSCRIPT

stretches when a force is applied to the top of the arc. Elongation of the device results in a strain in the active material, which creates a potential difference across the device. The device was simply supported, allowing for movement in the lateral direction. While these devices were typically used as actuators, Kymissis et al. (1998) [64] and Yoon et al. (2005) [65] revealed that they were also capable of generating useable energy as harvesters. The properties of the pre-stressed devices with varying different physical parameters were detailed in their study [64, 65] and it was reported that larger dome heights lead to larger strains and energy generation when the harvester was compressed; therefore, the thickness and type of the metal used to create the dome can affect the power harvesting performance of the device and should be optimized. In addition, the power harvesting capability of the device was increased by increasing the electrical conductivity of the adhesive layer between the passive metal layer and the piezoelectric material. This was achieved by the addition of metallic particles of nickel to the adhesive, which led to a 15% increase in the harvested energy. Danak et al. (2003) [66] also examined a method to enhance the energy harvesting performance of an initially curved PZT unimorph. A model was developed that predicted the relationship between generated charge and initial dome height, substrate thickness, PZT thickness, substrate stiffness and the power output of the device. It was identified that increasing the dome height offered the greatest increase in charge output and increasing the substrate and PZT thickness both lead to a higher charge output. However, increasing the substrate thickness had a greater influence compared to increasing the thickness of PZT; increasing the stiffness of the substrate could also generate more piezoelectric charge.

3. Post 2006: Piezoelectric nanogenerators

After 2007, there was significant attention on using one-dimensional (1D)

ACCEPTED MANUSCRIPT

piezoelectric nanostructures (PZT, $BaTiO_3$, ZnO, PVDF, CdS, GaN, etc.) for mechanical energy harvesting [67, 68]. Lin et al. (2013) [19] reported on the high output power density of their prototypes of ~5.3 mW cm^{-2}. Moreover it was identified that, due to substrate coupling effects, piezoelectric thin films may exhibit reduced piezoelectric coefficients [69, 70].

One dimensional (1D) nanomaterials, such as nanorods (NRs) and nanowires (NWs), are usually defined as having a length more than ~ 1 μm with a diameter less than 100 nm [71] and tend to be in single crystal form [72]; typically NRs have a lower aspect ratio than NWs [73]. Using piezoelectric 1D nanomaterials for mechanical energy harvesting is reported to have three benefits [68]: (i) when a strain gradient is experienced by a ferroelectric with a thickness of a few tens of nanometers, it exhibits ~ 400-500% improved piezoelectric effects as a result of flexoelectric effects due to the presence of a strain gradient; (ii) the lattice perfection of 1D materials provides improved mechanical properties that leads to superior critical strain, greater flexibility and extended operational lifetime, and (iii) 1D materials exhibit high sensitivity to a small force due to the small thickness and large aspect ratio that allows the formation of significant strain in nanowires under a mechanical load at the nano- or pico-Newton level. When a piezoelectric nanowire is deflected, an electric potential can be produced on the side surfaces due to distortion of the crystal lattice. For ZnO based NWs, the surface under tension provides a positive potential while a negative potential is generated on the surface under compression. In 2007, Gao and Wang [38] reported calculations of the potential distribution in a ZnO NW and stated the NW acted as a parallel plate capacitor. A ZnO NW with a diameter of 50 nm, a length of 600 nm, was bent by 145 nm at the tip by an 80 nN lateral force. Numerical modeling indicated that the maximum piezoelectric potential at the NW surface was directly proportional to the lateral displacement

ACCEPTED MANUSCRIPT

of the NW and inversely proportional to the length-to-diameter aspect ratio of the ZnO NW.

Initial investigations of the piezoelectric effect in NRs were obtained by straining a single nanorod with a conductive AFM. In 2006, the first study by Wang and Song [9] used nanorods of ZnO grown on a sapphire substrate via a vapor-liquid solid (VLS) method. This led to gold particles being left behind on the tip of each rod after catalyzing their growth, which provided a good electrical contact between the conductive AFM tip and the tip of the nanorod. Wang and Song hypothesized [68] that the Schottky barrier, namely the electronic potential energy barrier at a metal-semiconductor interface, formed between the ZnO and gold was important in producing a quantifiable output voltage, which was ~ 10 mV. They suggested that the stretched side of the rod had a positive potential, leading to a reverse bias with the Schottky junction so that no current might flow to screen the polarization [68]. On the compressed and negatively polarized side of the rod, the junction was forward biased and thus current can flow to screen the polarization. This means that the metal–ZnO contact creates a Schottky barrier that ensures the charge recuperation for piezoelectric charge-generation. Thus, Schottky contacts among the metal and ZnO are a key factor to the generation of current by NGs. An investigation of the piezoelectric output from individual ZnO nanorods was undertaken by straining a nanorod within a TEM so that the electrical output and structural changes could be directly inspected [1, 74, 75]. Such work offered more reliable results, compared to AFM, as the nanorod is physically bonded to the electrodes. However, careful use of the measurement method is still required as the reported current generation under static strain is not possible from the piezoelectric effect and implies that a small bias is present in the measurement system [76]. The reader is referred to the following papers for further discussion of the measurement system [14, 77].

ACCEPTED MANUSCRIPT

To support the experimental investigations of the piezoelectric output from strained nanorods, several theoretical models have been developed [21, 38]. For instance, Gao et al. [38] calculated the potential difference that would be produced across a bent nanorod. However, this neglected the impact of free carriers in ZnO, which were important in determining its overall effective piezoelectric properties, and therefore was later added to the model by the same research group [21], which confirmed that the free carriers lead to a non-symmetrical distribution of potential. Numerous advanced investigations of nanogenerators have included computational models of a strained nanorod, which often generated similar asymmetric distributions.

Recently, an integrated nanogenerator based on vertically aligned ZnO NWs has been reported. The peak open-circuit voltage and short circuit current were ~ 37 V and ~ 12 μA, respectively, from a 1 cm^2 nanogenerator [78]. The same research group also reported vertically aligned NW ZnO arrays that were sandwiched between two metal electrodes, as shown in **Fig. 3(a)**. Solidified PMMA was used to encapsulate the ZnO NWs and prevented them from making close contact with the top metal electrode [79]. The mechanism of the nanogenerator operation depended on the piezoelectric potential created in the ZnO NWs from an external strain [80]; dynamic straining of the NW exhibited a transient flow of electrons in the external load because of the driving force of the piezo-potential. The proposed benefit of using NWs was that they could be triggered by small physical motions and the excitation frequency can be a few Hz to several MHz, which is useful for random energy harvesting in the environment such as from small vibrations, body motion and air flow that are typically low frequency.

3.1 Recent advancements in fabrication of piezoelectric nanogenerators

ACCEPTED MANUSCRIPT

Several methods have been used to fabricate piezoelectric nanogenerators. In 2013, Suo Bai et al. [81] reported on the fabrication of 2D woven nanogenerators. During the assembly process, two types of fiber were woven together on the surface of a wooden block and slider, which served as a substrate. This approach imitated the woven structure of a textile and was composed of two kinds of fibers crossing each other, one type being ZnO nanowires and the other type were ZnO NWs coated with palladium (Pd) on their surface. Depending on the coupling of the piezoelectric and semiconducting properties of ZnO, it was possible to generate electricity from small external mechanical energy sources, such as wind and sound. The open-circuit voltage and short-circuit current of the woven NG were 3 mV and 17 pA, respectively. Moreover, the woven NG was used to power a microfiber/ZnO NWs hybrid UV sensor to form a wearable self-powered system, which could quantitatively sense UV light intensity [82].

The chemical vapor-phase growth method provided good electrode contact by leaving Au particles on the tips of the nanowires [83]; however, this was not well-matched to operation with plastic substrates, which were preferred for low-cost and flexible energy harvesters [84, 85]. As a result, this technique was superseded by using a hexamethylenetetramine-zinc nitrate growth method where a seeded substrate was employed in an equimolar (0.01-0.1 M) mixture and heated to 90 °C for 4 h to grow aligned ZnO nanorods on the substrate surface [86]. Later, this method became the dominant technique for ZnO nanorod growth and was used in the majority of ZnO nanogenerators [87, 88]. The approach was first validated for nanogenerator fabrication soon after the original report of the growth of ZnO nanorod arrays on polyimide substrates, such as Kapton. In this study, the nanorods were mechanically stabilized by spin-coating a poly(methyl methacrylate) (PMMA)

ACCEPTED MANUSCRIPT

solution between the nanorods, a method that became common in later devices [89].

Wang et al. [11, 68] fabricated the first prototype nanogenerator using a Pt-coated serrated electrode with vertically aligned ZnO NWs that were able to convert ultrasonic waves into electricity. The aligned ZnO NWs arrays were covered by a serrated silicon electrode coated with platinum, which were reported to enhance electrode conductivity and formed a Schottky contact at the interface with ZnO NWs. The ZnO NWs were grown on GaN substrates and the top electrode was composed of parallel serrated trenches fabricated on a (001) plane silicon wafer and coated with a thin layer of Pt. Some NWs were in direct contact with the top electrode, but some were positioned between the teeth of the electrode. Under the application of ultrasonic waves, the top electrode moved downward onto the ZnO NW, thereby leading to a lateral bending. The bending-induced piezoelectric potential was collected through the Pt film when the Schottky junction between the NW and Pt electrode was forward biased.

Recently, a number of devices have been fabricated using 'zig-zag' types electrodes, including those designed with gold-coated ZnO nanorods [90] . This pattern allowed the nanorods to be strained while fixed to a rigid substrate; this was particularly useful before flexible substrates became more common. In addition, other fabrication methods were also demonstrated to enable strain of piezoelectric arrays on rigid substrates [91]. By in-filling the nanorods with a polymer, such as PMMA, and exposing their surface using oxygen plasma etching, devices were made that converted compressive loads into electricity. The open-circuit voltage of these devices was ~ 80-100 mV with a short-circuit current density of 4-9 nA cm^{-2}. Later, the voltage generation was increased to over 300 mV by leaving ~1 μm of PMMA on top of the nanorods before coating with a gold electrode. This was developed into

ACCEPTED MANUSCRIPT

a device consisting of a ZnO array on silicon. When compressed with a linear motor, the device produced an open-circuit voltage of ~ 37 V after rectification through a bridge rectifier, and a higher short-circuit current density of 12 μA cm^{-2}. By connecting a number of nanogenerators in parallel, the authors were able to use the output to charge a capacitor to store the harvested energy, which will be discussed below in terms of the applications of nanogenerators.

In addition to efforts on ZnO nanorods, PZT-based nanorods have been fabricated using hydrothermal methods [92] by heating aqueous chemical precursors in a pressure vessel at 230 °C for 12 h on epitaxially-matched doped strontium titanate substrates. The Ti/Pt upper electrodes on silicon were pressed onto the top surface through which pressure was applied to produce voltage peaks of ~ 0.7 V and a current density of ~ 4 μA cm^{-2}. The PZT nanofibers [39], with a diameter and length of ~ 60 nm and 300 μm on a silicon substrate, produced an output voltage of approximately 1.63 V and the generated power under a periodic stress was 0.03 μW, as shown in **Fig. 4(a)**. In addition to PZT [92], barium titanate ($BaTiO_3$) is increasingly being used for energy harvesting and in 2014, Zhou and Sodano [93] developed an energy harvesting device using 1 μm long and 90 nm wide $BaTiO_3$ nanorods that were produced using a two-step hydrothermal procedure, whereby hydrothermally grown TiO_2 nanorods on a conductive fluorine-doped tin oxide (FTO) substrate were submerged in a Ba^{2+} solution to convert them to $BaTiO_3$, as shown in **Fig. 4(b)**. The nanogenerator devices were vibrated using a shaker table at 1*g* (9.8 m s^{-2}), achieving a peak-to-peak open-circuit voltage of ~ 623 mV, and a short-circuit current density of ~ 9 nA cm^{-2} with a power density of 6.27 μW cm^{-3} with a 120 MΩ resistive load. This was compared to ZnO nanorod-based devices tested, which produced 85 mV, 1.58 nA cm^{-2} and 0.4 μW cm^{-3} on a 50 MΩ load. The

ACCEPTED MANUSCRIPT

$BaTiO_3$ devices produced around 16 times more power than the ZnO rod-based device, which was credited to the higher electromechanical coupling coefficients of $BaTiO_3$ compared to ZnO, signifying the potential for $BaTiO_3$ as a lead-free piezoelectric alternative to PZT.

Recently a facile, lightweight, flexible, and cost-effective Er^{3+}- and Fe^{3+}-ion-doped PVDF-based piezoelectric nanogenerators (PENGs) were prepared via a simple solution casting method [94]. The established PENGs exhibited excellent energy-harvesting performance with a power density of ~160mW cm^{-3} and ~53.24 mW cm^{-3} under periodic finger loading of the Er^{3+}- and Fe^{3+}-stimulated PVDF film-based energy-harvesting arrays, respectively. The prepared self-powered PENG was also able to light up 54 commercially available light-emitting diodes.

3.2 Future prospects for piezoelectric nanogenerators

Piezoelectric nanogenerators have been intensively studied in order to increase the energy conversion efficiency and the power density of active materials. Studying the impact of nanowire and/or nanorod-metal Schottky contact on the energy harvesting properties is of importance to understand the overall improvement of the nanogenerator device performance. In this aspect, recent studies of nanostructured materials for energy harvesting, such as GaN nanowires, have also been undertaken [95], as shown in **Fig. 3(b)**. This demonstrated the impact of the GaN nanowire-Schottky metal nano-contact on the energy harvesting efficiency and three different metal nano-contacts of diamond, PtSi and Pt/Ir, were examined. Finally, the nanogenerator with platinum-based Schottky nano-contact produced a high piezoelectric energy and this was ~2.4 times higher than that of diamond-based contact.

By using piezoelectric materials, various types of energy harvesting devices have been explored, as highlighted thus far, with the aim to realize self-powered electronic devices

ACCEPTED MANUSCRIPT

such as mobile electronics and implanted medical devices. However, there are some challenges to be overcome for their use in these applications. Firstly, the output power of the piezoelectric energy harvesters is often low, i.e. between 1-5 μW, as seen from the power levels reported to date, thereby limiting their range of applications. Secondly, the energy harvester has to be durable to endure long-term exposure to vibrations. Thirdly, large scale and low-cost fabrication is desired. Finally, when energy harvesting from portable devices, they should be able to work under small mechanical stress levels such as small movements of body, heart, finger, i.e. there is a need to demonstrate a high sensitivity. To date, a limited number of energy harvesters are currently able to fulfill all of these requirements. In this regard, and in order to address the above issues, the research community has also focused on another type of energy harvester, termed as the triboelectric nanogenerator (TENG).

4. Triboelectric nanogenerator (TENG)

An early version of the triboelectric generator was a mechanical device that created static electricity or high voltage by contact charging. The most famous devices were the Wimshurst machine (circa 1880) and van de Graaff generator (circa 1929). Both instruments use accumulated static charges that are created by tribo-electrification, whereby tribo-charges are transferred from a rotating belt to a metal brush by corona discharging; e.g. the electric-field-induced arching or air. Once the accumulated charge density reaches a critical value, discharge over two opposite electrodes occurs. The traditional triboelectric generator is a high voltage source and there is no electric current apart from the discharging process. Although the triboelectric effect has been known for many years, the essential fundamental understanding of the process was relatively limited until recently. As with the piezoelectric effect, the triboelectric effect can be utilized to convert mechanical energy into electricity,

ACCEPTED MANUSCRIPT

however, the mechanism differs since it relies on contact-induced electrification in which a material is electrically charged after it makes contact with a different dielectric material through contact friction. The polarity of the induced charge depends on the relative polarity of the two materials in frictional contact with one another, with respect to the triboelectric series [17, 96, 97]. For a triboelectric nanogenerator reported in 2012 [98], the area power density of a single nanogenerator device reached ~500 Wm^{-2}, the volume power density reached ~15 MW m^{-3} and an instantaneous conversion efficiency of ~70% was achieved. The high output of the TENG makes it promising not only for common electronic devices but it is also being considered for large-scale energy from wind and ocean waves [88].

Based on the four types of triboelectric harvesting device geometry [99], as shown in **Fig. 5**, it is possible to fabricate various types of TENGs depending on specific technological applications [96]. These methods are the fundamental units for offering micro-scale power for small and smart electronic devices,and their assembly and integration could be the basis for harvesting large-scale energy. The TENG offers a different approach for harvesting mechanical energy compared to piezoelectric devices by using organic and inorganic materials. An energy conversion efficiency of 50-85% has been demonstrated and an output power density of 1200 W m^{-2} has been realized [96, 100]. TENGs can be used as a micro-scale power source for mobile and portable electronics [100] and an example of their potential to harvest energy higher power levels from the ocean and wind is shown in **Fig. 6**, which was proposed as a new field of 'blue energy' [96]. In 2016, Yong et al. [101] demonstrated harvesting wind via using a wind-rolling triboelectric nanogenerator (WR-TENG), as shown in **Fig. 7 (a)**. A single component of a WR-TENG produced an open-circuit voltage of ~ 11.2 V and a short circuit current of ~ 1.86 μA. In addition, the WR-

ACCEPTED MANUSCRIPT

TENG can be used as a sensor for self-powered wind velocity measurement as well as harvesting energy. Moreover, a facile and low cost technique was used to fabricate a triboelectric nanogenerator (NG) with a high electric output of ~ 1.2 W to an external load has been proposed [102], as shown in **Fig. 7 (b)**, in which a human palm can generate maximum short-circuit current of 2 mA, delivering 1.2 W to an external load. The output power density achieved was ~ 313 Wm^{-2} with a volume power density of ~ 54268 Wm^{-3}, an open circuit voltage ~ 1200 V and a maximum energy conversion efficiency of ~ 14.9%. This higher power was mainly due to the optimized nanogenerator device structure, appropriate materials selection and their surface modification. The operational mechanism revealed in this work was proposed to be useful in achieving large-scale mechanical energy harvesting from sources such as rolling wheels, wind power and ocean waves.

In 2012, Fan et al. [98] reported a simple and cost-effective all-polymer based triboelectric nanogenerator for mechanical energy harvesting, using a combination of tribo-electrification and electrostatic induction. The TENG device was formed by two polymer films, with dissimilar electron attracting abilities, and metal films deposited as electrodes. When the two polymer films are in contact, there is mechanical friction due to the natural nanoscale surface roughness, which generates equal and opposite charges on the contacting surfaces the films, thus, producing an electric potential at the interface. As the two films contact and separate, an alternating potential leads to electrons in the external load flowing back and forth. Such a polymer TENG yielded an output voltage of up to 3.3 V and a power density of 104 $\mu W\ cm^{-3}$. In addition, the output electric signals of the TENG also revealed the influence of mechanical triggering, so that the TENG device can be used as an active sensor. Whilst some conventional sensors require an external power source, TENG sensors

ACCEPTED MANUSCRIPT

provide an output electric signal without the need to supply an input power to the sensor tip. The TENG sensor has been used for sensing of vibration, motion, people and contact with objects [98].

Zhang et al. (2013) [103] fabricated a sandwich-shaped TENG where an aluminum film was placed between two polydimethylsiloxane (PDMS) membranes to achieve frequency multiplication by two contact electrification during one cycle of external force. In addition, the inclusion of micro/nano dual-scale structures (i.e., pyramids and V-shape grooves) on the upper PDMS surface was employed to enhance device performance. Owing to the bi-triboelectrification effects among the three layers, this sandwich-shaped TENG generated two triboelectric outputs under the external force in a single mechanical cycle. A peak output voltage of 465 V, current density of 13.4 $\mu A \cdot cm^{-2}$ and energy volume density of 53.4 $mW \cdot cm^{-3}$ were achieved. In addition, the nanogenerator was used to light up five commercial light-emitting diodes (LEDs) and drive an implantable 3-D microelectrode array for neural prosthesis without any energy storage unit. Recently, TENGs have received more attention due to their large efficiency for energy conversion and high output; these include reduced graphene oxide nanorods (rGO NRs)/PVDF [104] (**Fig. 8 (a)**), radial-arrayed rotary electrification [105] (**Fig. 8 (b)**), anti-reflection coated transparent TENG [106] (**Fig. 8 (c)**), smart floor with integrated TENGs [107] (**Fig. 8 (d)**), rotating TENG for water electrification [108] (**Fig. 8 (e)**), self-powered wind vector TENG sensor [109] (**Fig. 8 (f)**), hydropower harvesting TENGs [110] (**Fig. 8 (g)**) and hybridized blue energy and wind energy harvesting TENGs [111] (**Fig. 8 (h)**).

Over 70% of the Earth's surface is ocean and therefore represents a significant energy resource; for example, harvesting wave energy is of significant interest. TENG

ACCEPTED MANUSCRIPT

devices have the potential to be more suitable than electromagnetic generators (EMG) for wave energy harvesting in the frequency range of < 5 Hz, which is well suited for our daily life, the ocean and nature. However, the EMG approach is more effective at frequencies above 5 Hz although it can heavy, more costly and difficult to be installed in sea floor or at water surface for collecting the water wave energy [112]. Z.L. Wang suggested an idea of using TENG systems for wave harvesting; in this case the TENG was prepared using mostly organic materials and it was partially filled up with air, so that a network was created based on a large number of TENGs in the form of a fishing net that would flow at the vicinity of the water surface for water motion energy harvesting (2014) [96]. Wave motion could be used to drive the TENG to achieve contact-separation and sliding motion, so that the mechanical energy could converted into electrical power. The initial approximation determined that the power that could be produced is ~1 MW km^2, which could be multiplied by at least 10 based on future progress in material and structure design [96], although a number of challenges remain. The benefits offered by TENG systems are low-cost, small size, independent of day, night or weather and there are no significant safety concerns. A detailed comparison with existing methods for harvesting wave energy is also worthy of investigation.

Yufang Li et al. [113] introduced a single-electrode-based rotational triboelectric nanogenerator (SR-TENG) formed by two wheels and a belt for harvesting mechanical energy. Initially, four 1 -thick PMMA sheets were treated by laser cutting to form the two wheels. One wheel was connected to a rotational motor while another wheel surface was covered with a layer of PDMS and the elastic properties of PDMS enabled complete contact between the two tribo-surfaces. On top of the PDMS layer, half of the wheel was protected by an aluminium film and the other half overlaid with PTFE film. The wheel with PDMS was a

ACCEPTED MANUSCRIPT

rotatable wheel and a PTFE belt. The PTFE belt acted as a triboelectric polymer, while the Al film had the dual role of acting as a triboelectric layer and an electrode. Two working modes, the continuous discharge (CD) mode and the instantaneous discharge (ID) mode were demonstrated for the SR-TENG. The peak current of the SR-TENG with ID mode was ~ 20 μA, where the external load was ~ 10 MΩ, which was 33-times higher than short-circuit current peak of the SR-TENG in the CD mode. In addition, the SR-TENG with ID mode acted as a self-powered sensor for detecting the centrifugal angle of a rotating wheel and 20 LEDs were powered by the SR-TENG when the rotating speed was 1100 rpm. Recently, a TENG has also been used as a self-powered sensor for detecting static and dynamic processes arising from mechanical agitation using the voltage and current output signals of the TENG, with potential applications such as mechanical sensors, touch pads and smart skins (artificial skins).

The previous sections have overviewed piezoelectric and triboelectric approaches to energy harvesting. We will now examine attempts to make such devices flexible.

5. Flexible nanogenerator devices

5.1 Flexible piezoelectric nanogenerators

Large numbers of nanostructured energy harvesting devices have recently been produced using materials other than ZnO, such as PZT and barium titanate ($BaTiO_3$). Most of these nanogenerator devices resemble micro-electro-mechanical systems (MEMS) devices and their fabrication often involves a number of micro-fabrication procedures such as photolithography, etching, and lift-off. As previously discussed, even though devices produced on rigid substrates yield the highest output powers, the use of ZnO nanorods on flexible substrates is beneficial for the realization of flexible devices. As will be detailed in

ACCEPTED MANUSCRIPT

this section, nanorods can be readily grown in aligned arrays on flexible substrates. This provides the potential to strain the devices by bending the substrate, rather than being limited to only collecting energy from vibrations, or direct compression of the active material.

5.1.1 ZnO-based flexible piezoelectric device

In 2009, Choi et al. [114] demonstrated the use of a low temperature zinc nitrate-hexamethylenetetramine (HMT) growth approach to produce nanorod arrays on a flexible conductive indium-tin oxide (ITO)-coated polyethersulfone (PES) substrate. In this study, upper electrodes based on the same substrate, with and/or without a Pd-Au coating, were pressed onto the nanorod arrays. By using a Pd-Au coating higher outputs were produced, achieving the current density of 10 μA cm^{-2} when compressed by 0.9 kg force. These enhancements in performance were credited to the Schottky barrier formed by the Pd-Au. In this experimental investigation, despite testing the entire array on a flexible substrate, the substrate was not flexed at any point to strain the nanorods. However, the same group later reported similar devices with other upper electrodes based on carbon nanotubes or graphene, where the entire device was subjected to bending; this produced a lower current density output of ~ 5 and ~ 2 μA cm^{-2}, respectively.

ZnO NW-based nanogenerators can be formed on a wide-range of flexible substrates, such as metals, polymers and even curved substrates [115, 116]. Fiber-based nanogenerators have been developed for the conversion of vibration or mechanical energy into electricity using piezoelectric ZnO NWs radially grown around textile fibers (**Fig. 9**). The complete structure of the device was similar to a brush-to-brush assembly [30, 116], where one brush consisted of ZnO nanowires, while the metal nanowires acted as an additional brush. A cyclic relative sliding motion between the two nanofibers harvested power due to the deflection and

ACCEPTED MANUSCRIPT

bending of the ZnO nanowires. A prototype fiber-based nanogenerator exhibited advantages in the construction of a flexible, adjustable and wearable power source for smart clothing applications. Recently, Lee et al. [30, 117] produced a hybrid fiber based piezoelectric generator composed of ZnO NWs and a polymeric poly(vinylidene fluoride) (PVDF) coating on a conducting fiber to transform low-frequency (<1 Hz) mechanical energy into electrical power. By attaching this nanogenerator device to a human arm, the folding-releasing motion of the elbow could develop a voltage output of ~ 0.1 V, current density ~ 10 nA cm^{-2} and power density of ~ 16 μW cm^{-3}. This method revealed the improved performance and feasibility of the harvester as a power source for wearable electronic devices. Similarly, Li et al. [117] created a fiber nanogenerator based on carbon fibers that were cylindrically covered by textured ZnO thin films to form a flexible device. The ZnO film created a macroscopic piezo-potential across its inner and external surfaces, driving an electric current in the external load, where an output voltage of ~ 3.2 V and average current density of 0.15 μA cm^{-2} were obtained. The fiber based nanogenerator performed as a sensor to monitor the human heartbeat and was therefore of interest for use in medical diagnostic sensors and measurement apparatus.

Recently, Lu et al. [118] fabricated micro- and nano-structured piezoelectric fibers using thermo-plastic nanocomposites and the fibers exhibited a high output voltage of ~ 6 V under bending, as shown in **Fig. 10 (a)**. In addition, Yang et al. [119] demonstrated that ZnO nanowires can be used in flexible nanogenerators. In their work, the piezoelectric ZnO nanowires were fixed at both ends to electrodes and laterally packaged on a flexible substrate. Substrate bending produced a uniaxial tensile strain in the ZnO nanowire, leading to a piezoelectric potential along the wire that drives electrons to flow along the external circuit. A

ACCEPTED MANUSCRIPT

repeating bending-releasing progression of the ZnO nanowire (NW) in the PENG generated a pulsed and alternating current signal. The generated open-circuit voltage and short-circuit current were ~ 20-50 mV and ~ 400-750 pA, respectively. This method offers a different approach for biomechanical energy harvesting, for instance from finger movement and the motion or heartbeat of an animal, even if the motion is uneven with mechanical instabilities and fluctuations. For practical technological applications, it is important to enhance the output power of PENGs by integrating large numbers of nanowires in a parallel arrangement on a single flexible display device. Therefore, several lateral nanowire-array-based flexible nanogenerators were fabricated by incorporating 700 rows with each row containing ~ 20,000 lateral ZnO NWs. The entire device exhibited good flexibility and the nanowires were sufficiently strong to inhibit mechanical deformation. When the nanogenerator device was periodically deformed, a maximum voltage of ~ 1.26 V and a maximum current of ~ 28.8 nA were attained.

Combined multiple ZnO NW-based NG devices are possible for fabricating flexible energy harvesters that possess a higher output to power electronic devices. Zhu et al. [120] validated a high-output PENG based on a lateral ZnO NW array by utilizing a sweeping-printing method. Initially, the vertically-aligned ZnO NWs were transferred to a flexible substrate to form horizontally-aligned arrays with a crystallographic alignment. The metal electrodes were then created by conventional photolithographic procedures to connect the NWs together. The consistent growth and position of the NWs led to improved reliability of the piezoelectric potentials and a successful scale-up of the output performance and an open-circuit voltage of ~ 2.0 V and a peak output power density of ~ 11 mW cm^{-3} were observed. In addition, the PENG generated charge was stored into capacitors and utilized to power a

ACCEPTED MANUSCRIPT

commercial light-emitting diode (LED), demonstrating its potential in applications for low power electronic devices. However, the fabrication method was based on photolithographic tools, which was a complex process and limits the potential of PENGs for scale-up. To address this difficulty and improve the output energy performance, Hu et al. [121] developed a new PENG based on a composite assembly by simply dispersing conical ZnO NWs onto a flat polymer film. Owing to the piezoelectric potential superposition of each conical NW, the device produced a macroscopic induced potential difference between the top and bottom electrodes when subjected to mechanical deformation. The output voltage was ~2 V and current of ~50 nA, which can drive small industrial electronic devices, such as liquid crystal displays (LCDs). The proposed flexible PENG is a facile, low-cost, and scalable technology for small personal electronics and self-powered systems.

The use of different nanogenerator materials and fabrication methods for a range of device designs has been demonstrated. For example, devices have been demonstrated by using ZnO nanorods aligned laterally and vertically along a flexible substrate. Xu et al. [122] fabricated partially-covered strips of a seed layer so that the ZnO nanorods grew laterally, rather than perpendicularly to the substrate using lithographic methods. This fabrication method has a number of complex steps, although it led to the formation of well-organized set of lateral ZnO arrays that were joined in series, creating a high open-circuit voltage of 1.2 V, compared to low potential of 100 mV from a vertically-oriented device made by the same method. The output current density was also higher than the vertical device, at ~15 nA cm^{-2}. A lateral ZnO-based device was later produced using a more simple method of 'wiping' a ZnO nanorod array that was arranged laterally in order to transfer it to a secondary substrate, where alternating gold electrodes were used [122]. Even though this meant that the nanorods

ACCEPTED MANUSCRIPT

were randomly attached to the electrodes, and some of them were not connected the device produced a high open-circuit voltage of up to 2 V and a short-circuit current density of 100 nA cm^{-2} when subjected to bending.

As the use of flexible substrates became more common, the structure of a chemically-grown ZnO, filled with polymer of PMMA with a coated metal (often gold) electrode was examined in a number of research studies [123, 124]. Lee et al. (2011) [55] explored such a ZnO rod structure on a flexible Kapton polyimide substrate. The rods in this case were exposed by removing the PMMA surface by a plasma etching technique before a gold electrode was pressed on top. During bending, the device produced an open-circuit voltage of ~350 mV and short-circuit current density of ~125 nA cm^{-2}. This was increased to 2.1 V by stacking and connecting devices, however, detailed information about the device fabrication and analysis was not included. Later, Hu et al. [125] produced an open-circuit voltage of 10 V by not exposing the nanorod tips but leaving them covered with PMMA. The output voltage was amplified by covering both sides of the substrate with nanorod arrays, but the output current remained at only ~0.6 μA cm^{-2}. This indicates that by increasing the internal impedance of the device it is possible to increase the 'headline' peak open-circuit voltage, however, this may lead to a reduction of the overall output power from the nanogenerator subject to an external load.

It was considered that using a top electrode, such as gold, creates a Schottky barrier with ZnO nanostructures, which was thought to be essential to generate a measureable output from ZnO-based nanogenerator devices [9]. Such a requirement is now extensively considered to be related to screening by electrode contacts [13, 21]. This has also been tailored by addition of an insulating polymer (PMMA) layer, which may reduce screening,

ACCEPTED MANUSCRIPT

whilst also providing a resistive barrier. However, it has been found that using a p-type material as the top electrode contact to create a p-n junction with the nanorods of ZnO can generate higher output signals [126]. A p-type coating had been examined in the early studies of bending of ZnO nanorods using an AFM by functionalizing the surface with a p-type oligomer.

Briscoe et al. (2012) [127] fabricated a ZnO nanogenerator using a p-n junction, where the junctions were formed between n-type ZnO nanorods and the p-type polymer poly(3,4-ethylenedioxythiophene) poly(styrenesulfonate) (PEDOT:PSS) produced on an ITO-coated PET flexible substrate. Finally, the polymer (PEDOT:PSS) layer was coated only at the tips of the ZnO rods, allowing a highly conductive gold electrode to be simply coated on the surface while retaining a high freedom of movement in the ZnO nanorod array. When deformed, this device produced a maximum open-circuit voltage of ~ 10 mV and short-circuit current density of ~13 μA cm^{-2}, which were relatively low output levels. This was increased to ~1 V (open circuit voltage) and 1.88 mA cm^{-2} (current density) with 434 μW cm^{-2} (power density) on an optimum load of 6 kΩ by improving the nanogenerator device structure and reducing screening by conformably coating the ZnO surface with a thin layer of the p-type CuSCN. Although the output voltage generated by this device was lower than many devices comprising PMMA–Au Schottky contacts, it was later shown that by using a more conductive p-type polymer poly(3,4-ethylenedioxythiophene-Tosylate) (PEDOT:Tos) a higher output voltage of 95 mV was produced compared to PEDOT:PSS, which offered 18 mV when strained using an AFM tip [1].

Later, advanced flexible devices were manufactured by growing ZnO nanorods on the surface of 'common paper' as a substrate, which had the significant impact of providing a

ACCEPTED MANUSCRIPT

route to produce large-area flexible devices [128]. Unfortunately, no bottom electrode was employed in this case, hence a small output of 15 mV and 10 nA measured for these devices, which was later increased to 10 V and 600 nA by another group using cloth substrate [28, 128]. However, a nanogenerator device based on a cloth substrate has been described where a silver bottom electrode was coated on the cloth before ZnO growth, the output was tested using an AFM, and thus the flexibility of the cloth was not utilized [28, 128].

The majority of the flexible devices discussed so far have been manufactured on plastic sheets, such as polyimide, polyethylene terephthalate (PET) or polyestersulfone (PES). As previously mentioned, an interesting technological application for flexible nanogenerators is wearable technologies, so that the energy from the wide range of human motion can be captured and used for portable charging of devices. Such potential technological applications have been demonstrated by Qin et al. (2008) [116] using a ZnO nanorod-based energy harvester grown on a Kevlar fiber. The Kevlar fiber was first seeded by sputtering with a ZnO thin film, which then allowed the growth of ZnO nanorods on the surface by chemical synthesis.

Kim et al. [129] reported a fully-functioning, flexible energy harvesting device using ZnO nanorods on Au-coated woven polyester substrates. The device was finished by pressing another gold-coated polyester layer onto the surface as an upper electrode. The ZnO nanorods were contacted with both their base and tip so that the piezoelectric polarization, induced by straining the nanorods when the polyester cloth was bent, could be efficiently used to produce a voltage across an external load. An enhanced output was attained by placing a 40 μm thick polyethylene (PE) spacer between the ZnO nanorods and top electrode that when excited by acoustic vibrations at ~100 dB, the device created ~ 4 V open-circuit voltage and short-circuit

ACCEPTED MANUSCRIPT

current density of 0.15 μA cm^{-2}. Not only did this reveal the possibility of producing harvesting and sensing devices on textiles but it also demonstrated an output from acoustic vibrations, possibly enabled by the extremely flexible fabric substrate. By neglecting the PE spacer, a lower voltage of ~ 0.5 V was produced. The authors attributed the improvement to the presence of a PE layer where an electrostatic effect was activated due to its initial surface charge of -2×10^{-4} C m^{-2}, whereby it is performing as an electret generator, adding to the piezoelectric output from the ZnO nanorods.

ZnO nano-wall [123] structures have also been used in a more common ZnO/PMMA/Au arrangement, where the nano-walls may formed due to the high concentrations (15 mM) of polyethylenimine (PEI) during synthesis, though substrate effects cannot be ruled out as the bottom electrode material was not detailed. The device produced an open circuit voltage of ~ 2.5 V and short-circuit current of ~ 80 nA with a power output of 37.7 nW cm^{-2} achieved across a 75 MΩ load resistance when manually deformed. An example of such a structure has been produced using a zinc nitrate-hexamethylenetetramine (HMT) by a chemical procedure that would nominally create nanorods [130], but when used on an aluminium-coated polyethersulfone (PES) substrate ZnO nano-sheets were formed due to the interaction with the Al surface. An Au-coated polymer substrate was then pressed onto this nanosheet array, which produced open-circuit voltage of ~ 0.75 V and short-circuit current of 16 μA cm^{-2} using a force of 4 kgf (39.2 N). Even though the authors highlight the single polarity output was related to the 'layered double hydroxide' construction of Zn and Al, it is likely to be caused by a loss of contact between the free-standing electrode and the ZnO upon releasing the structure, as observed in the original AFM tests.

ZnO based nanogenerators that use nanoparticles [131] rather than nanorods have

ACCEPTED MANUSCRIPT

also been demonstrated by combining them with carbon nanotubes (CNTs) in a hybrid composite embedded in polymer of polydimethylsiloxane (PDMS). This composite sandwiched between conductive (PET/ITO) substrates and during bending produced an open-circuit voltage of ~ 0.4 V open-circuit voltage and a short-circuit current of ~ 50 nA. Manual pressing of the NG produced an open-circuit voltage of ~ 7.5 V and short-circuit current were ~ 2.5 μA and, by pressing with a foot, a peak output up to 30 V was achieved. This device was reported to also exhibit excellent durability and could withstand high levels of stress.

5.1.2 Additional flexible piezoelectric nanogenerators

In addition to ZnO, a range of other materials has been explored to produce flexible PENG devices. $BaTiO_3$ nanowire based powders were prepared hydrothermally without a substrate, via a reaction between barium hydroxide and sodium titanate nanowires [132]. The $BaTiO_3$ nanowire powders were dispersed in PDMS and cast onto a silicon substrate for curing, after which they were sandwiched between two ITO/PET substrates to create an energy harvester. The devices were tested by bending 5 mm at 0.22 mm sec^{-1}, which produced an open-circuit voltage up to 7 V and short-circuit current ~ 360 nA. The maximum output power of 1.2 mW was found on a 20 MΩ load. Moreover, flexible $BaTiO_3$ and composites with large areas were prepared by Park et al. [40, 133], as shown in **Fig. 10 (b-c)**. Among the various emerging nanofabrication procedures, transfer methods have received attention due to their ability to create various geometry-controlled nanowire materials on flexible substrates [134]. During the fabrication process, chromium and $BaTiO_3$ were deposited using a thermal evaporator and RF sputtering system, respectively.

Lead zirconate titanate (PZT) is a commonly used material in macro- and micro-scale piezoelectric energy harvesters due to its high electro-mechanical coupling and piezoelectric

ACCEPTED MANUSCRIPT

coefficients (e.g. d_{33} for PZT of 500-600 pC/N compared to ~12 pC/N for ZnO) [124]. Many technological applications using nanoscaled PZT have used lateral films of electrospun fibers. Cui et al. [124] prepared aligned electrospun PZT fibers on a PDMS coated iron oxide (Fe_3O_4) substrate, encapsulated with PDMS and contacted at each end with silver electrodes to form an energy harvester. When the fibers were deformed, they generated an open-circuit voltage of ~3.2 V and a short-circuit current of ~ 50 nA. Wu et al. [46] manufactured aligned arrays of PZT nanowires by electrospinning PZT/poly(vinylpyrrolidinone) (PVP) precursors onto a series of bridge-like electrodes. The electrospun film could then be detached and attached to a PET substrate using PDMS, with silver electrodes added at each end. In bending-mode, the devices created an open-circuit voltage of ~ 6 V and ~ 45 nA short-circuit current, with an average power of ~ 0.12 μW across a 100 MΩ load. An open-circuit voltage up to 209 V was observed for an electrospun PZT fiber array arranged perpendicular to the substrate by cutting sections of the film, rotating and stacking a number of layers, as reported by Gu et al. [22].

Various types of electrospun fibers of piezoelectric materials have also been investigated for energy harvesting. Kang et al. [135] prepared Mn-Doped $(K,Na)NbO_3$ (KNN) fibers by electrospinning in polyvinylpyrrolidone (PVP) and annealing at 750 °C. These were deposited on a polyether sulfone (PES) substrate by implanting in PDMS and were attached using interdigitated platinum electrodes. In bending-mode, the devices generated a maximum open-circuit voltage of ~ 0.3 V and short-circuit current of ~ 50 nA. In addition, vertically-aligned KNN nanorods [136] have also been used in an energy harvester. These KNN nanorods were manufactured hydrothermally on a conductive $SrRuO_3/SrTiO_3$ substrate at 190 °C, followed by annealing at 600 °C for 12 h. Epitaxial-

matching of the substrates was necessary to produce oriented nanorods, which were mostly fused at the base but separated at the tips, and were well aligned. Finally a nanogenerator was formed by attaching a gold-coated Kapton substrate to the top of the nanorods and poling. The piezoelectric response of individual nanorods and the output of the entire device were tested by mechanically applying a periodic compressive force. This produced ~0.4 V open-circuit voltage and short-circuit current of 7 nA at 1 kgf (9.8 N). A peak power density of 101 mW cm^{-3} was obtained for a 60 MΩ load resistance, where the volume was not specified.

In 2014, Jeong et al. [137], fabricated large area and flexible lead-free $(Na,K,Li)NbO_3$ which was combined with copper nanowires in a PDMS-embedded nanogenerator device. The power from the device was extracted more effectively from the insulating polymer matrix of PDMS using the conductive Cu nanowires; in this study an optimum power produced for a 1:2 Cu:KLNNbO_3, generating a 12 V open-circuit voltage and 1.2 μA short-circuit current. This method was acceptable to form a large-area nanogenerator, with 30×30 cm^2 device being easily produced, providing 140 V and 8 μA, with ~ 0.4 mW for an optimum load of ~ 40 MΩ. A PDMS-embedded device was created using $ZnSnO_3$ nano-cubes, produced from an aqueous chemical process. When compressed by rolling over the device using a car, the device produced an open-circuit voltage up to 20 V and short-circuit current density up to 1 μA cm^{-2}. In 2016, Park et al. [138] fabricated a polymer-based flexible nanogenerator for sensor applications, as shown in **Fig. 10 (d)**, which was used to measure a human pulse when applied directly to the skin. Recently the flexibility, stretchability, durability and harvesting capability of organic and/or inorganic materials such as $BiFeO_3$–PDMS composites [139] (**Fig. 11 (a)**), laterally aligned PZT [140] (**Fig. 11 (b)**), fine scale fibers of $Ba_{0.85}Ca_{0.15}Zr_{0.1}Ti_{0.9}O_3$ [141] (**Fig. 11 (c)**), nanotube arrays of $PbTiO_3$ [142] (**Fig. 11**

ACCEPTED MANUSCRIPT

(d)) and graphene/ZnO nanorod hybrids [143] (Fig. 12) based nanogenerators have been examined in order to improve the performance and multi-functionality of piezoelectric nanogenerators.

Today, energy harvesting devices based on piezoelectric PVDF polymers are being increasingly considered. Although PVDF-based devices are often not considered as 'nanogenerators', being compared to bulk, thin-film and microscale energy harvesting devices, they often benefit from the nanostructuring of the PVDF material and are often similar in terms of overall device design and strain method to many nanogenerators [117]. For example, PVDF is often in the form a flexible, thin, sheet-like device with or without a supportive substrate, which is pressed or flexed to produce a power output. For devices consisting of PVDF-based nanocomposites containing reduced graphene oxide (RGO) [144, 145] in the form of a flexible sheet, it was found that the addition of a small faction amount of RGO doubled the output power due to templating by the graphene. The power output of the device was evaluated by vibrating at 1*g* at a resonant frequency of 41 Hz, leading to an output power of ~ 36 nW on a 704 kΩ load. In addition, electrospun nanofibers of flexible PVDF have been examined for a number of energy harvesting applications, which have been recently reviewed [146-148].

5.2 Flexible and stretchable triboelectric devices

Recently, flexible TENG devices have also been considered in energy harvesting applications. In this aspect, nitrogen-doped carbon nanotube-(CNT) based flexible TENGs were prepared by Khan et al. [149]. This TENG consisted of two layers, including polyimide (PI), polydimethylsiloxane (PDMS) and CNTs served as a bottom layer, while polytetrafluoroethylene (PTFE with aluminum (Al) and polyimide (PI) was the top layer to

ACCEPTED MANUSCRIPT

create a flexible TENG based on CNTs fabricated via chemical vapor deposition (CVD). The fabricated TENG produced an output open circuit voltage of ~ 20 V, output short-circuit current of ~0.7 μA and an output power of 10.3 μW for a load of 40 MΩ. Finally, the charge produced by the flexible TENG was to charge commercial capacitors which were then used for lighting LEDs and power thermal sensors. In 2016, a polydimethylsiloxane (PDMS) and multiwall carbon nanotube (MWCNT) based flexible and biocompatible triboelectric nanogenerator was fabricated by Zhu et al. [150], as shown in **Fig. 13**. During their investigation, they varied the fraction of MWCNT from 2 wt % and 10 wt %. Under a vertical force of 3.0 N, the triboelectric output voltages of Prototype I (10 wt%) and Prototype II (2 wt %) were 30 V and 25 V respectively. Recently, in 2017, Wu et al. [35] reported a compact multi-layer flexible nanogenerator, which was prepared using fluorinated ethylene propylene with a silver electrode. By pressing the 4 × 4 cm^2 device, an output current peak of ~ 3 mA was measured, which was sufficiently large to power a wireless remote system with an effective emitting distance of 30 cm. In addition, a variety of self-powered triboelectric nanogenerators (TENGs), such as an auxetic foam-based triboelectric nanogenerator [151] (**Fig. 14 (a)**), a free-standing mode tribo-tronic tuning diode TENG [152] (**Fig. 14 (b)**), a single-thread-based triboelectric nanogenerator [153](**Fig. 14 (c)**), a textile based foldable wearable TENG [154](**Fig. 14 (d)**), a serpentine patterned electrode based flexible TENG [77] (**Fig. 14 (e)**), a graphene based crumpled substrate TENG [24] (**Fig. 14 (f)**), a two sliding mode TENG [155] (**Fig. 14 (g)**), a rolled TENG [156] (**Fig. 14 (h)**), a rubber based joint motion TENG [157] (**Fig. 14 (i)**) and an electrostatic actuation based TENG [158] (**Fig. 14 (j)**) have been prepared and demonstrated.

To harvest improved amounts of energy, advancements in TENGs are important.

ACCEPTED MANUSCRIPT

However, to date the stretchability and sensitivity of prototype devices remains low and they are restricted due to rigid materials, limiting device applications. In order to solve these issues, flexible interdigital-electrodes-based triboelectric generators (FITG) [159] (**Fig. 15 (a)**) and hydrophobic TENGs [160] (**Fig. 15 (b)**) have been considered.

Triboelectric nanogenerators normally consist of multiple components with a relatively high thickness of ~ 0.5-5 cm to enhance sensitivity. In this aspect, Chen et al. (2017) [161] recently demonstrated that an ultrathin flexible single electrode triboelectric nanogenerator (S-TENG) using nanoporous PTFE (180 μm) with surface modification of a Cu film (~20 nm) for a non-transparent TENG and a fluorinated ethylene propylene (FEP ~ 25 μm) thin film to fabricate a transparent TENG. Under the application of a pressing force of 140 N by a latex glove box, the non-transparent TENG exhibited an output current of ~ 60 μA and an open circuit voltage of ~ 150 V. The peak power was maximized at a load resistance of 6 MΩ, corresponding to 8.58 mW. For the same experimental conditions, the transparent S-TENG had a current and voltage output up to 78 μA and 340 V respectively, obtained when the device was subjected to an impact by a human palm covered with a latex glove. Using this device, the authors were able to light up 70 commercial LEDs. In addition, when tapped by a finger the device produced a current of ~ 1 μA and the sensitivity was ~0.947 μA MPa^{-1}. From these experimental results ultrathin TENGs have been shown to act not only as a mechanical energy harvester of human movements and ambient sources of motion, but also as effective sensors.

Recently, a graphene oxide (GO) based single-electrode TENG system has been fabricated by Guo et al. (2017) [162]. A poly(tetrafluoroethylene) (PTFE) polymer with a thickness of 0.07 mm was chosen as the substrate material due to its excellent physical and

ACCEPTED MANUSCRIPT

chemical properties such as its light-weight nature and high impact strength. Initially, a GO film prepared by the Hummers method was transferred to an Al electrode. The Al electrode was then fixed onto the PTFE substrate to make a stable TENG. In the control experiment, a PTFE film was used to replace the GO film for fabricating a single-electrode TENG, as shown in **Fig. 15 (c)**. Finally, the as-designed multifunctional TENG device could not only harvest mechanical energy from ambient movements with a power density of 3.13 Wm^{-2} but was also able to detect dynamic force with a sensitivity of ~ 382 μA MPa^{-1}. In 2017, Cheng et al. [163] fabricated a transparent and wrinkle structured TENG by fluorocarbon plasma on poly(dimethylsiloxane) (PDMS) and a variety of 'solaris' membranes, as shown in **Fig. 15 (d)**. It was reported that the C_4F_8 plasma-treated wrinkled PDMS had a higher performance than a flat PDMS-based and flat solaris-based TENG. Moreover, the results revealed that combining the high electron affinity fluorocarbon and wrinkled pattern PDMS enhanced TENG performance, which was mainly due to the increased surface area, high transparency of PDMS and the increase carrier concentration due to the fluorocarbon.

6. Hybrid energy harvesting nanogenerators

As a result of increasing interest in self-powered flexible micro- and nano-systems, energy harvesters based on different mechanisms have been extensively examined for harvesting energy from our surrounding environment, such as the piezoelectric nanogenerator (PENG) and triboelectric nanogenerator (TENG). In addition, pyroelectric nanogenerators and thermoelectric nanogenerators (ThENG) [164] for scavenging thermal energy have been explored. However, as the final goal is to improve the overall power output and realize maximum utilization of multi-type energies, the individual energy harvesters have recently been integrated as hybridized nanogenerators [165]. Wang et al. [166] fabricated a flexible

ACCEPTED MANUSCRIPT

triboelectric-piezoelectric hybrid nanogenerator (TPENG) based on P(VDF-TrFE) nanofibers and PDMS/MWCNT using an electro-spinning method and the device was used for wearable technological device applications. Double silver electrodes on a P(VDF-TrFE) film were used to characterize the output piezoelectric performance. This circuit was connected to a bottom silver electrode and a PDMS/MWCNT film to demonstrate the output performance of triboelectric mechanism. At the same time, the TPENG was loaded by a fingertip force that was monitored by a pressure sensor. The TPENG output voltage, power and power density under triboelectric mechanism were 25 V, 98.56 μW and 1.98 mW cm^{-3}, respectively, under a 5 N force. Additionally, an output peak-peak voltage of ~ 2.5 V, output power of ~9.74 μW and power density of 0.689 mW cm^{-3} were produced under piezoelectric operation at the same condition.

Similarly, Chen et al. [167] designed a ZnO nanowire array-based multimode energy harvester for simultaneous solar and mechanical energy harvesting, as shown in **Fig. 16**. They tested energy harvesting performance via series **(Fig. 16 (a))** and parallel **(Fig. 16 (b))** integration of a hybrid harvester that combined a solar cell (SC) and nanogenerator (NG). During series integration of the SC and NG under the application of both sun light and ultrasonic waves, the hybrid cell exhibited an open circuit voltage (U_{OC}) of 0.60 V with short circuit current density (J_{SC}) was about 6.9 μA cm^{-2}. On parallel integration of the SC and NG, under the application of both sun light and ultrasonic waves, the hybrid device exhibited U_{OC} of 0.102 V with J_{SC} of ~1.5 μA cm^{-2}. It was demonstrated that the two harvesting approaches of solar energy harvesting and mechanical energy harvesting could operate simultaneously or individually. Later, the same group fabricated a hybrid energy harvesting device using a nanowire array of ZnO (length ~2–3 μm and a 400-700 nm interspacing between the nanowires) for energy harvesting of both solar and

ACCEPTED MANUSCRIPT

mechanical energy [168]. The ZnO based hybrid energy harvester exhibited a maximum power density of ~ 34.5 μW cm^{-2} at J_{SC} =140 μA cm^{-2} and U_{OC} = 0.243 V, under the application of solar light with ultrasonic waves. This enhanced performance was attributed to the combination of both solar cell and nanogenerator comportments. Based on piezo-tribo-pyro-photoelectric effects, Kewei Zhang et al. [164] fabricated a single-structure-based multi-functional coupled nanogenerator, as shown in **Fig. 17**. The piezo-tribo-pyro-photoelectric nanogenerator consisted of three parts: (i) a PZT block, for piezoelectric, pyroelectric and photoelectric active system; (ii) polyamide (nylon) with fluorinated ethylene propylene (FEP) acting as the flexible vibrating film to introduce tribo-electrification and apply a strain to adjacent PZT during vibration; (iii) a bottom electrode of a thin silver (Ag) film under the PZT and (iv) a top electrode consisting of a thin indium tin oxide (ITO) film combined with Ag nanowires/polydimethylsiloxane (AgNWs/PDMS) film. The individual pyroelectric and individual photoelectric active system produced a larger output voltage, but smaller output current compared to the combined system. By combining a photoelectric active system, pyroelectric and tribo-pyro-photoelectric system into a single device and using the same output electrodes, a complementary power source with a peak current of ~5 μA, peak voltage of ~80 V and plateau voltage of ~50 V was attained. The hybrid nanogenerator that combined the functions of piezo-, tribo-, pyro- and photo-electric effects could charge a 10 μF capacitor to 5.1 V in 90s.

Recently, several researchers explained [169-172] the stepwise operation mechanism used to investigate the combined effects of piezoelectricity and triboelectricity in flexible substrate media, as shown in **Fig. 18**. While piezoelectricity and triboelectricity are two different phenomena they share several unique operational features of mechanical-to-electrical energy conversion. For example, both piezo-and tribo-electric materials respond well to many mechanical

ACCEPTED MANUSCRIPT

energy sources, such as compression, deflection/strain and vibration. In addition, their different working mechanisms suggest that their electricity generation procedures do not overlap with each other, since the triboelectric needs only the function of a material surface whereas the bulk part is responsible for the piezoelectric harvester. Therefore, these two properties can be collected for the equivalent type of mechanical-energy harvesting systems with combined electrical energy output. Pioneering work has demonstrated the possibility of integration of triboelectric and piezoelectric effects for mechanical-energy harvesting in one integrated system, as shown in **Fig. 18**.

7. Innovative applications of nanogenerators

It is well-known that the piezoelectric and triboelectric properties of materials offer a way to convert mechanical energy directly, from sources such as fluid flow, moving parts of machines and human body movements, into electrical power for microscale device uses. The device applications of PENG and/or TENG include self-powering conventional electronics such as Light Emitting Diodes (LEDs) [170, 173, 174] and Liquid Crystal Displays (LCDs) [175]. Examples including self-powered nano/micro gadgets [176], implantable power storage devices, smart wearable systems [177], such as wrist watches, power shoes and power shirts, are shown in **Fig. 19**. Compared with other applications, micro/nano sensors have attracted attention due to their potential device applications in sensing micro/nano-objects such as touch sensors, heat sensors, particles, cells and DNA. These PENG-based nanogenerators are important for fabricating small-scale sensors [169, 178, 179] and are focused on driving a nano-device by energy harvesting from its working environment instead of a conventional battery or any other energy storage and/or energy supply systems. In addition, nanogenerators can exploit small-scale device applications in medical treatments [175, 180-184], such as small physical motion during inhalation and the corresponding

ACCEPTED MANUSCRIPT

motion of the lung, heartbeat and muscle movement, as shown in **Fig. 20**.

Transparent and flexible TENG sensing array devices have been used for Touch Security Applications (TSA) [176, 185] and LCD touch screens [98, 175] powered by a transparent TENG, which covers the screen and converts the energy of a finger pressure into electricity [98, 176]. Recently a self-powered TENG based flexible Li-ion battery and super capacitor have been used for advanced energy storage/supply devices [27, 186], as shown in **Fig. 21 and 22**. Additionally, Wei Li et al. [187] reported the dual-functionality of a thin patch loudspeaker or microphone for flexible electronic devices; this was fabricated using a ferro-electret nanogenerator (FENG). By micro-plasma-discharging a FENG, the artificial voids inside the foam-structured ferro-electret forms numerous dipoles that enable the device to achieve high electromechanical transformation efficiency. They indicated that the mechanisms for direct and reverse interaction effects (that is, using mechanical energy to generate electrical energy and using electrical energy to harvest mechanical energy) were the key factors of the FENG-based loudspeaker/microphone device shown in **Fig. 22**.

Obviously, natural renewable sources such as light and thermal, ocean (blue energy) and wind power offers additional energy supplements to traditional energy strategies [188-190]. Energy from the ocean is abundant and has many forms, including water current energy, wave energy, tidal energy, thermal energy conversion and reverse osmosis. However, such ocean energy harvesting may face significant engineering challenges, low efficiency and high cost. In order to decrease these difficulties, ocean energy harvesting using electromagnetic generators (EMG) was advanced. [96, 191] However, the output power generation on this device is small at the low mechanical frequencies associated with ocean. Hence an alternative approach has been proposed using TENGs. [88, 179].

ACCEPTED MANUSCRIPT

In contrast to EMGs, TENGs, based on the combination of triboelectric and electrostatic induction, are reported to be more active at low frequencies. A spiral interdigital-electrode triboelectric nanogenerator and a wrap-around electromagnetic generator (W-EMG) have been reported for harvesting ocean energy system, as shown in **Fig. 23 (a)**. The hybrid blue energy harvesting nanogenerator can operate under either rotation mode or fluctuation mode to collect ocean current energy, tidal energy and wave energy. In addition, the features and benefits of outputs from both devices were systematically examined and compared. The results showed that the S-TENG has more benefits for collecting ocean energy at low frequency than a W-EMG; this will not only power electronic device units but also charge other energy storage devices, allowing the nanogenerator to produce electricity in a wide-range of working frequencies. In addition, Z. L. Wang's blue energy approach [96] involves networking millions of spherical balls based on triboelectric nanogenerators for harvesting low-frequency water wave energy; the concepts of the networks are shown in **Fig. 23 (b-c)**. This blue energy scheme was also executed by Kim et al. [192], as shown in **Fig. 23(d)**.

Chuan He (2017) et al. [193] recently fabricated an hourglass triboelectric nanogenerator that extracts the kinetic energy of falling particles and/or small objects. In this work, the particles used were a combination of polytetrafluoroethylene (PTFE) pellets and aluminum balls. From their investigations, they observed that for a falling particle volume ratio ~1:1 of PTFE pellets to aluminium balls 160 commercial light emitting diodes could be illuminated for ~18s intermittently. Furthermore, the fabricated hourglass-TENG can serve as a self-powered UV counterfeit detector, as shown in **Fig. 23 (e)**. From all these investigations it is evident that there is growing interest in TENG based devices for large-scale energy harvesting applications.

ACCEPTED MANUSCRIPT

8. Factors determining nanogenerators performance

This section details the current understanding of the environmental factors affecting the energy harvesting properties of piezoelectric, triboelectric and tribo-piezoelectric nanogenerators. The most common influential factors include humidity, temperature, adsorption of oxygen and other substances and an understanding of nanogenerators device packing. The surface morphology and materials are also key factors for enhancing the performance of the final device.

8.1 Humidity effects

Ambient air consists of a mixture of gases Nitrogen (N), Oxygen (O), Argon (Ar) and water vapor. In particular, oxygen and water vapor can affect the triboelectric and piezoelectric materials and thus the activity of nanogenerators. Whether in a vapor or liquid phase, the ubiquitous presence of water may penetrate through the TENG's package into the gap between two contacted surfaces. The contact electrification process in TENG can be influenced by water penetration, as it can infiltrate the gap or adsorb as a thin layer on each surface during operation of the TENG. This influence generally depends on the wettability of the working surfaces and the amount of water present [194-197].

It has been demonstrated that humid atmospheres can lead to degradation in the dielectric strength of piezoelectric materials [198]. The degradation of dielectric strength is related to ion and defect movement to electrodes and grain boundaries, initiating a reduction in the electrical resistance and breakdown strength of the material [199]. The resultant leakage current increases the power consumption and can eventually lead to failure of the device. In order to avoid this situation, encapsulation of polymer coatings has been used to protect devices, but these polymers are permeable and do not completely avoid water vapor

ACCEPTED MANUSCRIPT

transmission [200]. Airtight sealing has also been attempted as a solution but it required more complex arrangements and production costs can be high [201]. Several additional mechanisms for the degradation of materials due to the presence of water have been proposed: (i) the structural assimilation of interstitial atomic hydrogen [202]; (ii) increase in the surface conduction initiated by the adsorption of water [203]; and (iii) the replacement of oxygen vacancies through the ceramic [204].

8.2 Temperature effects

It is well known that the initial resistance of the piezoelectric and triboelectric materials is related to the temperature [198, 205]. A ferroelectric-based piezoelectric material loses its spontaneous polarization above a transition temperature, known as the Curie temperature (T_c). Typically, compared to nanosized materials (e.g. such as rods and wires), the Curie temperature (T_c) are lower for both PENG or TENG materials [206]. The Curie temperature of $BaTiO_3$ is relatively low at ~150°C and varies with doping [197, 207]; for example, $BaTiO_3$ can be modified via partial doping of either A-site doping (Ba^{2+} ions) or B-site doping (Ti^{4+} ions) [208]. A-site doping with cations of the same valence as Ba^{2+} leads to a reduction in Curie temperature (e.g. by substitution of Sr^{2+}) without any substantial transition broadening. It was confirmed that the partial replacement of titanium by tin, hafnium or zirconium usually led to a decrease in T_c and an increase in the maximum permittivity with content of dopant [208]. Since an ideal nanogenerator should be able to operate in a harsh environment for a prolonged time period, there is a need for improving the thermal stability which is an issue for many PENG and TENG materials. Among the various environmental factors, temperature is the one that most strongly affects the TENG's performance, that is, during triboelectric testing the electric charge generated tends to decrease with increasing

ACCEPTED MANUSCRIPT

temperature [209]. It is essential to note that, the working mechanism of TENGs is based on two main methods, which are contact electrification and electrostatic induction. The temperature-dependence of these two mechanisms have an important impact on the overall performance of the TENG due to heat transfer to or from the nanogenerator device [197].

8.3 Adsorption effects

Typically, nanogenerators have a large surface-to-volume ratio, which can leave them vulnerable to adsorption of substances other than water and oxygen from the surrounding atmosphere [197, 207]. These adsorbed substances can change device performance significantly via a resistance change. Some substances, such as alumina substrates [210], attack the major part of the active material and permanently change its chemical composition. Adsorption of external charges also affects the conductivity of inorganic nanogenerators. The adsorbed charges interact electrostatically with the internal free carriers and can be regarded as a floating gate (i.e. electrically isolated by the oxide layer). Finally, the resistance variations due to adsorbates will vary the piezoelectric materials leakage current and affect power generation. That is, for an n-type material, positive charges act in a similar way to a positive gate that attracts electrons and increases conductivity (lowers resistance), but the negative charges deplete the internal electrons and decrease conductance. Some adsorbates that are p-type semiconductors or high work function metals could form a Schottky barrier or p-n junctions with the n-type material (such as ZnO) [211, 212]. Such boundaries make a charge depletion region on n-type materials surface and decrease the carrier density. Subsequently, the screening effect is reduced and power output may be improved. In addition, during synthesis, reducing agents or hole depletion may increase the resistance, whereas the oxidizing agents or hole accumulation may decrease the resistance of p-type semiconducting

ACCEPTED MANUSCRIPT

materials [213]; this rule can be applied generally to non-wurtzite structured materials [214].

8.4 Surface morphology effects

The triboelectric process in TENGs is fundamentally a surface charging effect and therefore the surface morphology and friction behavior of the active materials will effectively determine the output of these devices. In order to increase performance and lifetime, researchers have expanded the effective friction areas by using micro- and nano-shaped dual-scale designs and formed micro- and nano-scale patterns onto tribo-surfaces. Dual-scale patterns, pyramid patterns and nanoscale patterns can enhance the roughness compared to the plane film, and thus TENG performance can be improved [17, 215, 216]. In addition to structural modifications, the material properties, such as the electron affinity, work function, friction can also play important roles in TENG output performance.

9. Conclusions

To harvest energy from ambient mechanical energy and provide power for various applications, such as touch and pressure sensors, self-powered portable electronics, flexible printed circuit boards and wearable medical devices, the development of flexible and stretchable materials and systems is essential for high performance device application. Hence, in this comprehensive review, we have presented the fundamental mechanisms, fabrication methods and applications of nanogenerators starting from traditional piezoelectric and triboelectric devices, along with recently reported flexible and hybrid devices. For traditional piezo- and tribo-electric nanogenerator devices, the stretchability and sensitivity are restricted due to their use of rigid materials. These nanogenerators' technical difficulties are rectified by developing flexible and hybrid device fabrication methods, where various material classifications have been utilized based on ZnO nanowires, nanorods, barium titanate

ACCEPTED MANUSCRIPT

($BaTiO_3$), lead zirconate titanate (PZT), poly(vinylidene fluoride) (PVDF), graphene-based 2D materials and composite materials. As a result of the flexible and/or hybrid device fabrication, the performances of the hybrid nanogenerators can be enhanced, when compared to conventional PENG and/or TENG and/or flexible devices. Among the various energy harvesters, the combination of flexible and hybrid piezo- and triboelectric nanogenerators can lead to improved performance and the flexible devices are easy to integrate as a hybrid device, which makes them good candidates for the applications described above. Flexible hybrid devices have the potential of harvesting energy from mechanical vibrations, human actions, rotating tires, ocean waves (blue energy), with a range of applications in self-powered nanogenerators that are able to operate without an external power supply for personal electronic devices, LED, LCD, sensing, detection, batteries, data processing and data transmission, medical sciences, environmental monitoring and even large-scale power production. Finally, some major perspectives and challenges to enhance the performance of the device have been discussed in detail so that commercial systems that utilize the reported materials and device architectures may be realized.

Acknowledgements

This study was supported by the Basic Science Research Program through the National Research Foundation of Korea (NRF) funded by The Ministry of Science, ICT and Future Planning (NRF-2016R1A2B2006311).

References

[1] J. Briscoe, S. Dunn, Piezoelectric nanogenerators–a review of nanostructured piezoelectric energy harvesters, Nano Energy, 14 (2015) 15-29.

[2] S. Roy, H. Gleeson, C. Shaw, R. Whatmore, Z. Huang, Q. Zhang, S. Dunn, Growth and

ACCEPTED MANUSCRIPT

characterisation of lead zirconate titanate (30/70) on indium tin oxide coated glass for oxide ferroelectric-liquid crystal display application, Integrated ferroelectrics, 29 (2000) 189-213.

[3] C. Bowen, H. Kim, P. Weaver, S. Dunn, Piezoelectric and ferroelectric materials and structures for energy harvesting applications, Energy & Environmental Science, 7 (2014) 25-44.

[4] C.R. Bowen, J. Taylor, E. LeBoulbar, D. Zabek, A. Chauhan, R. Vaish, Pyroelectric materials and devices for energy harvesting applications, Energy & Environmental Science, 7 (2014) 3836-3856.

[5] S. Roundy, E.S. Leland, J. Baker, E. Carleton, E. Reilly, E. Lai, B. Otis, J.M. Rabaey, P.K. Wright, V. Sundararajan, Improving power output for vibration-based energy scavengers, IEEE Pervasive computing, 4 (2005) 28-36.

[6] R. Amirtharajah, A.P. Chandrakasan, Self-powered signal processing using vibration-based power generation, IEEE Journal of solid-state circuits, 33 (1998) 687-695.

[7] C. Williams, R.B. Yates, Analysis of a micro-electric generator for microsystems, Sensors and Actuators A: Physical, 52 (1996) 8-11.

[8] P. Glynne-Jones, S.P. Beeby, N.M. White, Towards a piezoelectric vibration-powered microgenerator, IEE Proceedings-Science, measurement and technology, 148 (2001) 68-72.

[9] Z.L. Wang, J. Song, Piezoelectric nanogenerators based on zinc oxide nanowire arrays, Science, 312 (2006) 242-246.

[10] B. Saravanakumar, R. Mohan, K. Thiyagarajan, S.-J. Kim, Fabrication of a ZnO nanogenerator for eco-friendly biomechanical energy harvesting, RSC Advances, 3 (2013) 16646-16656.

[11] X. Wang, J. Song, J. Liu, Z.L. Wang, Direct-current nanogenerator driven by ultrasonic

ACCEPTED MANUSCRIPT

waves, Science, 316 (2007) 102-105.

[12] G. Zhu, R. Yang, S. Wang, Z.L. Wang, Flexible high-output nanogenerator based on lateral ZnO nanowire array, Nano Letters, 10 (2010) 3151-3155.

[13] X. Li, Y. Chen, A. Kumar, A. Mahmoud, J.A. Nychka, H.-J. Chung, Sponge-templated macroporous graphene network for piezoelectric ZnO nanogenerator, ACS Applied Materials & Interfaces, 7 (2015) 20753-20760.

[14] Y. Zi, L. Lin, J. Wang, S. Wang, J. Chen, X. Fan, P.K. Yang, F. Yi, Z.L. Wang, Triboelectric–Pyroelectric–Piezoelectric Hybrid Cell for High- Efficiency Energy- Harvesting and Self- Powered Sensing, Advanced Materials, 27 (2015) 2340-2347.

[15] F.-R. Fan, Z.-Q. Tian, Z.L. Wang, Flexible triboelectric generator, Nano Energy, 1 (2012) 328-334.

[16] H. Zhang, Y. Yang, T. C. Hou, Y. Su, C. Hu, Z.L. Wang, Triboelectric nanogenerator built inside clothes for self-powered glucose biosensors, Nano Energy, 2 (2013) 1019-1024.

[17] Z.L. Wang, Triboelectric nanogenerators as new energy technology for self-powered systems and as active mechanical and chemical sensors, ACS Nano, 7 (2013) 9533-9557.

[18] S. Lee, S.H. Bae, L. Lin, Y. Yang, C. Park, S.W. Kim, S.N. Cha, H. Kim, Y.J. Park, Z.L. Wang, Super- flexible nanogenerator for energy harvesting from gentle wind and as an active deformation sensor, Advanced Functional Materials, 23 (2013) 2445-2449.

[19] L. Lin, Y. Hu, C. Xu, Y. Zhang, R. Zhang, X. Wen, Z.L. Wang, Transparent flexible nanogenerator as self-powered sensor for transportation monitoring, Nano Energy, 2 (2013) 75-81.

[20] S. H. Shin, M.H. Lee, J. Y. Jung, J.H. Seol, J. Nah, Piezoelectric performance enhancement of ZnO flexible nanogenerator by a CuO–ZnO p–n junction formation, Journal

ACCEPTED MANUSCRIPT

of Materials Chemistry C, 1 (2013) 8103-8107.

[21] P.X. Gao, J. Song, J. Liu, Z.L. Wang, Nanowire piezoelectric nanogenerators on plastic substrates as flexible power sources for nanodevices, Advanced Materials, 19 (2007) 67-72.

[22] L. Gu, N. Cui, L. Cheng, Q. Xu, S. Bai, M. Yuan, W. Wu, J. Liu, Y. Zhao, F. Ma, Flexible fiber nanogenerator with 209 V output voltage directly powering a light-emitting diode, Nano Letters, 13 (2012) 91-94.

[23] M. Koo, K. I. Park, S.H. Lee, M. Suh, D.Y. Jeon, J.W. Choi, K. Kang, K.J. Lee, Bendable inorganic thin-film battery for fully flexible electronic systems, Nano Letters, 12 (2012) 4810-4816.

[24] S. Kim, M.K. Gupta, K.Y. Lee, A. Sohn, T.Y. Kim, K.S. Shin, D. Kim, S.K. Kim, K.H. Lee, H.J. Shin, Transparent flexible graphene triboelectric nanogenerators, Advanced Materials, 26 (2014) 3918-3925.

[25] J. Zhong, Q. Zhong, F. Fan, Y. Zhang, S. Wang, B. Hu, Z.L. Wang, J. Zhou, Finger typing driven triboelectric nanogenerator and its use for instantaneously lighting up LEDs, Nano Energy, 2 (2013) 491-497.

[26] X. Pu, L. Li, H. Song, C. Du, Z. Zhao, C. Jiang, G. Cao, W. Hu, Z.L. Wang, A self- charging power unit by integration of a textile triboelectric nanogenerator and a flexible lithium- ion battery for wearable electronics, Advanced Materials, 27 (2015) 2472-2478.

[27] J. Wang, X. Li, Y. Zi, S. Wang, Z. Li, L. Zheng, F. Yi, S. Li, Z.L. Wang, A flexible fiber- based supercapacitor–triboelectric- nanogenerator power system for wearable electronics, Advanced Materials, 27 (2015) 4830-4836.

[28] W. Zeng, L. Shu, Q. Li, S. Chen, F. Wang, X.M. Tao, Fiber- based wearable electronics: a review of materials, fabrication, devices, and applications, Advanced Materials, 26 (2014)

ACCEPTED MANUSCRIPT

5310-5336.

[29] J. Zhong, Y. Zhang, Q. Zhong, Q. Hu, B. Hu, Z.L. Wang, J. Zhou, Fiber-based generator for wearable electronics and mobile medication, ACS Nano, 8 (2014) 6273-6280.

[30] M. Lee, C.Y. Chen, S. Wang, S.N. Cha, Y.J. Park, J.M. Kim, L. J. Chou, Z.L. Wang, A hybrid piezoelectric structure for wearable nanogenerators, Advanced Materials, 24 (2012) 1759-1764.

[31] Y. Yang, H. Zhang, Z. H. Lin, Y.S. Zhou, Q. Jing, Y. Su, J. Yang, J. Chen, C. Hu, Z.L. Wang, Human skin based triboelectric nanogenerators for harvesting biomechanical energy and as self-powered active tactile sensor system, ACSNano, 7 (2013) 9213-9222.

[32] C. Hou, T. Huang, H. Wang, H. Yu, Q. Zhang, Y. Li, A strong and stretchable self-healing film with self-activated pressure sensitivity for potential artificial skin applications, Scientific reports, 3 (2013) 3138-3146.

[33] Y. Yang, H. Zhang, X. Zhong, F. Yi, R. Yu, Y. Zhang, Z.L. Wang, Electret film-enhanced triboelectric nanogenerator matrix for self-powered instantaneous tactile imaging, ACS Applied Materials & Interfaces, 6 (2014) 3680-3688.

[34] X. Chen, T. Jiang, Y. Yao, L. Xu, L. Zhao, Z.L. Wang, Stimulating Acrylic Elastomers by a Triboelectric Nanogenerator–Toward Self- Powered Electronic Skin and Artificial Muscle, Advanced Functional Materials, 26 (2016) 4906-4913.

[35] N. Wu, H. Jiang, W. Li, S. Lin, J. Zhong, F. Yuan, L. Huang, B. Hu, J. Zhou, Output Enhanced Compact Multilayer Flexible Nanogenerator for Self-Powered Wireless Remote System, Journal of Materials Chemistry A, (2017) 12787-12792.

[36] L. Lin, Q. Jing, Y. Zhang, Y. Hu, S. Wang, Y. Bando, R.P. Han, Z.L. Wang, An elastic-spring-substituted nanogenerator as an active sensor for self-powered balance, Energy &

ACCEPTED MANUSCRIPT

Environmental Science, 6 (2013) 1164-1169.

[37] X. Jiang, W. Huang, S. Zhang, Flexoelectric nano-generator: Materials, structures and devices, Nano Energy, 2 (2013) 1079-1092.

[38] Y. Gao, Z.L. Wang, Electrostatic potential in a bent piezoelectric nanowire. The fundamental theory of nanogenerator and nanopiezotronics, Nano Letters, 7 (2007) 2499-2505.

[39] X. Chen, S. Xu, N. Yao, Y. Shi, 1.6 V nanogenerator for mechanical energy harvesting using PZT nanofibers, Nano Letters, 10 (2010) 2133-2137.

[40] K. I. Park, S. Xu, Y. Liu, G. T. Hwang, S. J.L. Kang, Z.L. Wang, K.J. Lee, Piezoelectric BaTiO3 thin film nanogenerator on plastic substrates, Nano Letters, 10 (2010) 4939-4943.

[41] C.T. Huang, J. Song, C.M. Tsai, W.F. Lee, D.H. Lien, Z. Gao, Y. Hao, L.J. Chen, Z.L. Wang, Single- InN- Nanowire Nanogenerator with Upto 1 V Output Voltage, Advanced Materials, 22 (2010) 4008-4013.

[42] N.J. Ku, C.H. Wang, J.H. Huang, H.C. Fang, P.C. Huang, C.P. Liu, Energy Harvesting from the Obliquely Aligned InN Nanowire Array with a Surface Electron- Accumulation Layer, Advanced Materials, 25 (2013) 861-866.

[43] X. Wang, J. Song, F. Zhang, C. He, Z. Hu, Z. Wang, Electricity Generation based on One- Dimensional Group III Nitride Nanomaterials, Advanced Materials, 22 (2010) 2155-2158.

[44] J.H. Jung, M. Lee, J. I. Hong, Y. Ding, C.-Y. Chen, L.-J. Chou, Z.L. Wang, Lead-free NaNbO3 nanowires for a high output piezoelectric nanogenerator, ACS Nano, 5 (2011) 10041-10046.

[45] J.M. Wu, C. Xu, Y. Zhang, Z.L. Wang, Lead-free nanogenerator made from single

ACCEPTED MANUSCRIPT

ZnSnO3 microbelt, ACS Nano, 6 (2012) 4335-4340.

[46] J.M. Wu, K.-H. Chen, Y. Zhang, Z.L. Wang, A self-powered piezotronic strain sensor based on single ZnSnO3 microbelts, RSC Advances, 3 (2013) 25184-25188.

[47] T. C. Hou, Y. Yang, Z. H. Lin, Y. Ding, C. Park, K.C. Pradel, L. J. Chen, Z.L. Wang, Nanogenerator based on zinc blende CdTe micro/nanowires, Nano Energy, 2 (2013) 387-393.

[48] Y. F. Lin, J. Song, Y. Ding, S. Y. Lu, Z.L. Wang, Piezoelectric nanogenerator using CdS nanowires, Applied Physics Letters, 92 (2008) 022105.

[49] Y.F. Lin, J. Song, Y. Ding, S.Y. Lu, Z.L. Wang, Alternating the output of a CdS nanowire nanogenerator by a white- light- stimulated optoelectronic effect, Advanced Materials, 20 (2008) 3127-3130.

[50] J.M. Wu, C.C. Kao, Self-powered pendulum and micro-force active sensors based on a ZnS nanogenerator, RSC Advances, 4 (2014) 13882-13887.

[51] Y. Zhang, G. Gao, H.L. Chan, L. Dai, Y. Wang, J. Hao, Piezo- Phototronic Effect- Induced Dual- Mode Light and Ultrasound Emissions from ZnS: Mn/PMN–PT Thin- Film Structures, Advanced Materials, 24 (2012) 1729-1735.

[52] C. T. Huang, J. Song, W. F. Lee, Y. Ding, Z. Gao, Y. Hao, L. J. Chen, Z.L. Wang, GaN nanowire arrays for high-output nanogenerators, Journal of the American Chemical Society, 132 (2010) 4766-4771.

[53] C.H. Wang, W.S. Liao, Z.H. Lin, N.J. Ku, Y.C. Li, Y.C. Chen, Z.L. Wang, C.P. Liu, Optimization of the output efficiency of GaN nanowire piezoelectric nanogenerators by tuning the free carrier concentration, Advanced Energy Materials, 4 (2014) 1400392-1400397.

[54] S. Cha, S.M. Kim, H. Kim, J. Ku, J.I. Sohn, Y.J. Park, B.G. Song, M.H. Jung, E.K. Lee, B.L. Choi, Porous PVDF as effective sonic wave driven nanogenerators, Nano Letters, 11

ACCEPTED MANUSCRIPT

(2011) 5142-5147.

[55] M. Lee, J. Bae, J. Lee, C.-S. Lee, S. Hong, Z.L. Wang, Self-powered environmental sensor system driven by nanogenerators, Energy & Environmental Science, 4 (2011) 3359-3363.

[56] L. Kong, B. Orr, K. Wise, Integrated electrostatically resonant scan tip for an atomic force microscope, Journal of Vacuum Science & Technology B: Microelectronics and Nanometer Structures Processing, Measurement, and Phenomena, 11 (1993) 634-641.

[57] R. Beach, T. McGill, Piezoelectric fields in nitride devices, Journal of Vacuum Science & Technology B: Microelectronics and Nanometer Structures Processing, Measurement, and Phenomena, 17 (1999) 1753-1756.

[58] J. Chu, Z. Wang, R. Maeda, K. Kataoka, T. Itoh, T. Suga, Novel multibridge-structured piezoelectric microdevice for scanning force microscopy, Journal of Vacuum Science & Technology B: Microelectronics and Nanometer Structures Processing, Measurement, and Phenomena, 18 (2000) 3604-3607.

[59] D.L. Churchill, M.J. Hamel, C.P. Townsend, S.W. Arms, Strain energy harvesting for wireless sensor networks, Smart Structures and Materials 2003, 5055 (2003) 319-327.

[60] F. Mohammadi, A. Khan, R.E. Cass, Power generation from piezoelectric lead zirconate titanate fiber composites, MRS Online Proceedings Library Archive, 736 (2002).

[61] C. Lee, J. Joo, G. Han, J. Lee, S. Koh, Poly (vinylidene fluoride) transducers with highly conducting poly (3, 4-ethylenedioxythiophene) electrodes, Synthetic metals, 152 (2005) 49-52.

[62] S.R. Anton, H.A. Sodano, A review of power harvesting using piezoelectric materials (2003–2006), Smart materials and Structures, 16 (2007) R1.

ACCEPTED MANUSCRIPT

[63] K. Mossi, C. Green, Z. Ounaies, E. Hughes, Harvesting energy using a thin unimorph prestressed bender: geometrical effects, Journal of Intelligent Material Systems and Structures, 16 (2005) 249-261.

[64] J. Kymissis, C. Kendall, J. Paradiso, N. Gershenfeld, Parasitic power harvesting in shoes, in: Wearable Computers, 1998. Digest of Papers. Second International Symposium on, IEEE, 1998, pp. 132-139.

[65] H.-S. Yoon, G. Washington, A. Danak, Modeling, optimization, and design of efficient initially curved piezoceramic unimorphs for energy harvesting applications, Journal of Intelligent Material Systems and Structures, 16 (2005) 877-883.

[66] A.D. Danak, H. S. Yoon, G.N. Washington, Optimization of electrical output in response to mechanical input in piezoceramic laminated shells, in: ASME 2003 International Mechanical Engineering Congress and Exposition, American Society of Mechanical Engineers, 2003, pp. 309-315.

[67] G. Poulin-Vittrant, C. Oshman, C. Opoku, A. Dahiya, N. Camara, D. Alquier, L.-P.T.H. Hue, M. Lethiecq, Fabrication and characterization of ZnO nanowire-based piezoelectric nanogenerators for low frequency mechanical energy harvesting, Physics Procedia, 70 (2015) 909-913.

[68] X. Wang, Piezoelectric nanogenerators-Harvesting ambient mechanical energy at the nanometer scale, Nano Energy, 1 (2012) 13-24.

[69] Z.L. Wang, Piezoelectric Nanogenerators for Self- Powered Nanosensors and Nanosystems, Wiley encyclopedia of electrical and electronics engineering, (2012) 1-20.

[70] R. Hinchet, Electromechanical study of semiconductor piezoelectric nanowires. Application to mechanical sensors and energy harvesters, Doctoral dissertation in Grenoble,

ACCEPTED MANUSCRIPT

2014.

[71] Y. Huang, X. Duan, Q. Wei, C.M. Lieber, Directed assembly of one-dimensional nanostructures into functional networks, Science, 291 (2001) 630-633.

[72] C.M. Lieber, One-dimensional nanostructures: chemistry, physics & applications, Solid State Communications, 107 (1998) 607-616.

[73] H. Tang, Y. Lin, C. Andrews, H.A. Sodano, Nanocomposites with increased energy density through high aspect ratio PZT nanowires, Nanotechnology, 22 (2010) 015702.

[74] A. Asthana, H. Ardakani, Y. Yap, R. Yassar, Real time observation of mechanically triggered piezoelectric current in individual ZnO nanobelts, Journal of Materials Chemistry C, 2 (2014) 3995-4004.

[75] M. Alexe, S. Senz, M.A. Schubert, D. Hesse, U. Gösele, Energy harvesting using nanowires?, Advanced Materials, 20 (2008) 4021-4026.

[76] D. Damjanovic, Hysteresis in piezoelectric and ferroelectric materials, The science of hysteresis, 3 (2006) 337-465.

[77] P.K. Yang, L. Lin, F. Yi, X. Li, K.C. Pradel, Y. Zi, C.I. Wu, H. He Jr, Y. Zhang, Z.L. Wang, A Flexible, Stretchable and Shape- Adaptive Approach for Versatile Energy Conversion and Self- Powered Biomedical Monitoring, Advanced Materials, 27 (2015) 3817-3824.

[78] Z.L. Wang, G. Zhu, Y. Yang, S. Wang, C. Pan, Progress in nanogenerators for portable electronics, Materials Today, 15 (2012) 532-543.

[79] G. Zhu, A.C. Wang, Y. Liu, Y. Zhou, Z.L. Wang, Functional electrical stimulation by nanogenerator with 58 V output voltage, Nano Letters, 12 (2012) 3086-3090.

[80] R. Yang, Y. Qin, C. Li, G. Zhu, Z.L. Wang, Converting biomechanical energy into

ACCEPTED MANUSCRIPT

electricity by a muscle-movement-driven nanogenerator, Nano Letters, 9 (2009) 1201-1205.

[81] S. Bai, L. Zhang, Q. Xu, Y. Zheng, Y. Qin, Z.L. Wang, Two dimensional woven nanogenerator, Nano Energy, 2 (2013) 749-753.

[82] S.M. Hatch, J. Briscoe, S. Dunn, A Self- Powered ZnO Nanorod/CuSCN UV Photodetector Exhibiting Rapid Response, Advanced Materials, 25 (2013) 867-871.

[83] Z.L. Wang, ZnO nanowire and nanobelt platform for nanotechnology, Materials Science and Engineering: R: Reports, 64 (2009) 33-71.

[84] M.-C. Daniel, D. Astruc, Gold nanoparticles: assembly, supramolecular chemistry, quantum-size-related properties, and applications toward biology, catalysis, and nanotechnology, Chemical Reviews, 104 (2004) 293-346.

[85] D. Ito, M.L. Jespersen, J.E. Hutchison, Selective growth of vertical ZnO nanowire arrays using chemically anchored gold nanoparticles, ACSNano, 2 (2008) 2001-2006.

[86] M. Skompska, K. Zarębska, Electrodeposition of ZnO nanorod arrays on transparent conducting substrates–a review, Electrochimica Acta, 127 (2014) 467-488.

[87] Y. Xi, J. Song, S. Xu, R. Yang, Z. Gao, C. Hu, Z.L. Wang, Growth of ZnO nanotube arrays and nanotube based piezoelectric nanogenerators, Journal of Materials Chemistry, 19 (2009) 9260-9264.

[88] P. Pandey, N. Singh, M.Z. Haque, Development and optical study of hexagonal multi-linked ZnO micro-rods grown using hexamine as capping agent, Optik-International Journal for Light and Electron Optics, 124 (2013) 1188-1191.

[89] K. Savarimuthu, G. Rajamanickam, R. Shankararajan, R. Perumal, A. Rayarfrancis, Experimental Study on Flexible ZnO Based Nanogenerator Using Schottky Contact for Energy Harvesting Applications, IEEE Transactions on Nanotechnology, 16 (2017) 469-476.

ACCEPTED MANUSCRIPT

[90] J. Liu, P. Fei, J. Song, X. Wang, C. Lao, R. Tummala, Z.L. Wang, Carrier density and Schottky barrier on the performance of DC nanogenerator, Nano Letters, 8 (2008) 328-332.

[91] T.S. van den Heever, W.J. Perold, The performance of nanogenerators fabricated on rigid and flexible substrates, Microelectronic Engineering, 112 (2013) 41-45.

[92] Y. Lin, Y. Liu, H.A. Sodano, Hydrothermal synthesis of vertically aligned lead zirconate titanate nanowire arrays, Applied Physics Letters, 95 (2009) 123501.

[93] A. Koka, H.A. Sodano, A low- frequency energy harvester from ultralong, vertically aligned BaTiO3 nanowire arrays, Advanced Energy Materials, 4 (2014).

[94] N.A. Hoque, P. Thakur, S. Roy, A. Kool, B. Bagchi, P. Biswas, M.M. Saikh, F. Khatun, S. Das, P.P. Ray, Er3+/Fe3+ Stimulated Electroactive, Visible Light Emitting, and High Dielectric Flexible PVDF Film Based Piezoelectric Nanogenerators: A Simple and Superior Self-Powered Energy Harvester with Remarkable Power Density, ACS Applied Materials & Interfaces, 9 (2017) 23048-23059.

[95] N. Jamond, P. Chrétien, L. Gatilova, E. Galopin, L. Travers, J.-C. Harmand, F. Glas, F. Houzé, N. Gogneau, Energy harvesting efficiency in GaN nanowire-based nanogenerators: the critical influence of the Schottky nanocontact, Nanoscale, 9 (2017) 4610-4619.

[96] Z.L. Wang, Triboelectric nanogenerators as new energy technology and self-powered sensors–Principles, problems and perspectives, Faraday discussions, 176 (2015) 447-458.

[97] X. S. Zhang, M. D. Han, B. Meng, H. X. Zhang, High performance triboelectric nanogenerators based on large-scale mass-fabrication technologies, Nano Energy, 11 (2015) 304-322.

[98] F. R. Fan, L. Lin, G. Zhu, W. Wu, R. Zhang, Z.L. Wang, Transparent triboelectric nanogenerators and self-powered pressure sensors based on micropatterned plastic films,

ACCEPTED MANUSCRIPT

Nano Letters, 12 (2012) 3109-3114.

[99] R. Hinchet, W. Seung, S.W. Kim, Recent progress on flexible triboelectric nanogenerators for selfpowered electronics, ChemSusChem, 8 (2015) 2327-2344.

[100] L. Lin, S. Wang, Y. Xie, Q. Jing, S. Niu, Y. Hu, Z.L. Wang, Segmentally structured disk triboelectric nanogenerator for harvesting rotational mechanical energy, Nano Letters, 13 (2013) 2916-2923.

[101] H. Yong, J. Chung, D. Choi, D. Jung, M. Cho, S. Lee, Highly reliable wind-rolling triboelectric nanogenerator operating in a wide wind speed range, Scientific Reports, 6 (2016) 33977.

[102] G. Zhu, Z.-H. Lin, Q. Jing, P. Bai, C. Pan, Y. Yang, Y. Zhou, Z.L. Wang, Toward large-scale energy harvesting by a nanoparticle-enhanced triboelectric nanogenerator, Nano Letters, 13 (2013) 847-853.

[103] X. S. Zhang, M. D. Han, R. X. Wang, F. Y. Zhu, Z. H. Li, W. Wang, H. X. Zhang, Frequency-multiplication high-output triboelectric nanogenerator for sustainably powering biomedical microsystems, Nano Letters, 13 (2013) 1168-1172.

[104] N. Kaur, J. Bahadur, V. Panwar, P. Singh, K. Rathi, K. Pal, Effective energy harvesting from a single electrode based triboelectric nanogenerator, Scientific Reports, 6 (2016) 38835.

[105] G. Zhu, J. Chen, T. Zhang, Q. Jing, Z.L. Wang, Radial-arrayed rotary electrification for high performance triboelectric generator, Nature Communications, 5 (2014) 3426.

[106] Q. Liang, X. Yan, Y. Gu, K. Zhang, M. Liang, S. Lu, X. Zheng, Y. Zhang, Highly transparent triboelectric nanogenerator for harvesting water-related energy reinforced by antireflection coating, Scientific Reports, 5 (2015) 9080.

[107] C. He, W. Zhu, B. Chen, L. Xu, T. Jiang, C.B. Han, G.Q. Gu, D. Li, Z.L. Wang, Smart

ACCEPTED MANUSCRIPT

floor with integrated triboelectric nanogenerator as energy harvester and motion sensor, ACS Applied Materials & Interfaces, 9 (2017) 26126-26133.

[108] T. Kim, J. Chung, D.Y. Kim, J.H. Moon, S. Lee, M. Cho, S.H. Lee, S. Lee, Design and optimization of rotating triboelectric nanogenerator by water electrification and inertia, Nano Energy, 27 (2016) 340-351.

[109] Y. Yang, G. Zhu, H. Zhang, J. Chen, X. Zhong, Z.-H. Lin, Y. Su, P. Bai, X. Wen, Z.L. Wang, Triboelectric nanogenerator for harvesting wind energy and as self-powered wind vector sensor system, ACS Nano, 7 (2013) 9461-9468.

[110] Y. Xie, S. Wang, S. Niu, L. Lin, Q. Jing, Y. Su, Z. Wu, Z.L. Wang, Multi-layered disk triboelectric nanogenerator for harvesting hydropower, Nano Energy, 6 (2014) 129-136.

[111] Y. Xie, S. Wang, L. Lin, Q. Jing, Z.-H. Lin, S. Niu, Z. Wu, Z.L. Wang, Rotary triboelectric nanogenerator based on a hybridized mechanism for harvesting wind energy, ACS Nano, 7 (2013) 7119-7125.

[112] Z.L. Wang, J. Chen, L. Lin, Progress in triboelectric nanogenerators as a new energy technology and self-powered sensors, Energy & Environmental Science, 8 (2015) 2250-2282.

[113] Y. Li, G. Cheng, Z.-H. Lin, J. Yang, L. Lin, Z.L. Wang, Single-electrode-based rotationary triboelectric nanogenerator and its applications as self-powered contact area and eccentric angle sensors, Nano Energy, 11 (2015) 323-332.

[114] M.Y. Choi, D. Choi, M.J. Jin, I. Kim, S.H. Kim, J.Y. Choi, S.Y. Lee, J.M. Kim, S.W. Kim, Mechanically powered transparent flexible charge- generating nanodevices with piezoelectric ZnO nanorods, Advanced Materials, 21 (2009) 2185-2189.

[115] Q. Liao, Z. Zhang, X. Zhang, M. Mohr, Y. Zhang, H.-J. Fecht, Flexible piezoelectric nanogenerators based on a fiber/ZnO nanowires/paper hybrid structure for energy harvesting,

ACCEPTED MANUSCRIPT

Nano Res., 7 (2014) 917-928.

[116] Y. Qin, X. Wang, Z.L. Wang, Microfibre-nanowire hybrid structure for energy scavenging, Nature, 451 (2008) 809.

[117] Z. Li, Z.L. Wang, Air/Liquid- Pressure and Heartbeat- Driven Flexible Fiber Nanogenerators as a Micro/Nano- Power Source or Diagnostic Sensor, Advanced Materials, 23 (2011) 84-89.

[118] X. Lu, H. Qu, M. Skorobogatiy, Piezoelectric Micro and Nanostructured Fibers Fabricated from Thermoplastic Nanocomposites Using a Fiber Drawing Technique: Comparative Study and Potential Applications, ACS Nano, 11 (2017) 2103-2114.

[119] J. Yang, J. Chen, Y. Su, Q. Jing, Z. Li, F. Yi, X. Wen, Z. Wang, Z.L. Wang, Eardrum- Inspired Active Sensors for Self- Powered Cardiovascular System Characterization and Throat- Attached Anti- Interference Voice Recognition, Advanced Materials, 27 (2015) 1316-1326.

[120] G. Zhu, W.Q. Yang, T. Zhang, Q. Jing, J. Chen, Y.S. Zhou, P. Bai, Z.L. Wang, Self-powered, ultrasensitive, flexible tactile sensors based on contact electrification, Nano Letters, 14 (2014) 3208-3213.

[121] Y. Hu, Y. Zhang, C. Xu, G. Zhu, Z.L. Wang, High-output nanogenerator by rational unipolar assembly of conical nanowires and its application for driving a small liquid crystal display, Nano Letters, 10 (2010) 5025-5031.

[122] S. Xu, Y. Qin, C. Xu, Y. Wei, R. Yang, Z.L. Wang, Self-powered nanowire devices, Nature Nanotechnology, 5 (2010) 366-373.

[123] B. Saravanakumar, S. J. Kim, Growth of 2D ZnO nanowall for energy harvesting application, The Journal of Physical Chemistry C, 118 (2014) 8831-8836.

ACCEPTED MANUSCRIPT

[124] N. Cui, W. Wu, Y. Zhao, S. Bai, L. Meng, Y. Qin, Z.L. Wang, Magnetic force driven nanogenerators as a noncontact energy harvester and sensor, Nano Letters, 12 (2012) 3701-3705.

[125] Y. Hu, Y. Zhang, C. Xu, L. Lin, R.L. Snyder, Z.L. Wang, Self-powered system with wireless data transmission, Nano Letters, 11 (2011) 2572-2577.

[126] J. Song, X. Wang, J. Liu, H. Liu, Y. Li, Z.L. Wang, Piezoelectric potential output from ZnO nanowire functionalized with p-type oligomer, Nano Letters, 8 (2008) 203-207.

[127] J. Briscoe, M. Stewart, M. Vopson, M. Cain, P.M. Weaver, S. Dunn, Nanostructured p- n Junctions for Kinetic- to- Electrical Energy Conversion, Advanced Energy Materials, 2 (2012) 1261-1268.

[128] Y. Qiu, H. Zhang, L. Hu, D. Yang, L. Wang, B. Wang, J. Ji, G. Liu, X. Liu, J. Lin, Flexible piezoelectric nanogenerators based on ZnO nanorods grown on common paper substrates, Nanoscale, 4 (2012) 6568-6573.

[129] H. Kim, S.M. Kim, H. Son, H. Kim, B. Park, J. Ku, J.I. Sohn, K. Im, J.E. Jang, J.-J. Park, Enhancement of piezoelectricity via electrostatic effects on a textile platform, Energy & Environmental Science, 5 (2012) 8932-8936.

[130] K. H. Kim, B. Kumar, K.Y. Lee, H. K. Park, J.-H. Lee, H.H. Lee, H. Jun, D. Lee, S.-W. Kim, Piezoelectric two-dimensional nanosheets/anionic layer heterojunction for efficient direct current power generation, Scientific Reports, 3 (2013) 2017.

[131] H. Sun, H. Tian, Y. Yang, D. Xie, Y. C. Zhang, X. Liu, S. Ma, H. M. Zhao, T. L. Ren, A novel flexible nanogenerator made of ZnO nanoparticles and multiwall carbon nanotube, Nanoscale, 5 (2013) 6117-6123.

[132] K. I. Park, S.B. Bae, S.H. Yang, H.I. Lee, K. Lee, S.J. Lee, Lead-free BaTiO 3

ACCEPTED MANUSCRIPT

nanowires-based flexible nanocomposite generator, Nanoscale, 6 (2014) 8962-8968.

[133] K.I. Park, M. Lee, Y. Liu, S. Moon, G.T. Hwang, G. Zhu, J.E. Kim, S.O. Kim, D.K. Kim, Z.L. Wang, Flexible nanocomposite generator made of BaTiO3 nanoparticles and graphitic carbons, Advanced Materials, 24 (2012) 2999-3004.

[134] M. H. Seo, J. Y. Yoo, S. Y. Choi, J. S. Lee, K. W. Choi, C.K. Jeong, K.J. Lee, J. B. Yoon, Versatile Transfer of an Ultralong and Seamless Nanowire Array Crystallized at High Temperature for Use in High-Performance Flexible Devices, ACSNano, 11 (2017) 1520-1529.

[135] H.B. Kang, J. Chang, K. Koh, L. Lin, Y.S. Cho, High quality Mn-doped (Na, K) NbO3 nanofibers for flexible piezoelectric nanogenerators, ACS Applied Materials & Interfaces, 6 (2014) 10576-10582.

[136] P.G. Kang, B.K. Yun, K.D. Sung, T.K. Lee, M. Lee, N. Lee, S.H. Oh, W. Jo, H.J. Seog, C.W. Ahn, Piezoelectric power generation of vertically aligned lead-free (K, Na) NbO 3 nanorod arrays, RSC Advances, 4 (2014) 29799-29805.

[137] C.K. Jeong, K.I. Park, J. Ryu, G.T. Hwang, K.J. Lee, Large- Area and Flexible Lead- Free Nanocomposite Generator Using Alkaline Niobate Particles and Metal Nanorod Filler, Advanced Functional Materials, 24 (2014) 2620-2629.

[138] S. H. Park, H.B. Lee, S.M. Yeon, J. Park, N.K. Lee, Flexible and stretchable piezoelectric sensor with thickness-tunable configuration of electrospun nanofiber mat and elastomeric substrates, ACS Applied Materials & Interfaces, 8 (2016) 24773-24781.

[139] X. Ren, H. Fan, Y. Zhao, Z. Liu, Flexible lead-free BiFeO3/PDMS-based nanogenerator as piezoelectric energy harvester, ACS Applied Materials & Interfaces, 8 (2016) 26190-26197.

ACCEPTED MANUSCRIPT

[140] Q. L. Zhao, G. P. He, J. J. Di, W. L. Song, Z. L. Hou, P. P. Tan, D. W. Wang, M. S. Cao, Flexible Semitransparent Energy Harvester with High Pressure Sensitivity and Power Density Based on Laterally Aligned PZT Single-Crystal Nanowires, ACS Applied Materials & Interfaces, 9 (2017) 24696-24703.

[141] K.S. Chary, H.S. Panda, C.D. Prasad, Fabrication of Large Aspect Ratio Ba0. 85Ca0. 15Zr0. 1Ti0. 9O3 Superfine Fibers Based Flexible Nanogenerator Device: Synergistic Effect on Curie Temperature, Harvested Voltage and Power, Industrial & Engineering Chemistry Research, 56(2017) 10335-10342.

[142] Y.B. Lee, J.K. Han, S. Noothongkaew, S.K. Kim, W. Song, S. Myung, S.S. Lee, J. Lim, S.D. Bu, K.S. An, Toward Arbitrary- Direction Energy Harvesting through Flexible Piezoelectric Nanogenerators Using Perovskite PbTiO3 Nanotube Arrays, Advanced Materials, 29 (2017) 1604500.

[143] G. H. Nam, S. H. Baek, C. H. Cho, I. K. Park, A flexible and transparent graphene/ZnO nanorod hybrid structure fabricated by exfoliating a graphite substrate, Nanoscale, 6 (2014) 11653-11658.

[144] M.A. Rahman, B. C. Lee, D. T. Phan, G. S. Chung, Fabrication and characterization of highly efficient flexible energy harvesters using PVDF–graphene nanocomposites, Smart Materials and Structures, 22 (2013) 085017.

[145] Y. Mao, P. Zhao, G. McConohy, H. Yang, Y. Tong, X. Wang, Sponge- Like Piezoelectric Polymer Films for Scalable and Integratable Nanogenerators and Self- Powered Electronic Systems, Advanced Energy Materials, 4 (2014) 1301624.

[146] C. Chang, V.H. Tran, J. Wang, Y. K. Fuh, L. Lin, Direct-write piezoelectric polymeric nanogenerator with high energy conversion efficiency, Nano Letters, 10 (2010) 726-731.

ACCEPTED MANUSCRIPT

[147] J. Chang, M. Dommer, C. Chang, L. Lin, Piezoelectric nanofibers for energy scavenging applications, Nano Energy, 1 (2012) 356-371.

[148] Y. Yang, H. Zhang, G. Zhu, S. Lee, Z. H. Lin, Z.L. Wang, Flexible hybrid energy cell for simultaneously harvesting thermal, mechanical, and solar energies, ACSNano, 7 (2012) 785-790.

[149] S.A. Khan, H.L. Zhang, Y. Xie, M. Gao, M.A. Shah, A. Qadir, Y. Lin, Flexible Triboelectric Nanogenerator Based on Carbon Nanotubes for Self- Powered Weighing, Advanced Engineering Materials, 19 (2017) 1600710.

[150] Y. Zhu, B. Yang, J. Liu, X. Wang, L. Wang, X. Chen, C. Yang, A flexible and biocompatible triboelectric nanogenerator with tunable internal resistance for powering wearable devices, Scientific Reports, 6 (2016) 22233.

[151] S.L. Zhang, Y.C. Lai, X. He, R. Liu, Y. Zi, Z.L. Wang, Auxetic Foam- Based Contact- Mode Triboelectric Nanogenerator with Highly Sensitive Self- Powered Strain Sensing Capabilities to Monitor Human Body Movement, Advanced Functional Materials, (2017) 1606695.

[152] T. Zhou, Z.W. Yang, Y. Pang, L. Xu, C. Zhang, Z.L. Wang, Tribotronic tuning diode for active analog signal modulation, ACSNano, 11 (2016) 882-888.

[153] Y.C. Lai, J. Deng, S.L. Zhang, S. Niu, H. Guo, Z.L. Wang, Single- Thread- Based Wearable and Highly Stretchable Triboelectric Nanogenerators and Their Applications in Cloth- Based Self- Powered Human- Interactive and Biomedical Sensing, Advanced Functional Materials, 27 (2017) 1604462.

[154] W. Seung, M.K. Gupta, K.Y. Lee, K.-S. Shin, J.-H. Lee, T.Y. Kim, S. Kim, J. Lin, J.H. Kim, S.-W. Kim, Nanopatterned textile-based wearable triboelectric nanogenerator, ACS

ACCEPTED MANUSCRIPT

Nano, 9 (2015) 3501-3509.

[155] S. Wang, L. Lin, Y. Xie, Q. Jing, S. Niu, Z.L. Wang, Sliding-triboelectric nanogenerators based on in-plane charge-separation mechanism, Nano Letters, 13 (2013) 2226-2233.

[156] B.N. Chandrashekar, B. Deng, A.S. Smitha, Y. Chen, C. Tan, H. Zhang, H. Peng, Z. Liu, Roll- to- roll green transfer of CVD graphene onto plastic for a transparent and flexible triboelectric nanogenerator, Advanced Materials, 27 (2015) 5210-5216.

[157] F. Yi, L. Lin, S. Niu, P.K. Yang, Z. Wang, J. Chen, Y. Zhou, Y. Zi, J. Wang, Q. Liao, Stretchable- rubber- based triboelectric nanogenerator and its application as self- powered body motion sensors, Advanced Functional Materials, 25 (2015) 3688-3696.

[158] L. Zheng, Y. Wu, X. Chen, A. Yu, L. Xu, Y. Liu, H. Li, Z.L. Wang, Self- Powered Electrostatic Actuation Systems for Manipulating the Movement of both Microfluid and Solid Objects by Using Triboelectric Nanogenerator, Advanced Functional Materials, 27 (2017).

[159] Q. Leng, H. Guo, X. He, G. Liu, Y. Kang, C. Hu, Y. Xi, Flexible interdigital-electrodes-based triboelectric generators for harvesting sliding and rotating mechanical energy, Journal of Materials Chemistry A, 2 (2014) 19427-19434.

[160] J. Xiong, M.F. Lin, J. Wang, S.L. Gaw, K. Parida, P.S. Lee, Wearable All- Fabric- Based Triboelectric Generator for Water Energy Harvesting, Advanced Energy Materials, (2017).

[161] S.W. Chen, X. Cao, N. Wang, L. Ma, H.R. Zhu, M. Willander, Y. Jie, Z.L. Wang, An ultrathin flexible single- electrode triboelectric- nanogenerator for mechanical energy harvesting and instantaneous force sensing, Advanced Energy Materials, 7 (2017) 1601255.

[162] H. Guo, T. Li, X. Cao, J. Xiong, Y. Jie, M. Willander, X. Cao, N. Wang, Z.L. Wang,

ACCEPTED MANUSCRIPT

Self-Sterilized Flexible Single-Electrode Triboelectric Nanogenerator for Energy Harvesting and Dynamic Force Sensing, ACS Nano, 11 (2017) 856-864.

[163] X. Cheng, L. Miao, Z. Su, H. Chen, Y. Song, X. Chen, H. Zhang, Controlled fabrication of nanoscale wrinkle structure by fluorocarbon plasma for highly transparent triboelectric nanogenerator, Microsystems & Nanoengineering, 3 (2017) 16074.

[164] K. Zhang, S. Wang, Y. Yang, A One-Structure-Based Piezo-Tribo-Pyro-Photoelectric Effects Coupled Nanogenerator for Simultaneously Scavenging Mechanical, Thermal, and Solar Energies, Advanced Energy Materials, 7 (2017) 1601852.

[165] C. Xu, C. Pan, Y. Liu, Z.L. Wang, Hybrid cells for simultaneously harvesting multi-type energies for self-powered micro/nanosystems, Nano Energy, 1 (2012) 259-272.

[166] X. Wang, B. Yang, J. Liu, Y. Zhu, C. Yang, Q. He, A flexible triboelectric-piezoelectric hybrid nanogenerator based on P (VDF-TrFE) nanofibers and PDMS/MWCNT for wearable devices, Scientific Reports, 6 (2016) 36409.

[167] C. Xu, X. Wang, Z.L. Wang, Nanowire structured hybrid cell for concurrently scavenging solar and mechanical energies, Journal of the American Chemical Society, 131 (2009) 5866-5872.

[168] C. Xu, Z.L. Wang, Compact hybrid cell based on a convoluted nanowire structure for harvesting solar and mechanical energy, Advanced Materials, 23 (2011) 873-877.

[169] G. Suo, Y. Yu, Z. Zhang, S. Wang, P. Zhao, J. Li, X. Wang, Piezoelectric and Triboelectric Dual Effects in Mechanical-Energy Harvesting Using BaTiO3/Polydimethylsiloxane Composite Film, ACS Applied Materials & Interfaces, 8 (2016) 34335-34341.

ACCEPTED MANUSCRIPT

[170] W. S. Jung, M. G. Kang, H.G. Moon, S. H. Baek, S.-J. Yoon, Z. L. Wang, S. W. Kim, C. Y. Kang, High output piezo/triboelectric hybrid generator, Scientific Reports, 5 (2015) 9309.

[171] X. Wang, Z. Wen, H. Guo, C. Wu, X. He, L. Lin, X. Cao, Z.L. Wang, Fully packaged blue energy harvester by hybridizing a rolling triboelectric nanogenerator and an electromagnetic generator, ACS Nano, 10 (2016) 11369-11376.

[172] S. Wang, Z.L. Wang, Y. Yang, A One- Structure- Based Hybridized Nanogenerator for Scavenging Mechanical and Thermal Energies by Triboelectric–Piezoelectric–Pyroelectric Effects, Advanced Materials, 28 (2016) 2881-2887.

[173] C. Pan, L. Dong, G. Zhu, S. Niu, R. Yu, Q. Yang, Y. Liu, Z.L. Wang, High-resolution electroluminescent imaging of pressure distribution using a piezoelectric nanowire LED array, Nature Photonics, 7 (2013) 752-758.

[174] X. Wang, W. Peng, R. Yu, H. Zou, Y. Dai, Y. Zi, C. Wu, S. Li, Z.L. Wang, Simultaneously Enhancing Light Emission and Suppressing Efficiency Droop in GaN Microwire-Based UV LED by the Piezo-Phototronic Effect, Nano Letters, 17(2017) 3718-3724.

[175] X. Pu, M. Liu, X. Chen, J. Sun, C. Du, Y. Zhang, J. Zhai, W. Hu, Z.L. Wang, Ultrastretchable, transparent triboelectric nanogenerator as electronic skin for biomechanical energy harvesting and tactile sensing, Science Advances, 3 (2017) e1700015.

[176] Z. Yuan, T. Zhou, Y. Yin, R. Cao, C. Li, Z.L. Wang, Transparent and Flexible Triboelectric Sensing Array for Touch Security Applications, ACS Nano, 11 (2017) 8364-8369.

[177] P.G. Rosquist, G. Collins, A.J. Merrell, N.J. Tuttle, J.B. Tracy, E.T. Bird, M.K. Seeley, D.T. Fullwood, W.F. Christensen, A.E. Bowden, Estimation of 3D Ground Reaction Force

ACCEPTED MANUSCRIPT

Using Nanocomposite Piezo-Responsive Foam Sensors During Walking, Annals of Biomedical Engineering, (2017) 1-13.

[178] Y. Yang, Y. Zhou, J.M. Wu, Z.L. Wang, Single micro/nanowire pyroelectric nanogenerators as self-powered temperature sensors, ACS Nano, 6 (2012) 8456-8461.

[179] M. Al Ahmad, Piezoelectric extraction of ECG signal, Scientific Reports, 6 (2016) 37093.

[180] G. Jiji, A retrospect on the role of piezoelectric nanogenerators in the development of the green world, RSC Advances, 7 (2017) 33642-33670.

[181] C. Dagdeviren, B.D. Yang, Y. Su, P.L. Tran, P. Joe, E. Anderson, J. Xia, V. Doraiswamy, B. Dehdashti, X. Feng, Conformal piezoelectric energy harvesting and storage from motions of the heart, lung, and diaphragm, Proceedings of the National Academy of Sciences, 111 (2014) 1927-1932.

[182] G.T. Hwang, H. Park, J.H. Lee, S. Oh, K.I. Park, M. Byun, H. Park, G. Ahn, C.K. Jeong, K. No, Nanogenerators: Self- Powered Cardiac Pacemaker Enabled by Flexible Single Crystalline PMN- PT Piezoelectric Energy Harvester (Adv. Mater. 28/2014), Advanced Materials, 26 (2014) 4754-4754.

[183] G.T. Hwang, H. Park, J.H. Lee, S. Oh, K.I. Park, M. Byun, H. Park, G. Ahn, C.K. Jeong, K. No, Self- powered cardiac pacemaker enabled by flexible single crystalline PMN- PT piezoelectric energy harvester, Advanced Materials, 26 (2014) 4880-4887.

[184] Z. Li, G. Zhu, R. Yang, A.C. Wang, Z.L. Wang, Muscle- driven in vivo nanogenerator, Advanced Materials, 22 (2010) 2534-2537.

[185] D.B. Deutz, N.T. Mascarenhas, J.B.J. Schelen, D.M. de Leeuw, S. van der Zwaag, P. Groen, Flexible Piezoelectric Touch Sensor by Alignment of Lead- Free Alkaline Niobate

ACCEPTED MANUSCRIPT

Microcubes in PDMS, Advanced Functional Materials, 27(2017) 1700728.

[186] K. Zhao, Y. Yang, X. Liu, Z.L. Wang, Triboelectrification- Enabled Self- Charging Lithium- Ion Batteries, Advanced Energy Materials, 7(2017) 1700103.

[187] W. Li, D. Torres, R. Díaz, Z. Wang, C. Wu, C. Wang, Z.L. Wang, N. Sepúlveda, Nanogenerator-based dual-functional and self-powered thin patch loudspeaker or microphone for flexible electronics, Nature communications, 8 (2017) 15310.

[188] Z.L. Wang, On Maxwell's displacement current for energy and sensors: the origin of nanogenerators, Mater. Today, 20 (2017) 74.

[189] Y. Zi, H. Guo, J. Wang, Z. Wen, S. Li, C. Hu, Z.L. Wang, An inductor-free auto-power-management design built-in triboelectric nanogenerators, Nano Energy, 31 (2017) 302-310.

[190] Z.L. Wang, On Maxwell's displacement current for energy and sensors: the origin of nanogenerators, Mater. Today, 20 (2017) 74-82.

[191] Z. Wen, H. Guo, Y. Zi, M.-H. Yeh, X. Wang, J. Deng, J. Wang, S. Li, C. Hu, L. Zhu, Harvesting broad frequency band blue energy by a triboelectric–electromagnetic hybrid nanogenerator, ACS Nano, 10 (2016) 6526-6534.

[192] U. Khan, S.-W. Kim, Triboelectric nanogenerators for blue energy harvesting, ACS Nano, 10 (2016) 6429-6432.

[193] C. He, C.B. Han, G.Q. Gu, T. Jiang, B.D. Chen, Z.L. Gao, Z.L. Wang, Hourglass Triboelectric Nanogenerator as a "Direct Current" Power Source, Advanced Energy Materials, 7(2017) 1700644.

[194] F. Chaabouni, M. Abaab, B. Rezig, Metrological characteristics of ZnO oxygen sensor at room temperature, Sensors and Actuators B: Chemical, 100 (2004) 200-204.

[195] Z. Fan, D. Wang, P.-C. Chang, W. Y. Tseng, J.G. Lu, ZnO nanowire field-effect

ACCEPTED MANUSCRIPT

transistor and oxygen sensing property, Applied Physics Letters, 85 (2004) 5923-5925.

[196] X. Xue, Y. Nie, B. He, L. Xing, Y. Zhang, Z.L. Wang, Surface free carrier screening effect on the output of a ZnO nanowire nanogenerator and its potential as a self-powered active gas sensor, Nanotechnology, 24 (2013) 225501.

[197] V. Nguyen, R. Zhu, R. Yang, Environmental effects on nanogenerators, Nano Energy, 14 (2015) 49-61.

[198] G.H. Haertling, Ferroelectric ceramics: history and technology, Journal of the American Ceramic Society, 82 (1999) 797-818.

[199] J. Pritchard, C. Bowen, F. Lowrie, Multilayer actuators, British Ceramic Transactions, 100 (2001) 265-273.

[200] C. Sanchez, B. Julián, P. Belleville, M. Popall, Applications of hybrid organic–inorganic nanocomposites, Journal of Materials Chemistry, 15 (2005) 3559-3592.

[201] J. Pollock, The true cost of hermetic seals for aluminum housings, Microwave Journal, 40 (1997) 138-143.

[202] W. Chen, H.L. Chan, F. Yin, K. Ng, P. Liu, Water-induced degradation in lead zirconate titanate piezoelectric ceramics, Applied Physics Letters, 80 (2002) 3587-3589.

[203] C. Chan, F. Yeung. Electrical failure of multilayer ceramic capacitors subjected to environmental screening testing, IEEE Transactions on Components, Packaging, and Manufacturing Technology: Part C, 19 (1996) 138-143.

[204] L. Chen, X. Xiong, H. Meng, P. Lv, J. Zhang, Migration and redistribution of oxygen vacancy in barium titanate ceramics, Applied Physics Letters, 89 (2006) 071916.

[205] J.W. Peterson, The Influence of Piezo-Electrification on Tribo-Electrification, Physical Review, 76 (1949) 1882.

ACCEPTED MANUSCRIPT

[206] S. Zhang, F. Yu, Piezoelectric materials for high temperature sensors, Journal of the American Ceramic Society, 94 (2011) 3153-3170.

[207] I. Lipscomb, P. Weaver, J. Swingler, J. McBride, The effect of relative humidity, temperature and electrical field on leakage currents in piezo-ceramic actuators under dc bias, Sensors and Actuators A: Physical, 151 (2009) 179-186.

[208] F.D. Morrison, D.C. Sinclair, J. Skakle, A.R. West, Novel Doping Mechanism for Very- High- Permittivity Barium Titanate Ceramics, Journal of the American Ceramic Society, 81 (1998) 1957-1960.

[209] S. Matsusaka, H. Maruyama, T. Matsuyama, M. Ghadiri, Triboelectric charging of powders: A review, Chemical Engineering Science, 65 (2010) 5781-5807.

[210] B. D. Yan, S. Meilink, G. Warren, P. Wynblatt, Water adsorption and surface conductivity measurements on alpha-alumina substrates, IEEE transactions on components, hybrids, and manufacturing technology, 10 (1987) 247-251.

[211] Z.L. Wang, Piezopotential gated nanowire devices: Piezotronics and piezo-phototronics, Nano Today, 5 (2010) 540-552.

[212] S. Pearton, D. Norton, K. Ip, Y. Heo, T. Steiner, Recent progress in processing and properties of ZnO, Progress in Materials Science, 50 (2005) 293-340.

[213] S.R. Morrison, Semiconductor gas sensors, Sensors and Actuators, 2 (1981) 329-341.

[214] R. Caliò, U.B. Rongala, D. Camboni, M. Milazzo, C. Stefanini, G. De Petris, C.M. Oddo, Piezoelectric energy harvesting solutions, Sensors, 14 (2014) 4755-4790.

[215] S.-H. Shin, Y.H. Kwon, Y.-H. Kim, J.-Y. Jung, M.H. Lee, J. Nah, Triboelectric charging sequence induced by surface functionalization as a method to fabricate high performance triboelectric generators, ACS Nano, 9 (2015) 4621-4627.

ACCEPTED MANUSCRIPT

[216] Z.L. Wang, L. Lin, J. Chen, S. Niu, Y. Zi, Triboelectric Nanogenerators, Berlin, Heidelberg, Germany: Springer International Publishing, 2016.

Figure captions

Fig. 1 Working principle of (a) Piezoelectric Energy Harvesting Nanogenerators (PENG); polarization (P) conditions and directions (b) Without an applied force, pressure or strain (c) During an applied force (d) After the applied force is removed.

Fig. 2 (a) Schematic of traditional (i) Bimorph structure (ii) Unimorph structure based piezoelectric energy harvesters inspired from Ref[56] (b) Cross section of integrated electrostatically resonant scan tip for an atomic force microscope during 1993[56] *@ AIP Copyright permission* (c) Strain induced piezoelectric polarization induces a compensating two-dimensional electron gas (2DEG) at the AlGaN–GaN interface[57]*@ Copyright permission 1999 from AIP* (d)(i) SEM of piezoelectric micro-SFM, (ii) SFM force curve using the micro-fabricated device: *y* axis indicates piezoelectric current change, which is proportional to the cantilever vibration amplitude; *x* axis indicates frequencies of driving voltages applied to the PZT layers[58] *@Copyright permission 2000 from AIP.*

Fig. 3 (a)(i) ZnO NW nanogenerator (ii) SEM of device structure after spin-coating a PMMA on grown NWs with cross-sectional view (iii) SEM of coverage of NWs by the PMMA layer (iv-v) Nanogenerator activated manually (vi) Open-circuit voltage of the nanogenerator rectified by a bridge rectifier under a stress of 1 MPa and enlarged view of one cycle in the shadowed region (inset)[78]*@ Copyright permission2012 from ACS* (b) ZnO NR based PENG device setup shown in (i), (ii) Image of device and (iii) Connection view for measurements. (iv) Self-assembled GaN NWs grown on n-type doped Si(111) substrates (resistivity ~0.007 Ω·cm) (v) Variation of average output voltage generated by GaN NWs and harvested by the different AFM tips as a function of the constant normal force[95]*@ Copyright permission 2017 from RSC.*

Fig. 4 (a) Schematic of the PZT nanofiber nanogenerator in (i), (ii) Cross-section of poled PZT nanofiber in the generator, (iii) Schematic of power output mechanism of the PZT nanofibers in longitudinal mode. Color presents stress level in PDMS due to a pressure on top

ACCEPTED MANUSCRIPT

surface. (iv) Open circuit voltage from free vibration of a Teflon cantilever setup[39]@ *Copyright permission 2010 from ACS.* (b) $BaTiO_3$ NW energy harvester, (i) Schematic. (ii) Cross-sectional SEM of $BaTiO_3$ NW arrays. (iii) $BaTiO_3$ NW array based nanogenerator and energy harvesting device, which is smaller than a dime coin[93]@ *Copyright permission 2014 from Wiley*.

Fig. 5 Principle modes of triboelectric nanogenerators (TENGs) (a) Vertical contact-separation mode (b) Lateral sliding mode (c) Single-electrode mode and (d) Freestanding triboelectric-layer mode (inspired from Ref [99]).

Fig. 6 (a)(i) Schematic of disk TENG device. The inset (bottom left) is an enlarged figure of Kapton nanorod array on the surface area. (ii) Image of the two parts of a real disk TENG. (iii) Relationship between the open-circuit voltage/slope of the voltage and rotation speed. (iv) Schematic of working principle of the disk TENG with an electrons flow diagram in four consecutive stages within a full cycle of electricity generation at rotating speeds from 50 to 500 rpm; (v) Open-circuit voltage, (vi) Measured transferred charge density and (vii) Measured short-circuit current density[100]@ *Copyright permission 2013 from ACS*.

Fig. 7 (a) Schematic of the wind rolling triboelectric nanogenerator (WR-TENG) shown in (i), (ii) Expanded polystyrenesphere rotating inside the WR-TENG (air flow velocity of 2.2 ms^{-1}) (iii) Rolling I_{CC} outputs based on the sphere-electrode size ratio[101] @*Copyright permission 2014 from Nature*. (b) (i) Fabricated triboelectric NG, (ii) Electric energy generated by the current pulse in part a, which is equal to the Joule heating from the resistor of 1 M Ω. (iii-iv) Image of setup in which the NG acts as a direct power source for 200 green, red and blue LED bulbs, respectively and the estimated output open circuit voltage is ~ 1200 V[102]@ *Copyright permission 2013 from ACS*.

Fig. 8 Images of (a) rGO NRs/PVDF triboelectric nanogenerator top and side view[104]@ *Copyright permission 2016 from Nature* (b) Rotary electrification for high performance triboelectric generator[105]@ *Copyright permission 2014 from Nature* (c) Transparent TENG (T-TENG) placed above a paper with alphabets on it. Bottom image is comparison of the T-TENG and the TENG composed of a commercial 50 μm PTFE film[106]@ *Copyright permission 2015 from Nature*. (d)Smart Floor with Integrated Triboelectric Nanogenerator[107]@ *Copyright permission 2017 from ACS.* (e) (i-ii) Design of rotating triboelectric nanogenerator lighting up 30 LED's[108]@ *Copyright permission 2016 from Elsevier* (f) Side and cross sectional view of wind energy harvesting TENG[109] shown in (i-ii)@ *Copyright permission 2013 from ACS.* (g) Image of multi-layered disk TENG coupled with a water turbine for harvesting water flow energy and lighting up 100 LEDs in (i). (ii) M-TENG energy harvesting system showing the detailed structural design (iii) Real-time measurement of current signal of the system[110]@ *Copyright permission 2014 from Elsevier* (h) Structure of the rotary triboelectric nanogenerator (R-TENG) with the enlarged image of nanowire-like structures on the surface of PTFE[111]@ *Copyright permission 2013 from ACS*.

Fig. 9 (a) ZnO fiber-based PENG (i) Experimental set-up (ii) SEM of 'teeth-to-teeth' interface of two fibers covered by nanowires (NWs), top coated with Au (iii) Schematic of

ACCEPTED MANUSCRIPT

the teeth-to-teeth contact between two fibers (iv) Piezoelectric potential created across nanowires I and II on pulling the top fiber by an external force. (v) When the top fiber is pulled, the Au-coated nanowires rubs across the uncoated nanowires, resulting in output of electric current, as indicated by arrowheads. (vi) Enhancement of output current by reducing the inner resistance (Ri) of the nanogenerator[116]@ *Copyright permission 2008 from Nature*.

Fig. 10 (a) (i) Schematic and (ii) photo of a BTO-PVDF based PENG in bent state (iii-iv) Open-circuit voltage and short circuit current of the PENG during bend and release actions. Equivalent circuits are inserted in the graphs[118]@ *Copyright permission 2017 from ACS*. (b). (i-ii) Flexible $BaTiO_3$ nanogenerator (area ~ 82 mm^2 and filling factor of 16.4%) supported on a plastic substrate after PDMS is peeled off (iii-iv) Energy harvesting during periodic bending and unbending on forward bias condition[40]@ *Copyright permission 2010 from ACS*. (C). (c) (i) Photograph of the p-NC stretched by tweezers. Inset shows NCG device (3 cm x 4 cm) bent by fingers. (ii) Large-area type NCG device (13 cm x 13 cm) fabricated by spin-casting or Mylar bar-coating. (iii) Schematic of the cross sectional structure of NCG devices and calculated piezo-potential distributions for explaining the role of CNTs. The CNTs act as dispersing agent (*insert* (ii) and stress reinforcing agents (v) which are well supported by the calculated piezo potential difference (iii and vi))[133]@ *Copyright permission 2012 from Wiley*. (d) (i) Schematic and images of a flexible PENG for skin deflection by arterial distension (ii) Real-time sensor output waveforms measured from radial and carotid pulses[138]@ *Copyright permission 2016 from ACS*.

Fig. 11 (a) $BiFeO_3$-PDMS composite based PENG bent by fingers shown in (i). (ii) Red and green LEDs driven from hand pressing and release (iii) Durability test of the PENG. Inset shows an enlarged view of the open circuit voltage signal in the durability test process[139]@ *Copyright permission 2016 from ACS*. (b) Flexible semitransparent energy harvester with high pressure sensitivity in (i). (ii) FE-SEM image of the PZT NWs laterally aligned on electrodes. (iii) FTPH with large bending. (iv) Pressure dependence of output AC voltage and its linear fit[140]@ *Copyright permission 2017 from ACS*. (c) Nanofibers mat based PENG during tapping in (i). (ii) Measured output voltage during tapping (iii) Nanofibers mat based PENG during bending and (iv) Measured output voltage during bending[141]@ *Copyright permission 2017 from ACS*. (d) $PbTiO_3$ (PTO) NTs/Ti fibers devices for PENG illustrating arbitrary bending motion using two of PTO NTs/Ti fibers in the PDMS polymer matrix (left), radially grown PTO NTs array on the Ti fiber (middle), PTO crystal structure indicating perovskite phase (top right), and individual PTO NTs (bottom right) as shown in (i); (ii) photograph of the p-NGs devices standing on a field, images showing the p-NGs devices in inset; (iii) EDS spectra of $PbTiO_3$ (PTO) NTs/Ti fibers and (iv) output voltage signals from double wire p-NGs bended by 0°, 180°, 90°, and 270°[142]@ *Copyright permission 2017 from Wiley*.

Fig. 12 (a) Fabrication steps of the graphene/ZnO NR on a graphite substrate. (b) Surface of the graphene/ZnO NRs after exfoliation. Inset shows exfoliated free-standing graphene/ZnO NR composite based PENG. (c) Piezoelectric output potential measured from the ZnO NR/PDMS-based piezoelectric nanogenerator with an exfoliated graphene electrode. (d) Output voltage with frequency of mechanical force. Inset shows device structure[143]@ *Copyright permission 2014 from RSC*.

ACCEPTED MANUSCRIPT

Fig. 13 (a) Schematic of prototype TENG nanogenerator (b) Three layers of the nanogenerator prototype. (c) Electrons are transferred from PDMS/MWCNT to PDMS when they contact each other. (d) Electrons transfer between electrodes at separation state. (e) Vertical forces are applied on the generator again. (f) PDMS and PDMS/MWCNT at full-separated state. (a) Electric potential between the triboelectric material surfaces with 0.1 mm interval. (b) Electric potential with 5 mm interval. (c) Electric potential with 10 mm interval. (a) Fabricated nanogenerator at the initial and full-contact states. (b) TENG lighting 16 LED bulbs configured in parallel. (c) Charging voltage and time of the two capacitors with different capacitance values[150]@ *Copyright permission 2016 from Nature.*

Fig. 14 (a) Auxetic triboelectric nanogenerator[151]@ *Copyright permission 2017 from Wiley* (b) TENG in free-standing mode[152]@ *Copyright permission 2015 from Wiley.* (c) Single-thread-based triboelectric nanogenerator[153]@ *Copyright permission 2017 from ACS.* (d) Flexible, foldable Wearable TENG[154]@ *Copyright permission 2015 from ACS.* (e) Photographs of the FTENG[77]@ *Copyright permission 2015 from Wiley.* (f) TENG by graphene based crumpled substrate[24]@ *Copyright permission 2014 from Wiley.* (g) structural design and pictorial image of the TENG in two sliding states[155]@ *Copyright permission 2013 from ACS* (h) TENG roll of graphene/EVA/PET film after delamination[156]@ *Copyright permission 2015 from Wiley.* (i) Operational modes from joint motion TENG[157]@ *Copyright permission 2015 from Wiley* and (j) Two water droplets before and after the confluence; below image shows two kinds of phenothalin and potassium hydroxide droplets (pink colour) before and after the confluence[158]@ *Copyright permission 2017 from Wiley*.

Fig. 15 (a) (i-iii) Schematic for sliding mode, image and short circuit current and open circuit potential versus rotation of the flexible interdigital-electrodes-based triboelectric generator respectively[159]@ *Copyright permission 2014 from RSC.*(b) Fabrication of water energy harvesting TENG, (i) the variation in weight percentage of the HCOENPs coated on PET fabric as a function of washing time in harsh environment. Insert is photograph of HCOENPs-coated PET fabric that holds dye aqueous droplets after being washed for 72 h. (ii-iii) All-fabric-based DMTEG constructed as a wristband, for harvesting water energy to drive commercial LEDs. All fabric-based WTEG with effective dimensions of 1.5 cm × 1.5 cm for output tests; effective dimensions of 3 cm × 3 cm for driving LEDs, (iv) Instantaneous power density generated from DMTEG with external resistance. Insert shows current without resistance[160] @ *Copyright permission 2017 from Wiley*. (c) Low thickness of graphene based S-TENG fabrication shown in (i-iii), (iv-v) Short-circuit current produced by different contact materials[162] @ *Copyright permission 2017 from Wiley.* (d) Fabrication of highly transparent and high-performance TENG as shown in (i), (ii-iii)comparisons of output voltage and current of TENGs using different contact-electrification materials[163]@ *Copyright permission 2017 from Nature*.

Fig.16 (a) Hybrid energy harvesting cell composed of serially integrated solar cell (SC) and nanogenerator (NG) (i) Schematic of a serially combined cells, the top electrode used for to

ACCEPTED MANUSCRIPT

harvest solar energy and bottom was used to harvest mechanical energy, whereas ITO layer acts as cathode and GaN substrate acts as the anode. Microscopic image of (ii) Solar cell unit and (iii) Nanogenerator unit, the inserts (1) and (2) are cross-section view of the hybrid cell. (d) Energy band diagram of the serially integrated solar cell (SC) and nanogenerator (NG) device for high performance. Whereas CB, VB and EF represents conduction band, valence band and Fermi level respectively. (b) Parallel integrated hybrid device (i) Schematic structure, where Pt-coated silicon substrate acts as the anode, and the ITO acts as the cathode. (b) Energy band diagram of parallel integrated hybrid device. The top two diagrams and the below one diagram are the band structures of SC and NG before parallel integration and after parallel integration respectively[167] *@ Copyright permission 2003 from ACS.*

Fig. 17 (a) Device architecture and working mechanism of the single-structure-based piezo-tribo-pyro-photoelectric effects coupled nanogenerator. b) Physical mechanism of pyroelectric effect in PyENG. c) Light-induced charge separation and corresponding distribution of charge density in the PVC with ITO/PZT/Ag sandwich structure. d) Working principle of the vibrating TPiENG[164]*@ Copyright permission 2017 from Wiley.*

Fig. 18 (a) (i) Operation mechanism to investigate combined effects of piezoelectricity and triboelectricity, (ii) Flexible hybrid NG, (iii) Output voltage under three testing modes: hybrid, triboelectric, and piezoelectric[169]*@ Copyright permission 2016 from ACS*. (b) Structural design of blue energy hybrid nanogenerator. (i) Schematic of the R-TENG and EMG. (*Insert* SEM of nanowires on PTFE thin film, schematic of TENG, which consists of a group of aluminum rods and PTFE thin film coated with the copper interdigitated electrodes, schematic of EMG unit, which consists of a pair of magnets and a coil) (ii) TENG and EMG hybrid nanogenerator. TENG is 45 cm^3 in volume and 28.3 g in weight. The EMG is 337 cm^3 in volume and 311.8 g in weight. (iii) Charging curves of a 20 μF capacitor using TENG only, EMG only, and hybrid nanogenerator, showing hybrid charging offers both high charging voltage and fast charging speed. (iv) Robustness and stability investigation of the TENG[171]*@ Copyright permission 2016 from ACS*. (c) (i) Photographs of fabricated hybrid generator at initial and full-contact states. (ii) Charging voltage and time ofthree capacitors with different capacitance values. (iii) Snapshots of the 550 LED bulbs configured in series before and when lit up. (iv) Snapshots of the 600 LED bulbs configured in series and parallel before and when hit by a 0.2-N mechanical force[170]*@ Copyright permission 2015 from Nature*. (d) (i) Schematic of the hybridized nanogenerator. (ii) Photograph of the flexible hybridized nanogenerator (iii) Measured output current of the TENG–PiENG[172]*@ Copyright permission 2016 from Wiley*.

Fig. 19 (a) (i-v) LEDs array on a PET film showing flexibility of PENG[173]*@ Copyright permission 2015 from Nature*, (b) (i-ii) GaN MW-based LEDs using PENG[174]*@ Copyright permission 2017 from ACS*, (c) flexible piezoelectric touch sensor[185]*@ Copyright permission 2017 from Wiley*, (d) (i-ii) Nanocomposite piezo-responsive foam (NCPF) sensor with wires embedded to measure the voltage response during impacts on shoes[177]*@ Copyright permission 2017 from Springer*. (e) (i-ii) Self-Powered Temperature Sensors[178]*@ Copyright permission 2012 from ACS*, (f) Heart beat measurement of piezoelectric sensor[179]*@ Copyright permission 2016 from Nature.*

ACCEPTED MANUSCRIPT

Fig. 20 (a) In vivo evaluation of optimal placement and orientation of PZT MEHs on the heart, and assessment of voltage output by varying the heart rate via dobutamine infusion and use of pacemaker (b) In vivo evaluation of PZT MEHs on lung and diaphragm (c) Performance of a PZT MEH evaluated with chest open and closed and scaling of power output in multilayer stacked designs[181]@ *Copyright permission 2014 from PNAS*, (d) A schematic and experimental condition of the artificial cardiac pace making using electrical energy from the flexible PMN-PT energy harvester. The inset is a flexible PMN-PT thin film stimulator used to stimulate the living heart of rat[183]@ *Copyright permission 2014 from Wiley*, (e) Energy harvesting sensor from the breath and heartbeat of a live rat using an SWG attached to (i) rat diaphragm and (ii) rat heart[184]@ *Copyright permission 2010 from Wiley*.

Fig. 21 (a) Transparent and flexible triboelectric sensing array for touch security applications (i-ii) and working principle (iii-iv)[176] @ *Copyright permission 2017 from ACS*; (b)(i) Tactile sensing by STENG; Biomechanical energy harvesting by the STENG (ii) Image of 20 green LEDs lit by VHB-STENG (iii-iv) Image of LCD screen powered by a transparent VHB-STENG, which covers the screen and converts finger pressing into electricity[175]@ *Copyright permission 2017 from Science*; (c) (i-ii) Sensing electrical output and optical measurement of the FTNG and (iii) FTNG device attached on the screen of a smart phone that indicates the high transparency of the NG device[98]@ *Copyright permission 2012 from ACS;* (d) (i) Self-powered TENG based flexible Li-ion battery. Photographs of the (ii) twisted and (iii) bent Li-ion batteries to light up a green LED[186]@ *Copyright permission 2017 from Wiley*.

Fig. 22 (a) Flexible Fiber-Based Supercapacitor–Triboelectric-Nanogenerator (i) Planar FSC (ii) bent FSC[27]@ *Copyright permission 2015 from Wiley;* (b) (i) Mechanism of transformation from acoustic energy to electric energy. (ii) FENG-based microphone system for recording music sound (iii) Experimental setup for free-standing FENG-based loudspeaker and (iii) recorded sound wave[187]@ *Copyright permission from 2017 Nature.*

Fig. 23 (a) Demonstration of hybrid nanogenerator as a blue energy power source, inserts are LED's[191]@ *Copyright permission from 2016 ACS.* (b) Model of a blue energy dream (by Prof. Z. L Wang) by networking millions of spherical balls based on triboelectric nanogenerators for harvesting low-frequency water wave energy. The inset is the designed spherical TENG. The lower right corner is an imaginary structure of the networks[190]@ *Copyright permission from 2017 Elsevier.* (c) Blue energy model[96]@ *Copyright permission from 2014 RSC;* (d) Blue energy harvesting TENG's fabricated by Sang Woo Kim group[192]@ *Copyright permission from 2016 ACS*, and (e) hourglass triboelectric nanogenerator (HG-TENG) (i) photographic image of TENG device (ii) Operating process of the HG-TENG (iii) pictures of a row of LEDs lit up by the HG-TENGs in real time during one falling process[193]@ *Copyright permission from 2017 Wiley.*

ACCEPTED MANUSCRIPT

Figure 1
Click here to download high resolution image

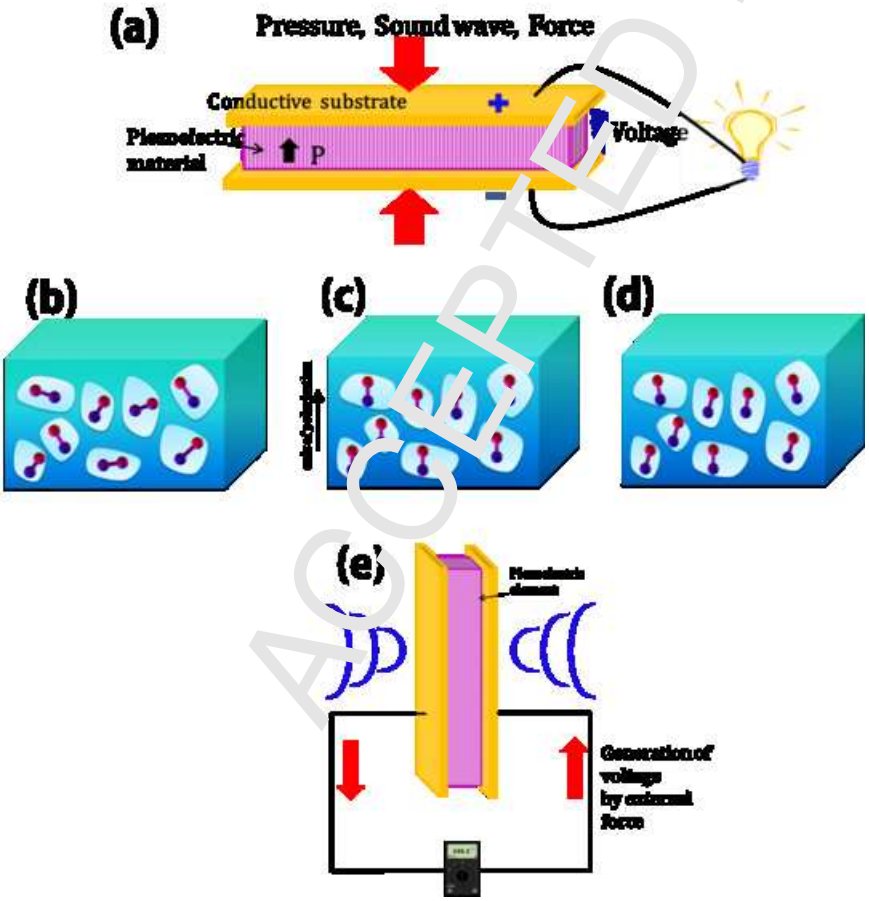

ACCEPTED MANUSCRIPT

ACCEPTED MANUSCRIPT

Figure 2
Click here to download high resolution image

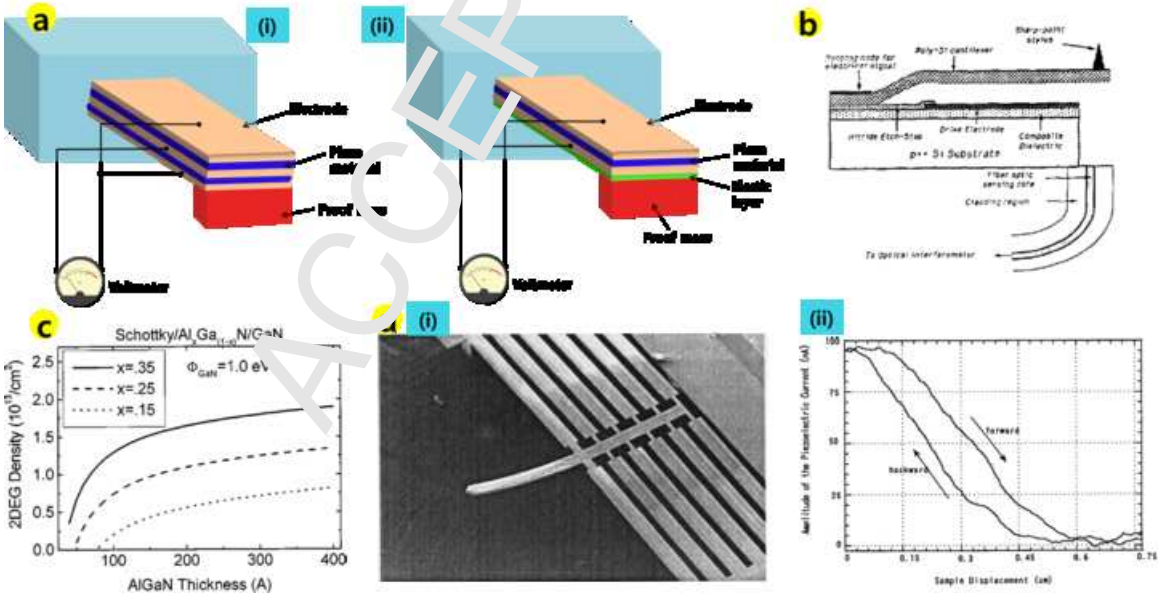

ACCEPTED MANUSCRIPT

Figure 3
Click here to download high resolution image

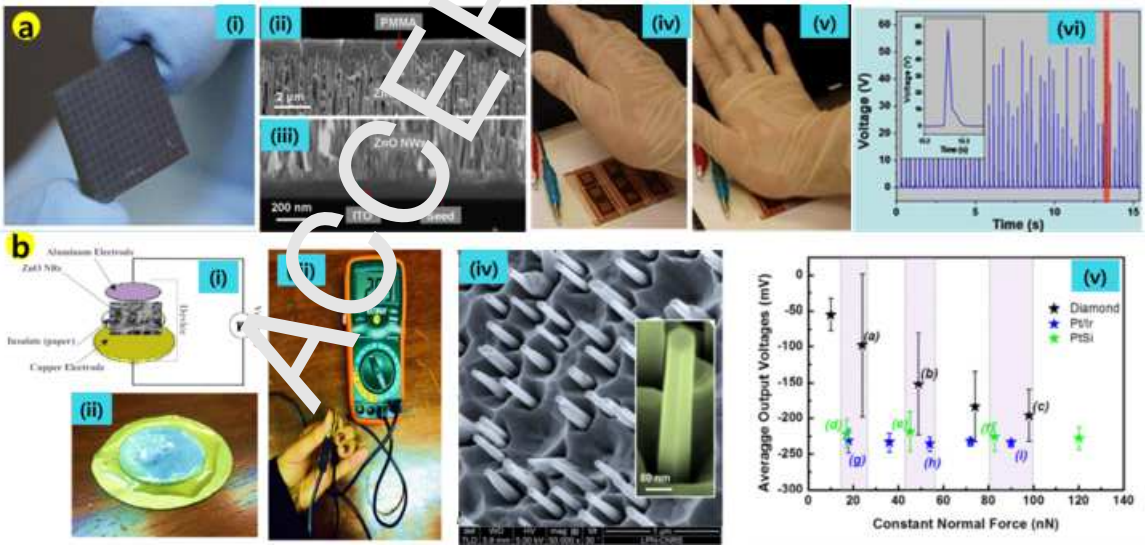

ACCEPTED MANUSCRIPT

Figure 4
Click here to download high resolution image

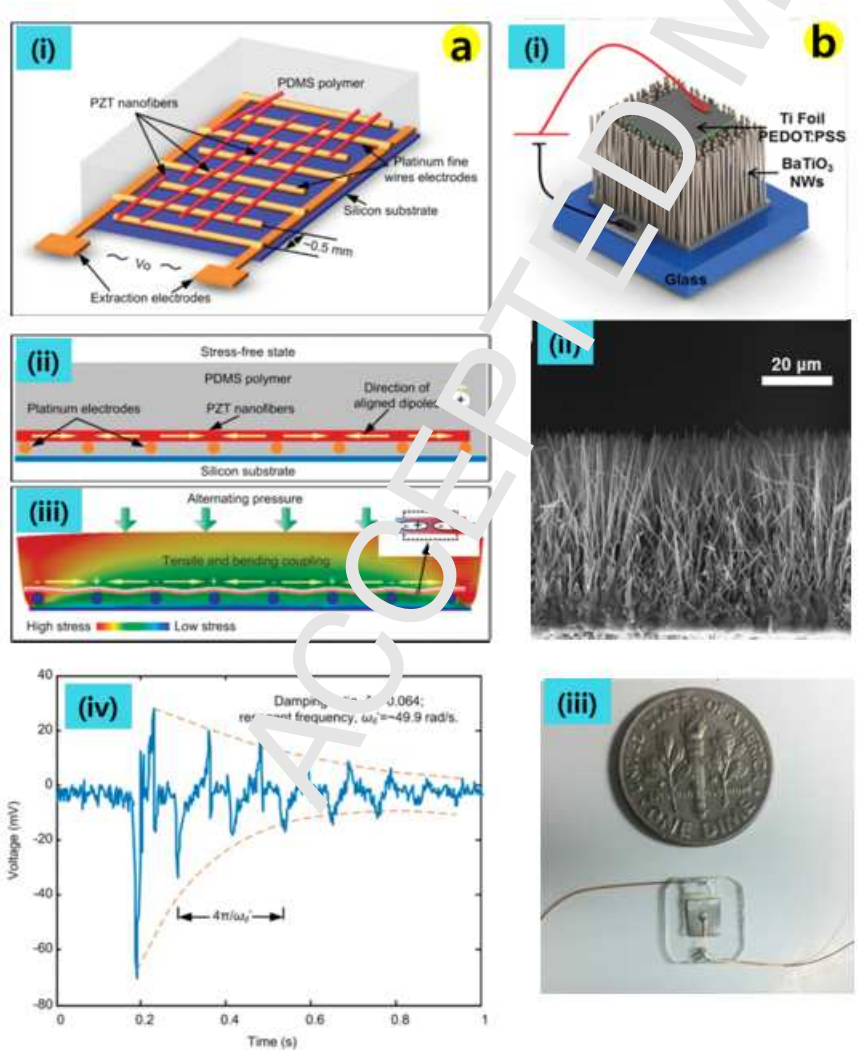

ACCEPTED MANUSCRIPT

Figure 5
Click here to download high resolution image

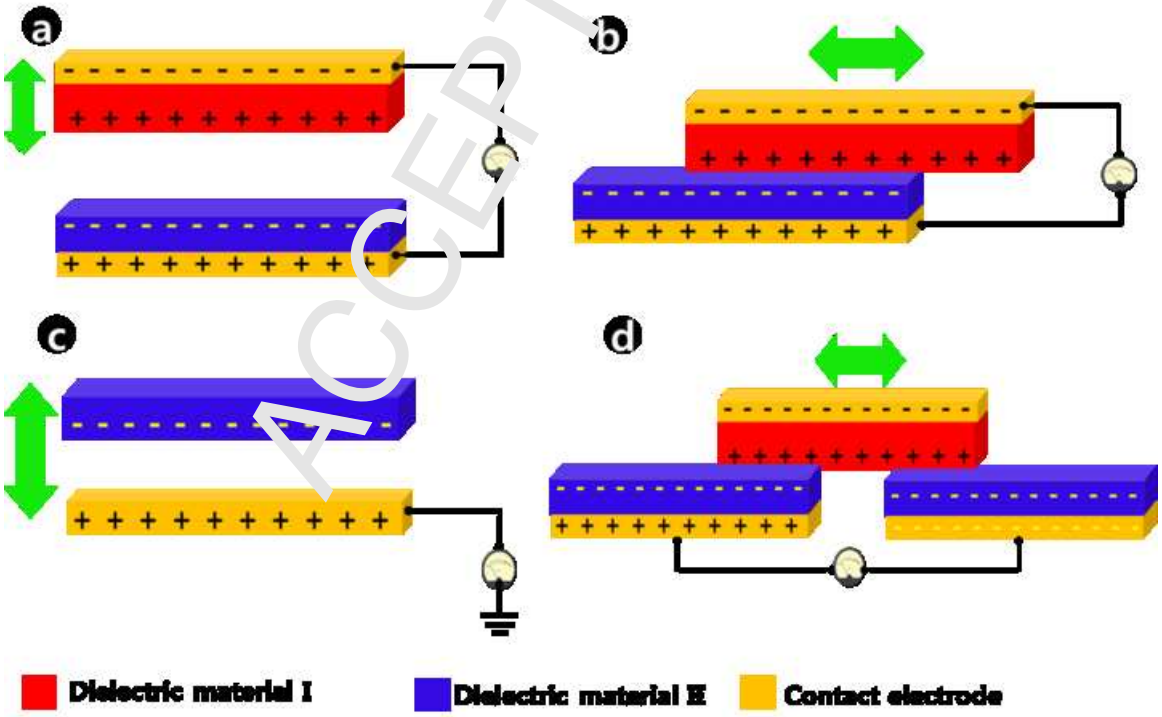

ACCEPTED MANUSCRIPT

ACCEPTED MANUSCRIPT

Figure 6
Click here to download high resolution image

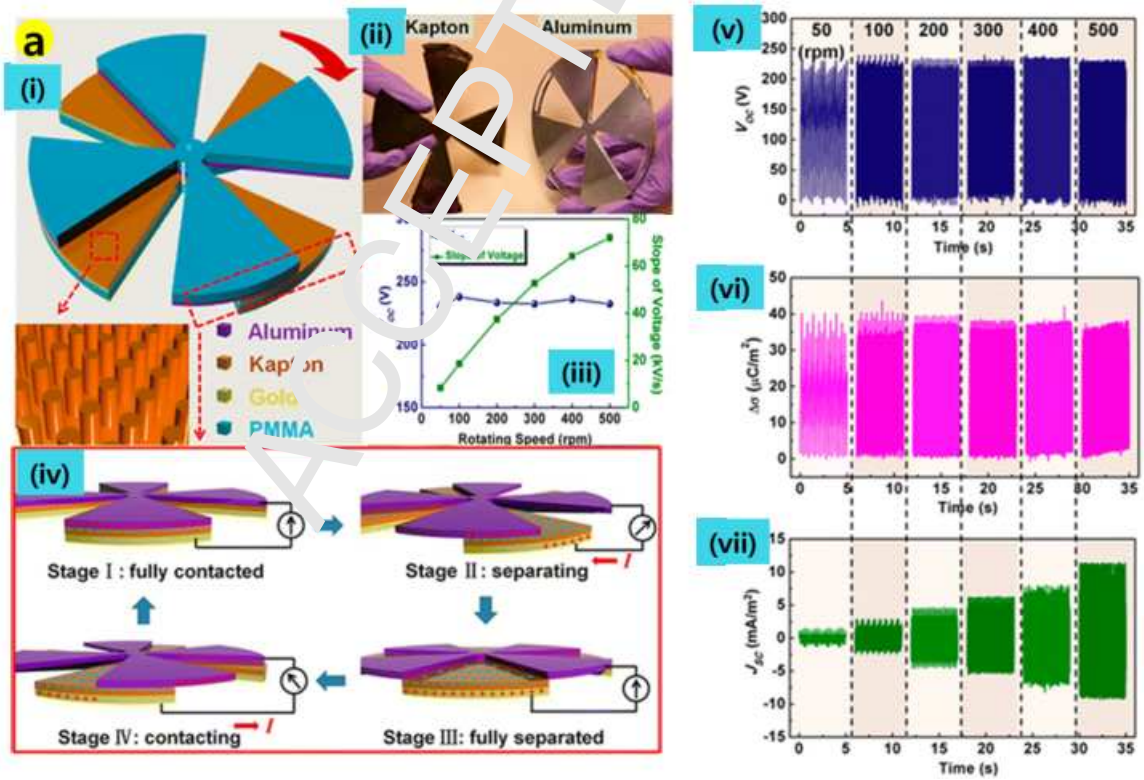

ACCEPTED MANUSCRIPT

ACCEPTED MANUSCRIPT

Figure 7
Click here to download high resolution image

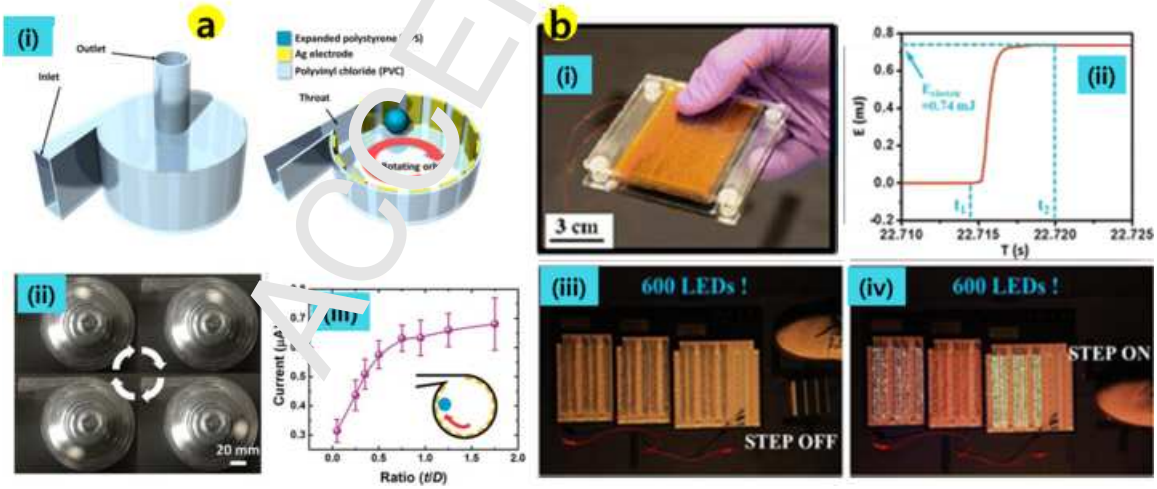

ACCEPTED MANUSCRIPT

ACCEPTED MANUSCRIPT

Figure 8
Click here to download high resolution image

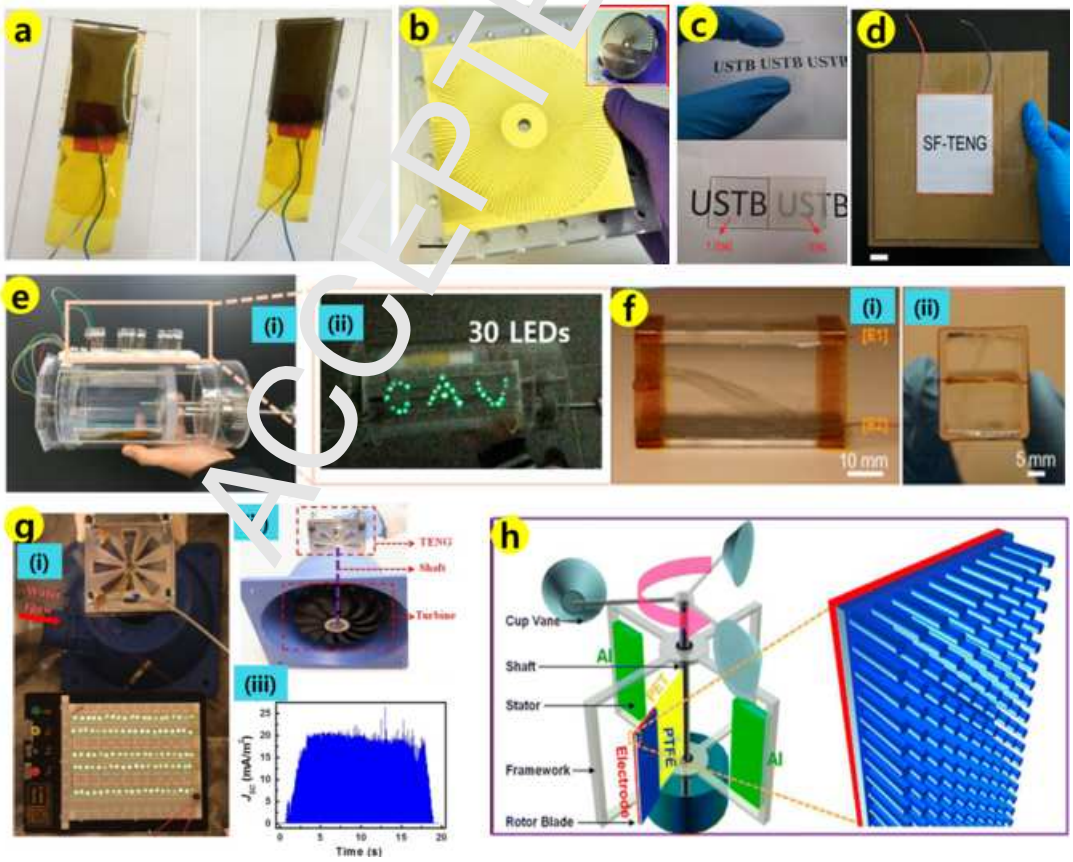

ACCEPTED MANUSCRIPT

ACCEPTED MANUSCRIPT

Figure 9
Click here to download high resolution image

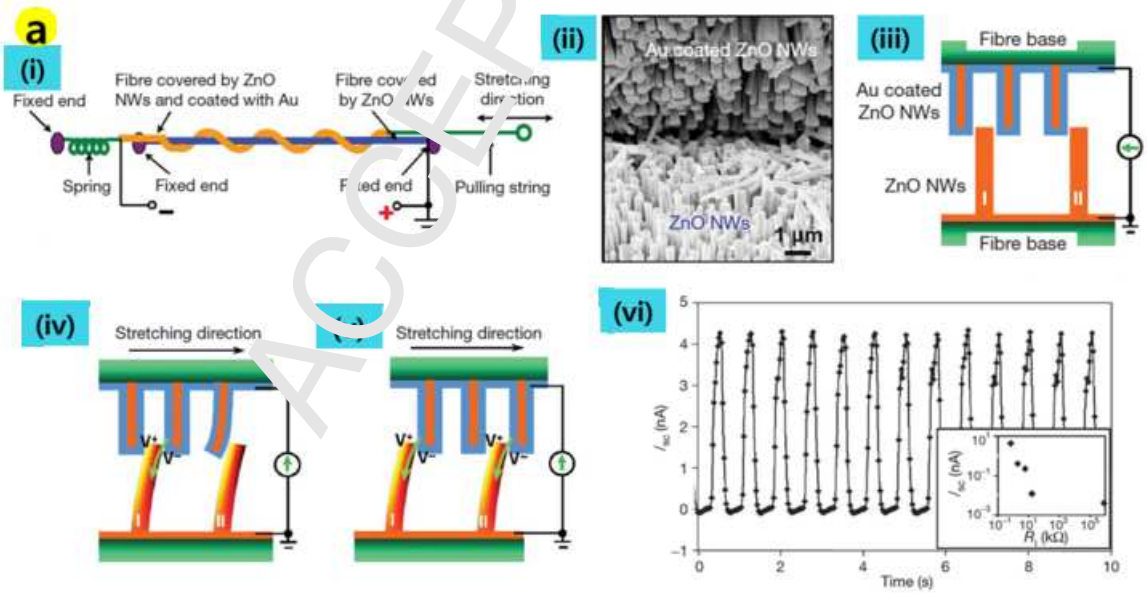

ACCEPTED MANUSCRIPT

Figure 10
Click here to download high resolution image

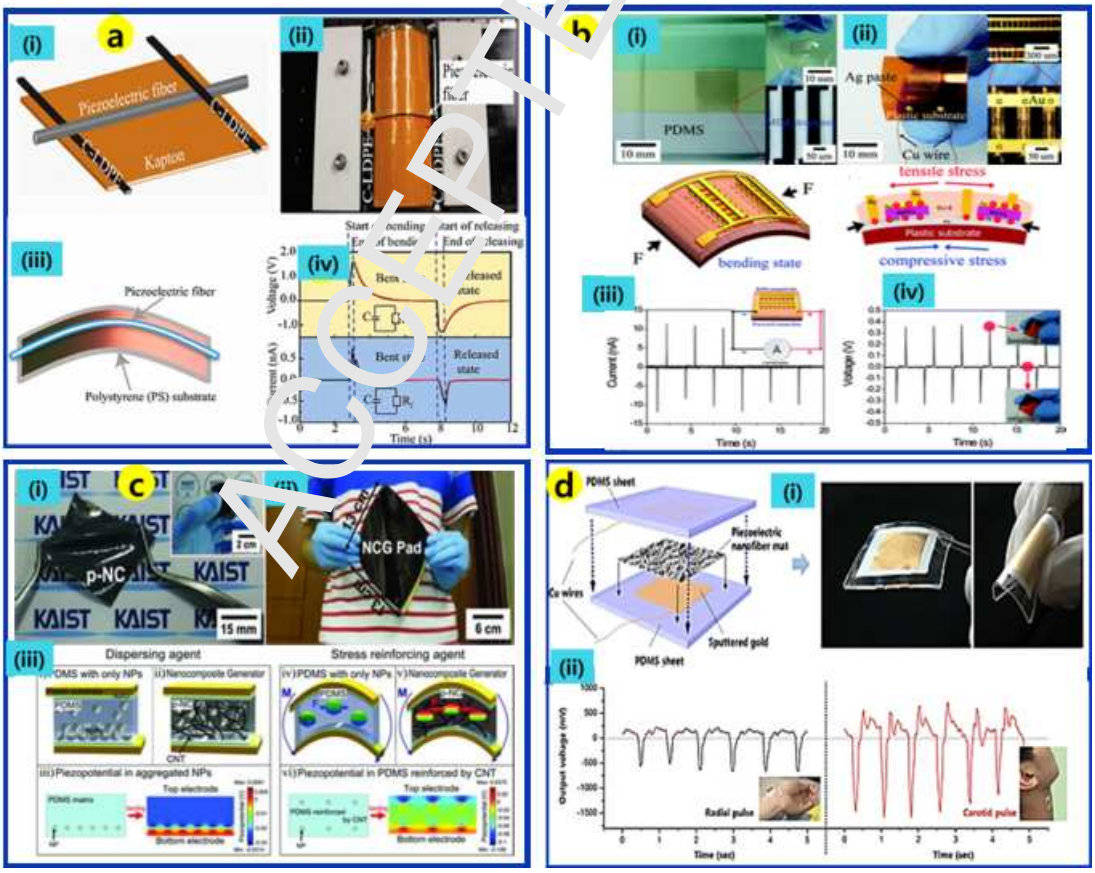

ACCEPTED MANUSCRIPT

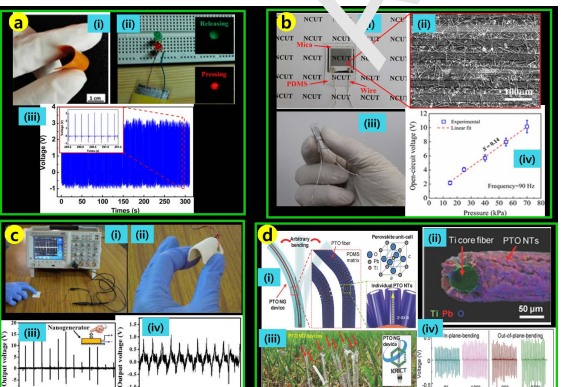

ACCEPTED MANUSCRIPT

Figure 12
Click here to download high resolution image

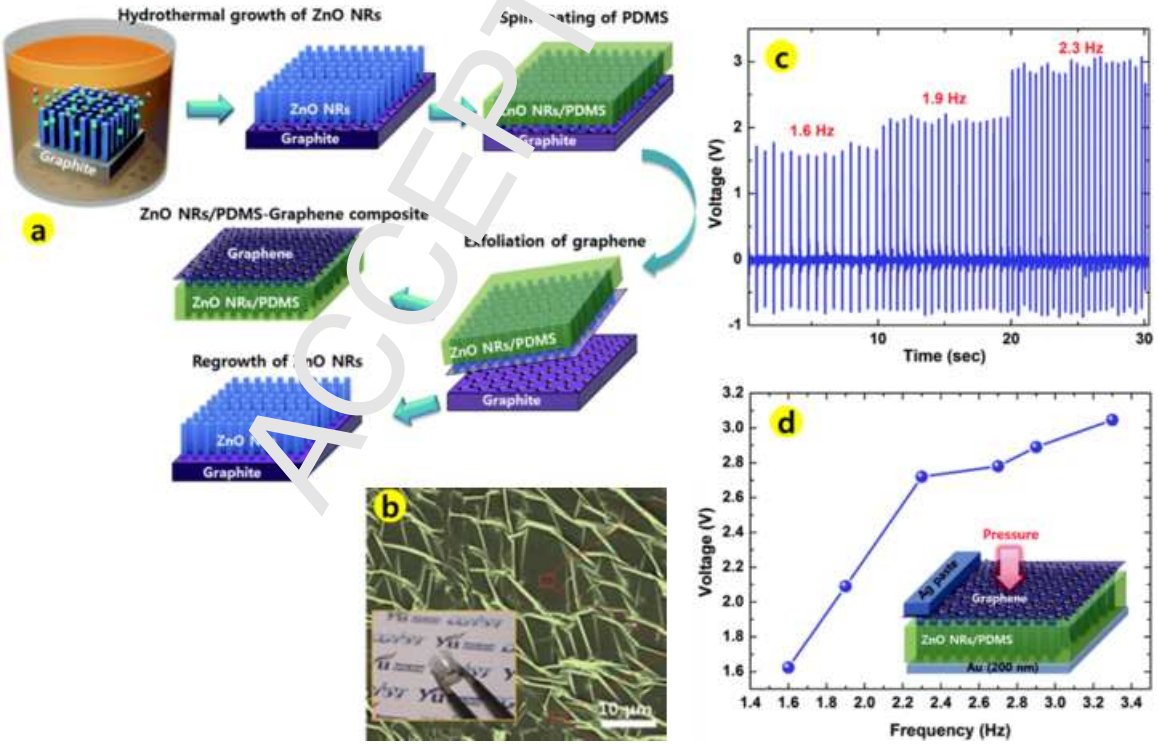

ACCEPTED MANUSCRIPT

Figure 13
Click here to download high resolution image

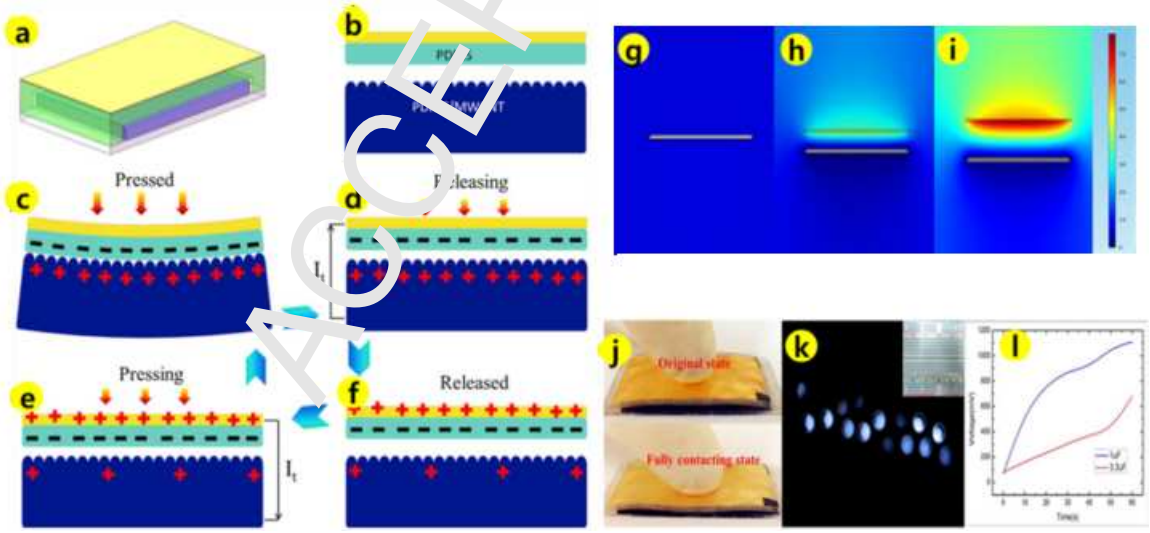

ACCEPTED MANUSCRIPT

ACCEPTED MANUSCRIPT

Figure 14
Click here to download high resolution image

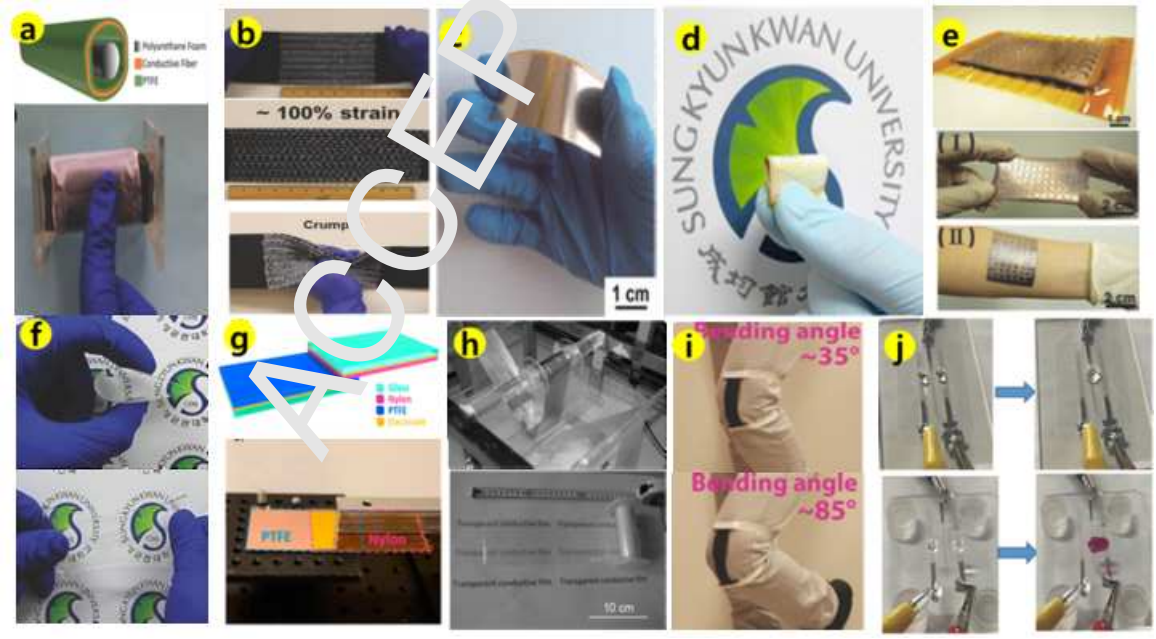

ACCEPTED MANUSCRIPT

Figure 15
Click here to download high resolution image

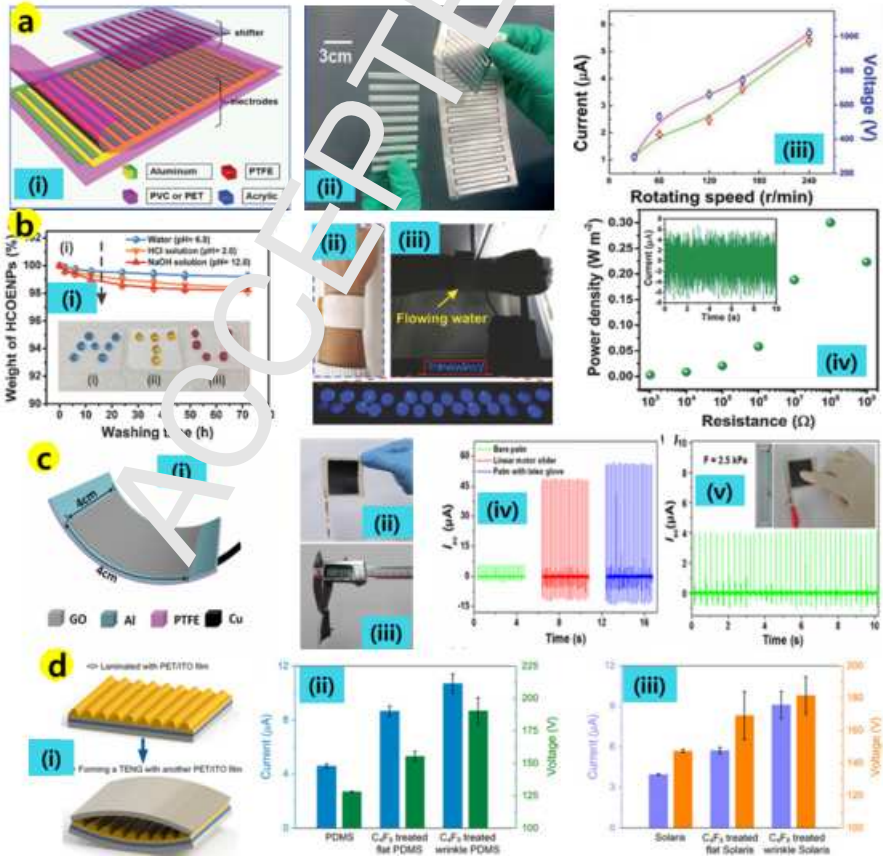

ACCEPTED MANUSCRIPT

ACCEPTED MANUSCRIPT

Figure 16
Click here to download high resolution image

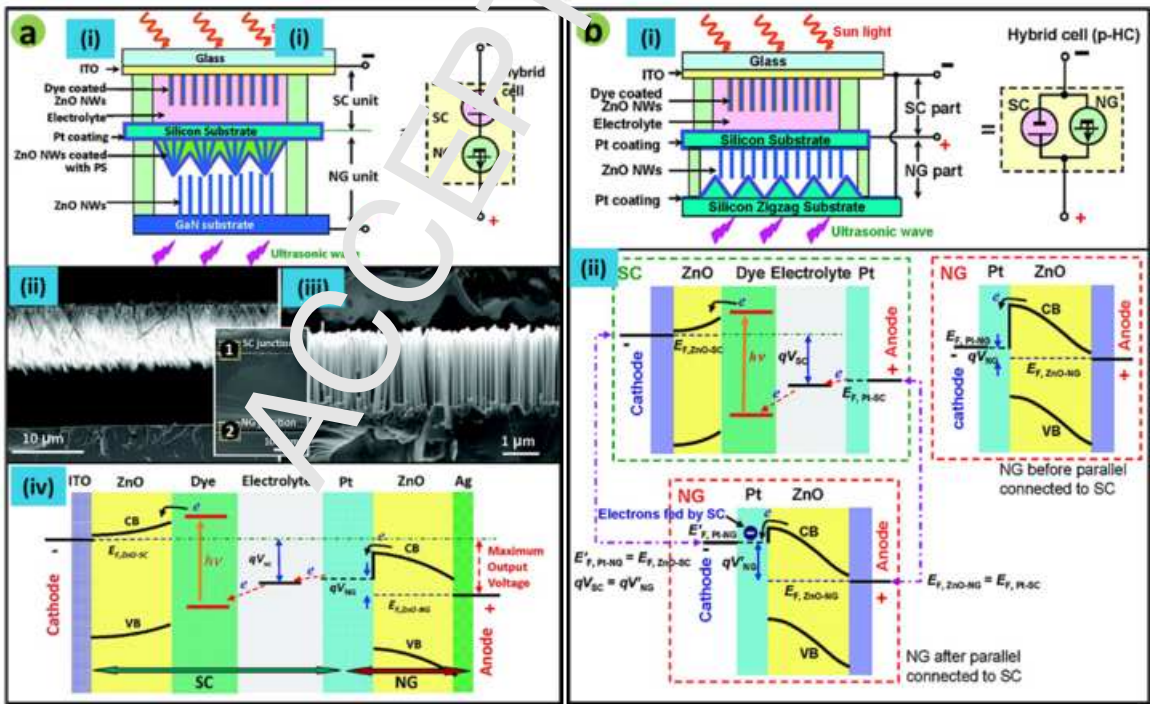

ACCEPTED MANUSCRIPT

Figure 17
Click here to download high resolution image

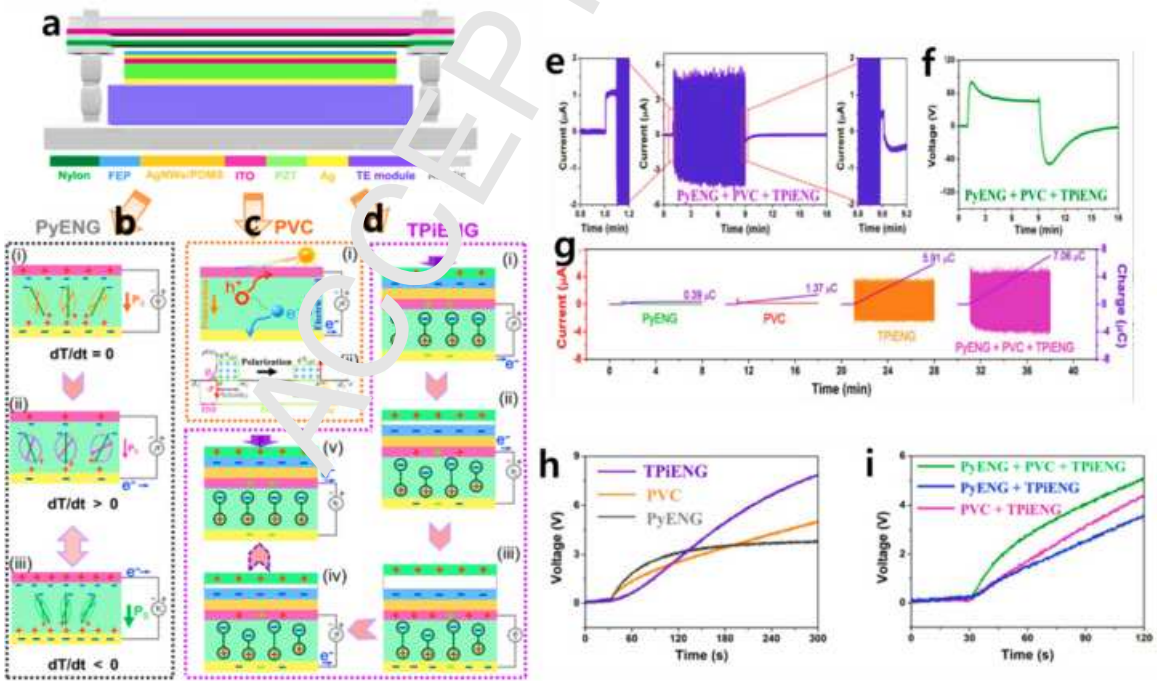

ACCEPTED MANUSCRIPT

Figure 18
Click here to download high resolution image

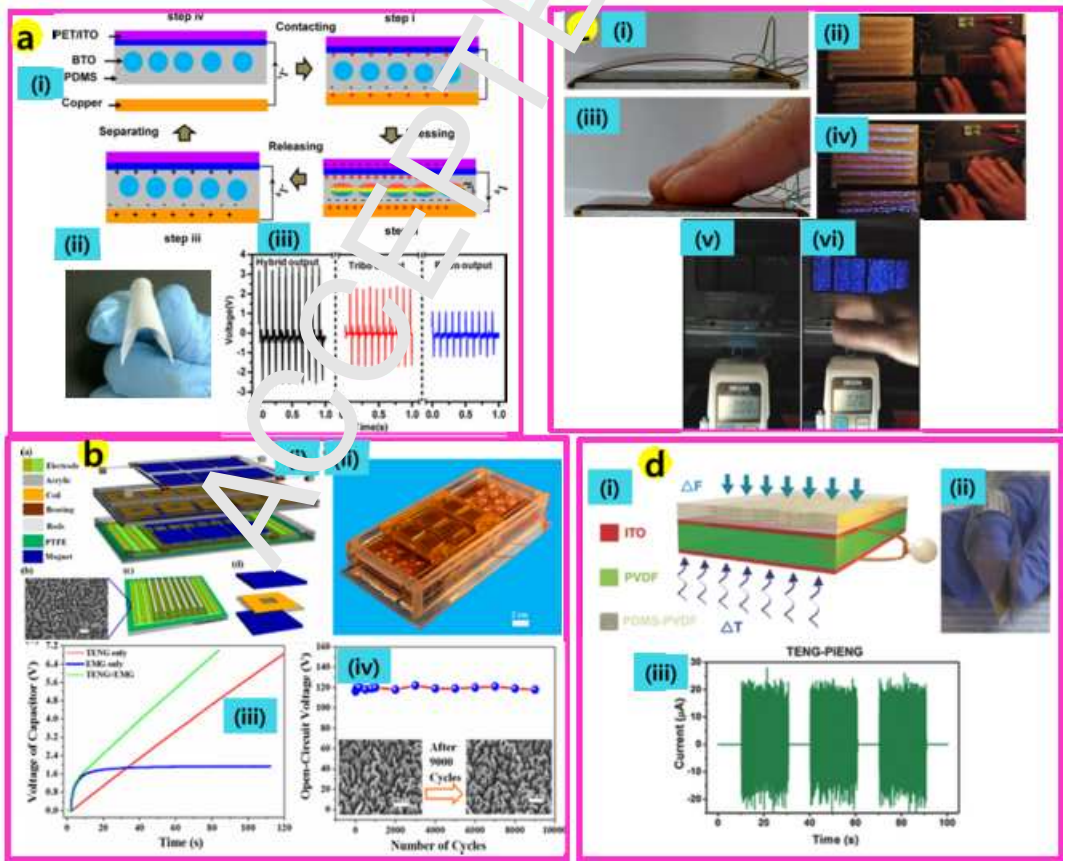

ACCEPTED MANUSCRIPT

Figure 19
Click here to download high resolution image

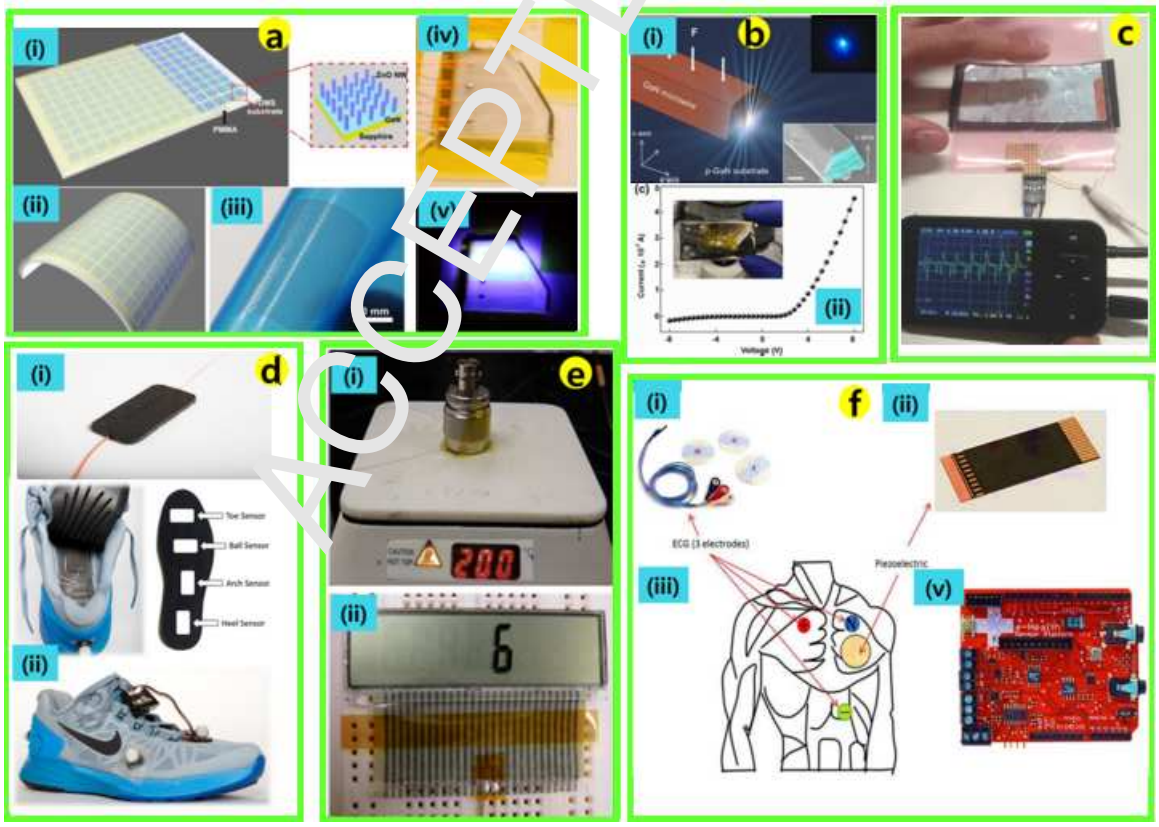

ACCEPTED MANUSCRIPT

Figure 20
Click here to download high resolution image

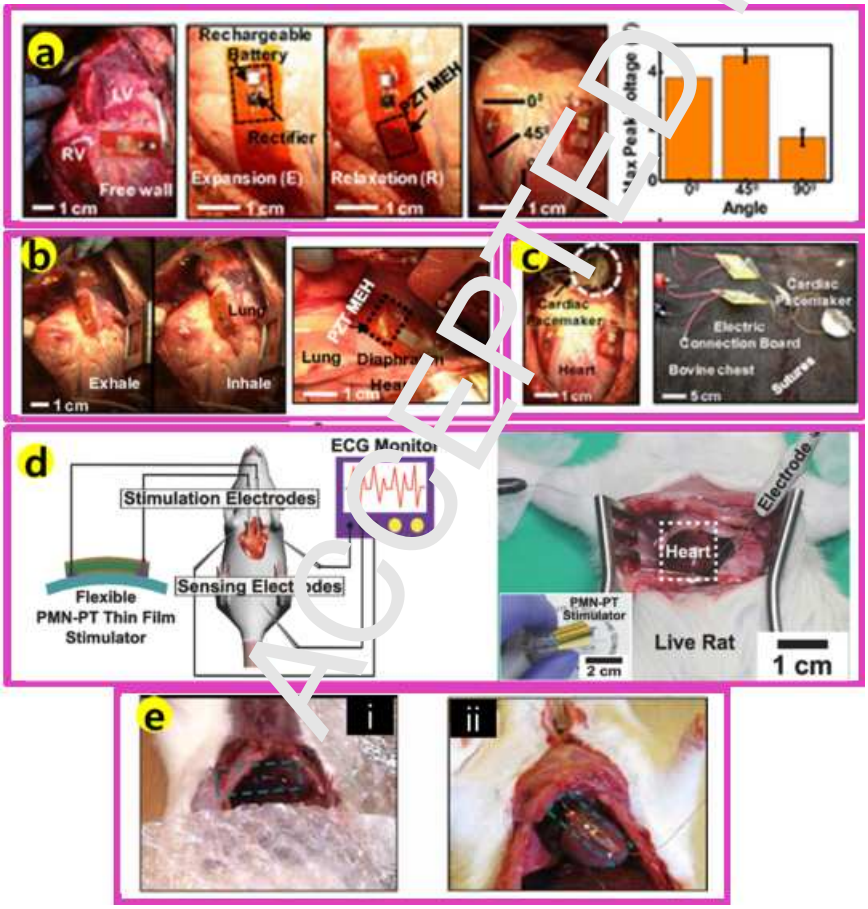

ACCEPTED MANUSCRIPT

Figure 21
Click here to download high resolution image

ACCEPTED MANUSCRIPT

Figure 22
Click here to download high resolution image

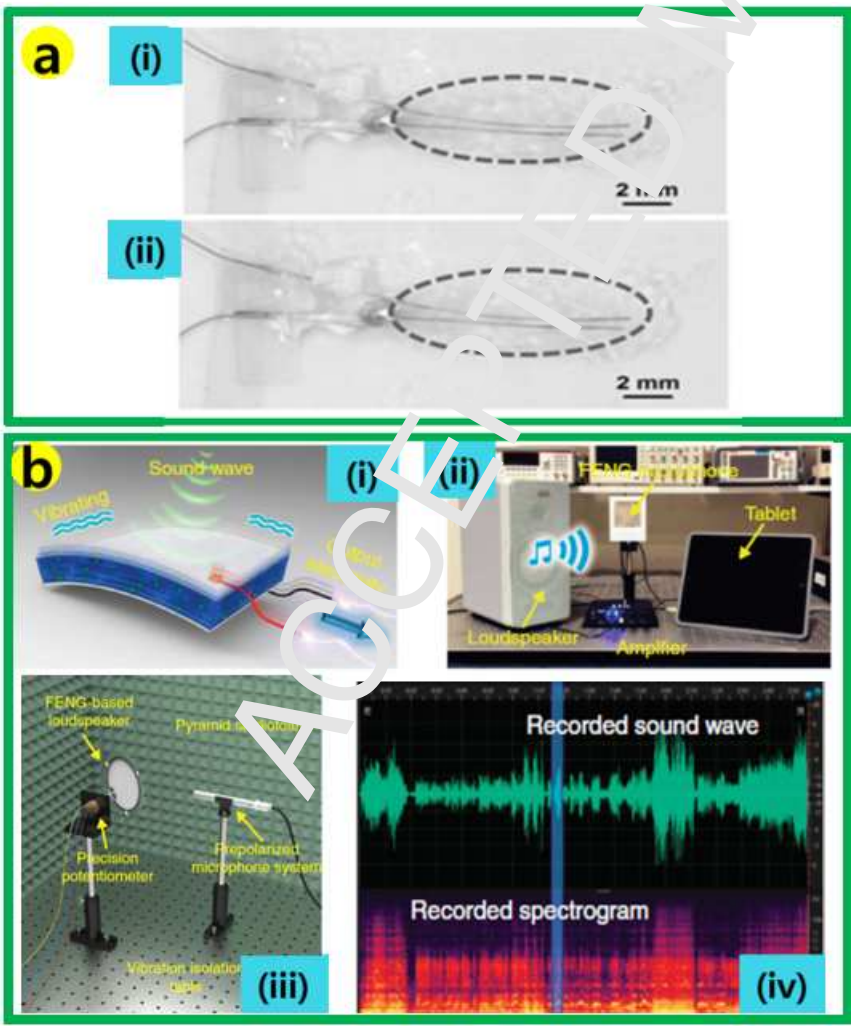

ACCEPTED MANUSCRIPT

ACCEPTED MANUSCRIPT

Figure 23
Click here to download high resolution image

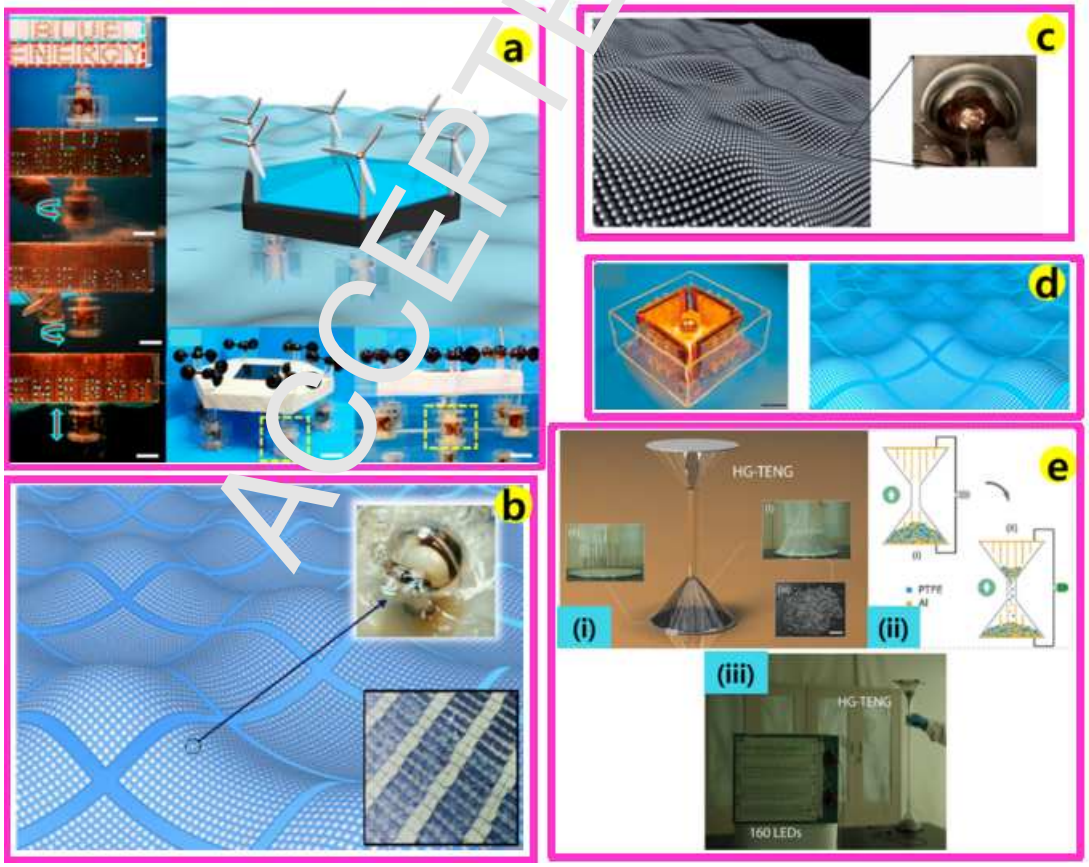

ACCEPTED MANUSCRIPT